Appendix 6.9.2

HAC PACKAGE MODEL

6.9.2.1 PREDICTION OF HAC DAMAGE IN THE ES-3100 PACKAGE

Finite element analysis of an ES-3100 package under Hypothetical Accident Conditions (HAC) is used to predict the deformed outer diameters of the drum at node points along the vertical axis of an upright package. Selected node points are designated in a downward direction from the top of the drum as "UR," "MUR," "MR," "MLR," and "LR." Table 6.9.2.1-1 lists diameters at the five node points measured along the 90–270° and 0–180° axes. These dimensions represent major and minor axes at each deformation point on the assumption that the drum cross section is ellipsoidal. A corresponding equivalent circular diameter is also listed for each node point in Table 6.9.2.1-1.

A set of KENO V.a calculation models based on reduced package diameters at the "MR," "MLR," and "LR" deformation points are derived from the Normal Conditions of Transport (NCT) geometry model. These geometry models are evaluated for the purpose of establishing a bounding geometry model for representing the ES-3100 package under HAC. The primary changes made to the KENO V.a geometry input statements in the NCT model are reductions in the drum's radii. The change to the drum's inner radius also affects the outer radius of both the angle iron and the Kaolite located inside the containment vessel outer liner. The volume fractions for these materials are adjusted in the KENO V.a calculation models so that material masses of the affected package components are conserved. Table 6.9.2.1-2 provides data for transforming the KENO V.a calculation model from an NCT model into an HAC model.

6.9.2.2 CRITICALITY CALCULATIONS

Sets of criticality calculations are performed for the "MR," "MLR," and "LR" models at five different package water contents over the range of HAC. The five package water contents of the void spaces external to the containment vessel and the interstitial space between drums are as follows: 1e-20 spg water, 1e-04 spg water, 0.1 spg water, 0.3 spg water, and 1.0 spg water. The water content in the Kaolite corresponds to the dry condition (VF= 0.0287) where neutronic interaction between the packages of an array is maximized.

An infinite array of packages is evaluated in order to eliminate any biases arising from spectral leakage effects in the reflector of the finite array. The k_{eff} values for each KENO V.a case are based on 500,000 neutron histories produced by running for 215 generations with 2,500 neutrons per generation and truncating the first 15 generations of data. Each package modeled has 36 kg of 100% enriched uranium in the form of broken metal content.

Each case is rerun using a different starting random number in order to produce sets of computed k_{eff} values that are statistically independent. The random starting number, the mean value (k_{eff}), and the corresponding standard error (s_i) computed for ten individual runs are shown in Tables 6.9.2.2-1, -2, and -3. The same statistical method (described in DAC-FS-900000-A014) used in the evaluation of Kaolite models (Appendix 6.9.3, Sect. 6.9.3.4) is also used here for determining whether or not differences in neutronic performance between the package models are statistically significant.

Table 6.9.2.1-1. Deformation of the ES-3100 drum at five node points, projected by finite element analysis "Case 3100 RUN1HL Lower Bound Kaolite May 2004"

Deformation point	FEA node	Diameter at 90° (in.)	Diameter at 180° (in.)	Equivalent circular diameter	
				(in.)	(cm)
UR	098194	20.02	15.60	17.6724	44.8878
MUR	100238	20.74	15.07	17.6791	44.9050
MR	101589	20.74	14.18	17.1492	43.5588
MLR	103012	22.00	13.44	17.1954	43.6762
LR	105786	20.92	12.92	16.4404	41.7586

Table 6.9.2.1-2. Parameter changes for converting an NCT package model into an HAC package model

Parameter	Reference NCT package model	HAC model at MR node point of package	HAC model at MLR node point of package	HAC model at LR node point of package
Package Model Dimension				
OR_{Drum} (cm)	23.32990	21.77942	21.83809	20.87929
IR_{Drum} (cm)	23.17750	21.62702	21.68569	20.72689
$th_{Drum\ wall}$ (cm)	0.15240	0.15240	0.15240	0.15240
OR_{Lid} (cm)	23.11400	21.56352	21.62219	20.66339
IR_{Lid} (cm)	22.96160	21.41112	21.46979	20.51099
$th_{Kaolite}$ (cm)	12.10310	10.55262	10.61129	9.65249
Kaolite of the Body Weldment Inner Liner				
Mass (g)	117563.0	97080.4	97829.7	85839.8
Volume (cm^3)	134888.0	111387.0	112246.0	98489.5
Volume fraction multiplier [a]	–	1.21099	1.20171	1.36956
VF for water component of Kaolite	0.52294	0.63327 [b]	0.62843 [b]	0.71620 [b]
VF for dry mix component of Kaolite	0.34864	0.42220 [b]	0.41897 [b]	0.47749 [b]
Angle Iron				
Mass (g)	5621.76	4521.40	4561.66	3917.54
Volume (cm^3)	708.030	569.446	574.516	493.393
VF	1.0	1.24337	1.23239	1.43502
Drum Steel				
Mass (g)	25446.3	23397.6	23474.2	22231.2
Volume (cm^3)	3204.82	2946.80	2956.50	2799.90
VF	1.0	1.08756	1.08401	1.14462

[a] Volume fraction multiplier is an NCT density multiplier for conserving mass in components having modified volumes in the HAC calculation models.

[b] Volume Fraction (VF) for Kaolite components calculated by multiplying the VF used in the NCT model by volume fraction multiplier for the HAC model.

Table 6.9.2.2-1. Neutron multiplication factors with standard deviations for the ES-3100 package models at the "MR" and "MLR" node points

moifr	Random Number	"A" cases	k_{eff}	s	"B" cases	k_{eff}	s
1.0e-20	109E77866CF6	mrandnum_01_01	1.04965	0.00119	lrrandnum_01_01	1.05093	0.00133
1.0e-20	16AA4A58735C	mrandnum_01_02	1.05132	0.00131	lrrandnum_01_02	1.05009	0.00118
1.0e-20	1814171B652A	mrandnum_01_03	1.05368	0.00123	lrrandnum_01_03	1.05057	0.00118
1.0e-20	1A423B9472C7	mrandnum_01_04	1.05165	0.00145	lrrandnum_01_04	1.05066	0.00120
1.0e-20	20E876D82248	mrandnum_01_05	1.05344	0.00106	lrrandnum_01_05	1.04882	0.00129
1.0e-20	3F6E65CA7440	mrandnum_01_06	1.05188	0.00157	lrrandnum_01_06	1.05316	0.00127
1.0e-20	479D21DB7509	mrandnum_01_07	1.05149	0.00148	lrrandnum_01_07	1.05229	0.00134
1.0e-20	55D4371D3A23	mrandnum_01_08	1.05083	0.00113	lrrandnum_01_08	1.05186	0.00131
1.0e-20	6E1A14672B8F	mrandnum_01_09	1.04910	0.00106	lrrandnum_01_09	1.05236	0.00113
1.0e-20	77A0308C0E44	mrandnum_01_10	1.05254	0.00106	lrrandnum_01_10	1.05098	0.00120
1.0e-04	109E77866CF6	mrandnum_03_01	1.04994	0.00132	lrrandnum_03_01	1.05122	0.00123
1.0e-04	16AA4A58735C	mrandnum_03_02	1.05023	0.00118	lrrandnum_03_02	1.05324	0.00121
1.0e-04	1814171B652A	mrandnum_03_03	1.05090	0.00139	lrrandnum_03_03	1.05143	0.00123
1.0e-04	1A423B9472C7	mrandnum_03_04	1.05072	0.00115	lrrandnum_03_04	1.05048	0.00121
1.0e-04	20E876D82248	mrandnum_03_05	1.05052	0.00119	lrrandnum_03_05	1.05095	0.00137
1.0e-04	3F6E65CA7440	mrandnum_03_06	1.05383	0.00131	lrrandnum_03_06	1.05029	0.00119
1.0e-04	479D21DB7509	mrandnum_03_07	1.05205	0.00153	lrrandnum_03_07	1.05124	0.00108
1.0e-04	55D4371D3A23	mrandnum_03_08	1.05343	0.00106	lrrandnum_03_08	1.05080	0.00116
1.0e-04	6E1A14672B8F	mrandnum_03_09	1.04831	0.00132	lrrandnum_03_09	1.05074	0.00122
1.0e-04	77A0308C0E44	mrandnum_03_10	1.05353	0.00111	lrrandnum_03_10	1.05094	0.00111
0.10	109E77866CF6	mrandnum_06_01	0.97948	0.00120	lrrandnum_06_01	0.98315	0.00118
0.10	16AA4A58735C	mrandnum_06_02	0.98104	0.00125	lrrandnum_06_02	0.98605	0.00124
0.10	1814171B652A	mrandnum_06_03	0.98056	0.00134	lrrandnum_06_03	0.98690	0.00120
0.10	1A423B9472C7	mrandnum_06_04	0.97895	0.00114	lrrandnum_06_04	0.98347	0.00126
0.10	20E876D82248	mrandnum_06_05	0.98058	0.00113	lrrandnum_06_05	0.98770	0.00124
0.10	3F6E65CA7440	mrandnum_06_06	0.97966	0.00119	lrrandnum_06_06	0.98734	0.00140
0.10	479D21DB7509	mrandnum_06_07	0.97953	0.00145	lrrandnum_06_07	0.98417	0.00133
0.10	55D4371D3A23	mrandnum_06_08	0.97993	0.00130	lrrandnum_06_08	0.98712	0.00136
0.10	6E1A14672B8F	mrandnum_06_09	0.97972	0.00138	lrrandnum_06_09	0.98533	0.00142
0.10	77A0308C0E44	mrandnum_06_10	0.98157	0.00134	lrrandnum_06_10	0.98412	0.00116
0.30	109E77866CF6	mrandnum_08_01	0.93412	0.00118	lrrandnum_08_01	0.93910	0.00146
0.30	16AA4A58735C	mrandnum_08_02	0.93227	0.00138	lrrandnum_08_02	0.93757	0.00117
0.30	1814171B652A	mrandnum_08_03	0.93390	0.00131	lrrandnum_08_03	0.93940	0.00146
0.30	1A423B9472C7	mrandnum_08_04	0.93252	0.00144	lrrandnum_08_04	0.93676	0.00130
0.30	20E876D82248	mrandnum_08_05	0.93334	0.00132	lrrandnum_08_05	0.93851	0.00111
0.30	3F6E65CA7440	mrandnum_08_06	0.93168	0.00132	lrrandnum_08_06	0.93914	0.00149
0.30	479D21DB7509	mrandnum_08_07	0.93514	0.00123	lrrandnum_08_07	0.94011	0.00131
0.30	55D4371D3A23	mrandnum_08_08	0.93564	0.00132	lrrandnum_08_08	0.93900	0.00139
0.30	6E1A14672B8F	mrandnum_08_09	0.93597	0.00136	lrrandnum_08_09	0.93781	0.00117
0.30	77A0308C0E44	mrandnum_08_10	0.93525	0.00128	lrrandnum_08_10	0.93965	0.00118

Table 6.9.2.2-1. Neutron multiplication factors with standard deviations for the ES-3100 package models at the "MR" and "MLR" node points

moifr	Random Number	"A" cases	k_{eff}	s	"B" cases	k_{eff}	s
1.00	109E77866CF6	mrandnum_15_01	0.93103	0.00139	lrrandnum_15_01	0.93344	0.00126
1.00	16AA4A58735C	mrandnum_15_02	0.93082	0.00131	lrrandnum_15_02	0.93281	0.00121
1.00	1814171B652A	mrandnum_15_03	0.92890	0.00148	lrrandnum_15_03	0.93468	0.00132
1.00	1A423B9472C7	mrandnum_15_04	0.93062	0.00145	lrrandnum_15_04	0.93592	0.00126
1.00	20E876D82248	mrandnum_15_05	0.93055	0.00125	lrrandnum_15_05	0.93251	0.00143
1.00	3F6E65CA7440	mrandnum_15_06	0.92950	0.00117	lrrandnum_15_06	0.93374	0.00121
1.00	479D21DB7509	mrandnum_15_07	0.92952	0.00116	lrrandnum_15_07	0.93572	0.00138
1.00	55D4371D3A23	mrandnum_15_08	0.92805	0.00154	lrrandnum_15_08	0.93498	0.00145
1.00	6E1A14672B8F	mrandnum_15_09	0.93117	0.00140	lrrandnum_15_09	0.93224	0.00114
1.00	77A0308C0E44	mrandnum_15_10	0.93218	0.00120	lrrandnum_15_10	0.93158	0.00131

Table 6.9.2.2-2.Neutron multiplication factors with standard deviations for the ES-3100 package models at the "MLR" and "LR" node points

moifr	Random Number	"A" cases	k_{eff}	s	"B" cases	k_{eff}	s
1.0e-20	109E77866CF6	mlrrandnum_01_01	1.05024	0.00139	lrrandnum_01_01	1.05093	0.00133
1.0e-20	16AA4A58735C	mlrrandnum_01_02	1.05051	0.00135	lrrandnum_01_02	1.05009	0.00118
1.0e-20	1814171B652A	mlrrandnum_01_03	1.05121	0.00128	lrrandnum_01_03	1.05057	0.00118
1.0e-20	1A423B9472C7	mlrrandnum_01_04	1.04954	0.00120	lrrandnum_01_04	1.05066	0.00120
1.0e-20	20E876D82248	mlrrandnum_01_05	1.05249	0.00110	lrrandnum_01_05	1.04882	0.00129
1.0e-20	3F6E65CA7440	mlrrandnum_01_06	1.04924	0.00132	lrrandnum_01_06	1.05316	0.00127
1.0e-20	479D21DB7509	mlrrandnum_01_07	1.05105	0.00111	lrrandnum_01_07	1.05229	0.00134
1.0e-20	55D4371D3A23	mlrrandnum_01_08	1.05039	0.00129	lrrandnum_01_08	1.05186	0.00131
1.0e-20	6E1A14672B8F	mlrrandnum_01_09	1.05161	0.00125	lrrandnum_01_09	1.05236	0.00113
1.0e-20	77A0308C0E44	mlrrandnum_01_10	1.05041	0.00129	lrrandnum_01_10	1.05098	0.00120
1.0e-04	109E77866CF6	mlrrandnum_03_01	1.05108	0.00151	lrrandnum_03_01	1.05122	0.00123
1.0e-04	16AA4A58735C	mlrrandnum_03_02	1.05245	0.00116	lrrandnum_03_02	1.05324	0.00121
1.0e-04	1814171B652A	mlrrandnum_03_03	1.05169	0.00138	lrrandnum_03_03	1.05143	0.00123
1.0e-04	1A423B9472C7	mlrrandnum_03_04	1.05303	0.00102	lrrandnum_03_04	1.05048	0.00121
1.0e-04	20E876D82248	mlrrandnum_03_05	1.05191	0.00115	lrrandnum_03_05	1.05095	0.00137
1.0e-04	3F6E65CA7440	mlrrandnum_03_06	1.05017	0.00110	lrrandnum_03_06	1.05029	0.00119
1.0e-04	479D21DB7509	mlrrandnum_03_07	1.05232	0.00128	lrrandnum_03_07	1.05124	0.00108
1.0e-04	55D4371D3A23	mlrrandnum_03_08	1.05100	0.00144	lrrandnum_03_08	1.05080	0.00116
1.0e-04	6E1A14672B8F	mlrrandnum_03_09	1.05046	0.00145	lrrandnum_03_09	1.05074	0.00122
1.0e-04	77A0308C0E44	mlrrandnum_03_10	1.05130	0.00134	lrrandnum_03_10	1.05094	0.00111

Table 6.9.2.2-2.Neutron multiplication factors with standard deviations for the ES-3100 package models at the "MLR" and "LR" node points

moifr	Random Number	"A" cases	k_{eff}	s	"B" cases	k_{eff}	s
0.1	109E77866CF6	mlrrandnum_06_01	0.98071	0.00129	lrrandnum_06_01	0.98315	0.00118
0.1	16AA4A58735C	mlrrandnum_06_02	0.98006	0.00110	lrrandnum_06_02	0.98605	0.00124
0.1	1814171B652A	mlrrandnum_06_03	0.98043	0.00116	lrrandnum_06_03	0.98690	0.00120
0.1	1A423B9472C7	mlrrandnum_06_04	0.98253	0.00109	lrrandnum_06_04	0.98347	0.00126
0.1	20E876D82248	mlrrandnum_06_05	0.98256	0.00135	lrrandnum_06_05	0.98770	0.00124
0.1	3F6E65CA7440	mlrrandnum_06_06	0.98093	0.00127	lrrandnum_06_06	0.98734	0.00140
0.1	479D21DB7509	mlrrandnum_06_07	0.97959	0.00127	lrrandnum_06_07	0.98417	0.00133
0.1	55D4371D3A23	mlrrandnum_06_08	0.98033	0.00111	lrrandnum_06_08	0.98712	0.00136
0.1	6E1A14672B8F	mlrrandnum_06_09	0.97940	0.00117	lrrandnum_06_09	0.98533	0.00142
0.1	77A0308C0E44	mlrrandnum_06_10	0.98318	0.00134	lrrandnum_06_10	0.98412	0.00116
0.3	109E77866CF6	mlrrandnum_08_01	0.93254	0.00147	lrrandnum_08_01	0.93910	0.00146
0.3	16AA4A58735C	mlrrandnum_08_02	0.93186	0.00142	lrrandnum_08_02	0.93757	0.00117
0.3	1814171B652A	mlrrandnum_08_03	0.93200	0.00135	lrrandnum_08_03	0.93940	0.00146
0.3	1A423B9472C7	mlrrandnum_08_04	0.93197	0.00150	lrrandnum_08_04	0.93676	0.00130
0.3	20E876D82248	mlrrandnum_08_05	0.93601	0.00124	lrrandnum_08_05	0.93851	0.00111
0.3	3F6E65CA7440	mlrrandnum_08_06	0.93249	0.00118	lrrandnum_08_06	0.93914	0.00149
0.3	479D21DB7509	mlrrandnum_08_07	0.93299	0.00128	lrrandnum_08_07	0.94011	0.00131
0.3	55D4371D3A23	mlrrandnum_08_08	0.93500	0.00133	lrrandnum_08_08	0.93900	0.00139
0.3	6E1A14672B8F	mlrrandnum_08_09	0.93201	0.00122	lrrandnum_08_09	0.93781	0.00117
0.3	77A0308C0E44	mlrrandnum_08_10	0.93238	0.00153	lrrandnum_08_10	0.93965	0.00118
1.0	109E77866CF6	mlrrandnum_15_01	0.93180	0.00126	lrrandnum_15_01	0.93344	0.00126
1.0	16AA4A58735C	mlrrandnum_15_02	0.93020	0.00159	lrrandnum_15_02	0.93281	0.00121
1.0	1814171B652A	mlrrandnum_15_03	0.92956	0.00117	lrrandnum_15_03	0.93468	0.00132
1.0	1A423B9472C7	mlrrandnum_15_04	0.92837	0.00165	lrrandnum_15_04	0.93592	0.00126
1.0	20E876D82248	mlrrandnum_15_05	0.93220	0.00120	lrrandnum_15_05	0.93251	0.00143
1.0	3F6E65CA7440	mlrrandnum_15_06	0.93177	0.00141	lrrandnum_15_06	0.93374	0.00121
1.0	479D21DB7509	mlrrandnum_15_07	0.93217	0.00144	lrrandnum_15_07	0.93572	0.00138
1.0	55D4371D3A23	mlrrandnum_15_08	0.92921	0.00125	lrrandnum_15_08	0.93498	0.00145
1.0	6E1A14672B8F	mlrrandnum_15_09	0.92980	0.00177	lrrandnum_15_09	0.93224	0.00114
1.0	77A0308C0E44	mlrrandnum_15_10	0.93070	0.00126	lrrandnum_15_10	0.93158	0.00131

Table 6.9.2.2-3.Neutron multiplication factors with standard deviations for the ES-3100 package models at the "MR" and "LR" node points

moifr	Random Number	"A" cases	k_{eff}	s	"B" cases	k_{eff}	s
1.0e-20	109E77866CF6	mrandnum_01_01	1.04965	0.00119	lrrandnum_01_01	1.05093	0.00133
1.0e-20	16AA4A58735C	mrandnum_01_02	1.05132	0.00131	lrrandnum_01_02	1.05009	0.00118
1.0e-20	1814171B652A	mrandnum_01_03	1.05368	0.00123	lrrandnum_01_03	1.05057	0.00118
1.0e-20	1A423B9472C7	mrandnum_01_04	1.05165	0.00145	lrrandnum_01_04	1.05066	0.00120
1.0e-20	20E876D82248	mrandnum_01_05	1.05344	0.00106	lrrandnum_01_05	1.04882	0.00129
1.0e-20	3F6E65CA7440	mrandnum_01_06	1.05188	0.00157	lrrandnum_01_06	1.05316	0.00127
1.0e-20	479D21DB7509	mrandnum_01_07	1.05149	0.00148	lrrandnum_01_07	1.05229	0.00134
1.0e-20	55D4371D3A23	mrandnum_01_08	1.05083	0.00113	lrrandnum_01_08	1.05186	0.00131
1.0e-20	6E1A14672B8F	mrandnum_01_09	1.04910	0.00106	lrrandnum_01_09	1.05236	0.00113
1.0e-20	77A0308C0E44	mrandnum_01_10	1.05254	0.00106	lrrandnum_01_10	1.05098	0.00120
1.0e-04	109E77866CF6	mrandnum_03_01	1.04994	0.00132	lrrandnum_03_01	1.05122	0.00123
1.0e-04	16AA4A58735C	mrandnum_03_02	1.05023	0.00118	lrrandnum_03_02	1.05324	0.00121
1.0e-04	1814171B652A	mrandnum_03_03	1.05090	0.00139	lrrandnum_03_03	1.05143	0.00123
1.0e-04	1A423B9472C7	mrandnum_03_04	1.05072	0.00115	lrrandnum_03_04	1.05048	0.00121
1.0e-04	20E876D82248	mrandnum_03_05	1.05052	0.00119	lrrandnum_03_05	1.05095	0.00137
1.0e-04	3F6E65CA7440	mrandnum_03_06	1.05383	0.00131	lrrandnum_03_06	1.05029	0.00119
1.0e-04	479D21DB7509	mrandnum_03_07	1.05205	0.00153	lrrandnum_03_07	1.05124	0.00108
1.0e-04	55D4371D3A23	mrandnum_03_08	1.05343	0.00106	lrrandnum_03_08	1.05080	0.00116
1.0e-04	6E1A14672B8F	mrandnum_03_09	1.04831	0.00132	lrrandnum_03_09	1.05074	0.00122
1.0e-04	77A0308C0E44	mrandnum_03_10	1.05353	0.00111	lrrandnum_03_10	1.05094	0.00111
0.10	109E77866CF6	mrandnum_06_01	0.97948	0.00120	lrrandnum_06_01	0.98315	0.00118
0.10	16AA4A58735C	mrandnum_06_02	0.98104	0.00125	lrrandnum_06_02	0.98605	0.00124
0.10	1814171B652A	mrandnum_06_03	0.98056	0.00134	lrrandnum_06_03	0.98690	0.00120
0.10	1A423B9472C7	mrandnum_06_04	0.97895	0.00114	lrrandnum_06_04	0.98347	0.00126
0.10	20E876D82248	mrandnum_06_05	0.98058	0.00113	lrrandnum_06_05	0.98770	0.00124
0.10	3F6E65CA7440	mrandnum_06_06	0.97966	0.00119	lrrandnum_06_06	0.98734	0.00140
0.10	479D21DB7509	mrandnum_06_07	0.97953	0.00145	lrrandnum_06_07	0.98417	0.00133
0.10	55D4371D3A23	mrandnum_06_08	0.97993	0.00130	lrrandnum_06_08	0.98712	0.00136
0.10	6E1A14672B8F	mrandnum_06_09	0.97972	0.00138	lrrandnum_06_09	0.98533	0.00142
0.10	77A0308C0E44	mrandnum_06_10	0.98157	0.00134	lrrandnum_06_10	0.98412	0.00116
0.30	109E77866CF6	mrandnum_08_01	0.93412	0.00118	lrrandnum_08_01	0.93910	0.00146
0.30	16AA4A58735C	mrandnum_08_02	0.93227	0.00138	lrrandnum_08_02	0.93757	0.00117
0.30	1814171B652A	mrandnum_08_03	0.93390	0.00131	lrrandnum_08_03	0.93940	0.00146
0.30	1A423B9472C7	mrandnum_08_04	0.93252	0.00144	lrrandnum_08_04	0.93676	0.00130
0.30	20E876D82248	mrandnum_08_05	0.93334	0.00132	lrrandnum_08_05	0.93851	0.00111
0.30	3F6E65CA7440	mrandnum_08_06	0.93168	0.00132	lrrandnum_08_06	0.93914	0.00149
0.30	479D21DB7509	mrandnum_08_07	0.93514	0.00123	lrrandnum_08_07	0.94011	0.00131
0.30	55D4371D3A23	mrandnum_08_08	0.93564	0.00132	lrrandnum_08_08	0.93900	0.00139
0.30	6E1A14672B8F	mrandnum_08_09	0.93597	0.00136	lrrandnum_08_09	0.93781	0.00117
0.30	77A0308C0E44	mrandnum_08_10	0.93525	0.00128	lrrandnum_08_10	0.93965	0.00118

Table 6.9.2.2-3.Neutron multiplication factors with standard deviations for the ES-3100 package models at the "MR" and "LR" node points

moifr	Random Number	"A" cases	k_{eff}	s	"B" cases	k_{eff}	s
1.00	109E77866CF6	mrandnum_15_01	0.93103	0.00139	lrrandnum_15_01	0.93344	0.00126
1.00	16AA4A58735C	mrandnum_15_02	0.93082	0.00131	lrrandnum_15_02	0.93281	0.00121
1.00	1814171B652A	mrandnum_15_03	0.92890	0.00148	lrrandnum_15_03	0.93468	0.00132
1.00	1A423B9472C7	mrandnum_15_04	0.93062	0.00145	lrrandnum_15_04	0.93592	0.00126
1.00	20E876D82248	mrandnum_15_05	0.93055	0.00125	lrrandnum_15_05	0.93251	0.00143
1.00	3F6E65CA7440	mrandnum_15_06	0.92950	0.00117	lrrandnum_15_06	0.93374	0.00121
1.00	479D21DB7509	mrandnum_15_07	0.92952	0.00116	lrrandnum_15_07	0.93572	0.00138
1.00	55D4371D3A23	mrandnum_15_08	0.92805	0.00154	lrrandnum_15_08	0.93498	0.00145
1.00	6E1A14672B8F	mrandnum_15_09	0.93117	0.00140	lrrandnum_15_09	0.93224	0.00114
1.00	77A0308C0E44	mrandnum_15_10	0.93218	0.00120	lrrandnum_15_10	0.93158	0.00131

6.9.2.3 STATISTICAL EVALUATION

An evaluation of KENO V.a calculation results is made to determine if there is a statistically significant difference between the mean k_{eff} for the "MR" and "MLR" models, for the "MLR" and "LR" models, and for the "MR" and "LR" models. Cases are classified into five groups based on the amount of water assumed to be present in the shipping package. The symbol "I" is used to specify the case. The mean difference and standard deviation for each of the five sets of pair-wise differences are defined as follows:

(a) $d_i = (k_{effBi} - k_{effAi})/n$ and
(b) $s_{di} = \sqrt{[\,[\,n\Sigma d_i^{\,2} - (\,\Sigma d_i\,)^2\,] / n(n-1)\,]}$ (conservatively defined for the t-test appropriate for small sample sizes),

where A_i and B_i denote the model types, and n denotes the sample size of ten. It is reasonable to assume that the paired differences have been randomly selected from a normally distributed population of paired differences with mean (μ_d) and standard deviation (σ_d), then the sampling distribution of

$$(d - \mu_d) / (s_d/\sqrt{n})$$

is a *t* distribution having n-1 degrees of freedom.

The evaluation of the mean differences (d_i) for the 10 sets of cases is accomplished through hypothesis testing, a statistical tool used to provide evidence that a difference exists or does not exist. The t_i values are given in Table 6.9.2.3-1. A value of 3.25 is obtained from the standard table for critical values for the t distribution from which the decision to accept or reject the null hypothesis H_0 is made with a Type I error probability (α) of 0.01.

For $|t| < 3.25$, the H_0 hypothesis is not rejected. Acceptance of the null hypothesis is the result of insufficient evidence to reject it. Thus, it can be concluded that the mean estimates of the difference in k_{eff} between the "MR" and "MLR" calculation models, between the "MLR" and "LR" calculation models, and between the "MR" and "LR" calculation models are not statistically significant for the dry condition where neutronic interaction between packages is significant. Also, the mean estimate of the difference in k_{eff} between the "MR" and "MLR" calculation models is not statistically significant for wet or flooded conditions where the packages of the array become isolated.

Table 6.9.2.3-1. T-test values for establishing the statistical significance of the differences in calculated k_{eff} values for the ES-3100 package models at the "MR," "MLR," and "LR" node points

moifr	"MR" cases (k_{eff})	"MLR" cases (k_{eff})	d_i	S_{di}	t[a]
1.0E-20	1.05154	1.05075	0.00089	1.58991e-03	1.77
1.0E-04	1.05146	1.05165	-0.00019	2.17840e-03	-0.28
0.1	0.98008	0.98091	-0.00087	1.33870e-03	-2.06
0.3	0.93404	0.93300	0.00106	1.88912e-03	1.77
1.0	0.93030	0.93067	-0.00034	1.68664e-03	-0.65
moifr	**"MLR" cases (k_{eff})**	**"LR" cases (k_{eff})**	**d_i**	**S_{di}**	**t**
1.0E-20	1.05075	1.05116	-0.00050	1.92087e-03	-0.83
1.0E-04	1.05165	1.05113	0.00041	9.36819e-04	1.38
0.1	0.98091	0.98546	-0.00456	2.28535e-03	-6.31
0.3	0.93300	0.93863	-0.00578	1.59574e-03	-11.45
1.0	0.93067	0.93369	-0.00318	2.30797e-03	-4.36
moifr	**"MR" cases (k_{eff})**	**"LR" cases (k_{eff})**	**d_i**	**S_{di}**	**t**
1.0E-20	1.05154	1.05116	0.00039	2.35840e-03	0.52
1.0E-04	1.05146	1.05113	0.00021	2.19813e-03	0.31
0.10	0.98008	0.98546	-0.00543	1.66324e-03	-10.33
0.30	0.93404	0.93863	-0.00472	1.46294e-03	-10.21
1.00	0.93030	0.93369	-0.00353	2.50750e-03	-4.45

[a] critical value = 3.25 for 10 cases.

For $|t| > 3.25$, the H_0 hypothesis is rejected. Therefore, it can be concluded that the mean estimate of the difference in k_{eff} between the "MLR" and "LR" calculation models, and between the "MR" and "LR" calculation models, is statistically significant for wet or flooded conditions where the packages of the array become isolated. The negative t-values indicate that the calculated k_{eff} value for the "LR" model is slightly higher than for the "MR" and "MLR" models. This result is consistent with an expected increase in k_{eff} due to "tighter or closer" water reflector surrounding the package content.

Although flattening of the side of the package represents a reduction in the diameter of the drum, the points at which minimum flattening occurs provide an indication of the reduction of lattice spacing between packages of an array under HAC. The composite of the minimum deformation points at perpendicular axes (90–270° and 0–180°) represents the modified lattice spacing in an array of ES-3100 packages. As illustrated in Table 6.9.2.3-2, the equivalent diameter of the package for "composite" lattice spacing is not significantly different from the 18.37-in. diameter of the pre-test package. Even though significant crushing of the drum midsection and bottom occurs, the effective center-to-center spacing of the contents actually increases under HAC. Selective rearrangement of alternating packages would be required to achieve a more compact array; however, this event is not credible.

As described in Sect. 6.3.1.2, a close-pack (triangular-pitch) array of packages would be represented by a reduced package in a rectangular-pitch configuration. For HAC, the 17.26-in. reduced diameter for the "composite close-pack" package is slightly larger than the 17.20-in. diameter of the "MLR" calculation model used in the HAC calculations of Sect. 6.6. Therefore, packages evaluated with the "MLR" calculation model of packages in a rectangular-pitch configuration are deemed adequate for the HAC criticality evaluation. Considering both the irregular shape of the deformed drums and that array spacing is determined by overall (maximum) dimensions rather than by mean or minimum dimensions of a damaged package, the use of the "MLR" model for representing the ES-3100 package under HAC is conservative and bounding.

Table 6.9.2.3-2. Deformation of the ES-3100 drum projected by finite element analysis "Case 3100 RUN1HL Lower Bound Kaolite May 2004"

	FEA node	Diameter at 90^O (in.)	Diameter at 180^O (in.)	Equivalent circular diameter (in.)
Composite	103012/098194	22.00	15.60	18.56
Pre-test drum	-	18.37	18.37	
Pre-test, close-pack	-	17.08	17.08	
Composite, close-pack	103012/098194	-	-	17.26

THIS PAGE INTENTIONALLY LEFT BLANK.

Appendix 6.9.3

PACKAGE MATERIAL COMPOSITIONS

THIS PAGE INTENTIONALLY LEFT BLANK.

Appendix 6.9.3

PACKAGE MATERIAL COMPOSITIONS

Table 6.4 (Sect. 6.3.2) provides basic information for deriving the compositions for the ES-3100 package (Figs. 6.1 and 6.2). The atomic densities presented in Table 6.4 can be verified using additional information provided in Appendix 6.9.5. The following sections provide the rationale, the justification, or both for the material compositions used in the criticality calculations.

6.9.3.1 HEU AND UNIRRADIATED TRIGA CONTENTS

HEU considered for shipment in the ES-3100 is categorized into the following material forms: highly enriched uranium (HEU) solid or broken metal; HEU oxide; uranyl nitrate hexahydrate (UNH) crystals. In the interest of adding conservatism, uranium is modeled as ^{235}U and ^{238}U, while the ^{234}U and ^{236}U isotopes are excluded. Any positive change in neutron multiplication represented by the presence of the ^{234}U is covered by the higher than actual ^{235}U content. (Rothe et al. 1978) The theoretical density of 100 wt % ^{235}U HEU is 18.8111 g/cm^3. This value is determined by adjusting the density of natural uranium included in the SCALE Standard Composition Library with 100 wt % weight factors. The theoretical density of HEU oxide types are 10.96 g/cm^3 for UO_2, 8.30 g/cm^3 for U_3O_8, and 7.29 g/cm^3 for UO_3. The theoretical density of UNH crystals is 2.79 g/cm^3. Table 6.9.3.1-1 provides details of the calculated weight percentages input to KENO V.a calculated on the basis of the stoichiometric formula of $UO_2(NO_3)_2$+$6H_2O$ and crystalline density. The maximum enrichment considered in the analysis is 100 wt % ^{235}U, although actual material enrichments are lower. The unirradiated solid form TRIGA fuel is uranium zirconium hydride ($UZrH_x$) where "x" is ≤2, having a density of 8.65 g/cm^3.

Table 6.9.3.1-1. Calculation of constituent weight-percentage values for uranyl nitrate hexahydrate crystals used in KENO V.a calculation models

Avogadro No. (N_o)	6.0221370E+23					
UNH						
$UO_2(NO_3)_2$+$6H_2O$	Atoms/Molecule	At. wt [a]	Mole. wt.	wt %	calc. Ni	NiAi
Hydrogen	12	1.0078	12.0936	2.4233	4.0401e+22	4.0716e+22
Nitrogen	2	14.0031	28.0062	5.6117	6.7333e+21	9.4286e+22
Oxygen	14	15.9949	223.9286	44.8690	4.7132e+22	7.5388e+23
U-235		235.0441		100.0000		
U-238		238.0510		0.0000		
Uranium	1	235.0441	235.0441	47.0962	3.3666e+21	7.9130e+23
			499.0725	100.0002		
summations				100.0002	9.7633e+22	1.6802e+24
At. Wt. material						
assumed density	2.7900					
den.=($\sum N_iA_i$)/No						2.7900

[a] *Source*: *Nuclides and Isotopes*, 14th ed., General Electric Company, 1989.

HEU broken metal. The critical mass of fissile material is dependent on factors such as the form and shape of the material, bulk density if the material is broken into pieces, and the enrichment. Broken metal can be compared to the minimum critical mass of submerged metal lattices of regular-shaped fissile material. Using experimental data, the approximation of a heterogeneous mixture of fissile material and moderator to a homogenous mixture is justified as follows.

Figure 6.9.3.1-1 depicts the experimentally determined minimum critical mass of U (~ 94) lattices immersed in water as a function of the volume-to-surface area ratio of the fissile element. (TID-7028). The critical mass is shown to increase from 850 g to 21 kg over the range of volume-to-surface ratios from 0 to 0.18 in. The critical mass is nearly constant in the range of volume-to-surface ratios from 0.18 to 0.8 in. For pieces greater than 1-in. cubes, the minimum critical mass will not be less than 21 kg. For smaller pieces, the minimum critical mass is a nearly linear function of the volume-to-surface-area ratio of the fissile element.

Figure 6.9.3.1-2 depicts the experimentally determined minimum critical mass of U (~ 94) metal water and solution systems as a function of the concentration of ^{235}U. The figure with added data reveals that: (1) a minimum critical mass exists for each metal lattice system plotted, and (2) as the bulk density of uranium or the uranium concentration increases, the curves for the critical mass of metal lattice systems converge with the curve for highly enriched solution experiments or the curve for calculated homogenous metal water mixtures. Conversely stated, the critical mass is greater for a heterogenous system than for a homogenous system, and this difference increases as the H/X ratio increases. Therefore, the practice of approximating a heterogeneous mixture of fissile material and moderator as a homogenous mixture is justifiable and also conservative at the higher H/X ratios.

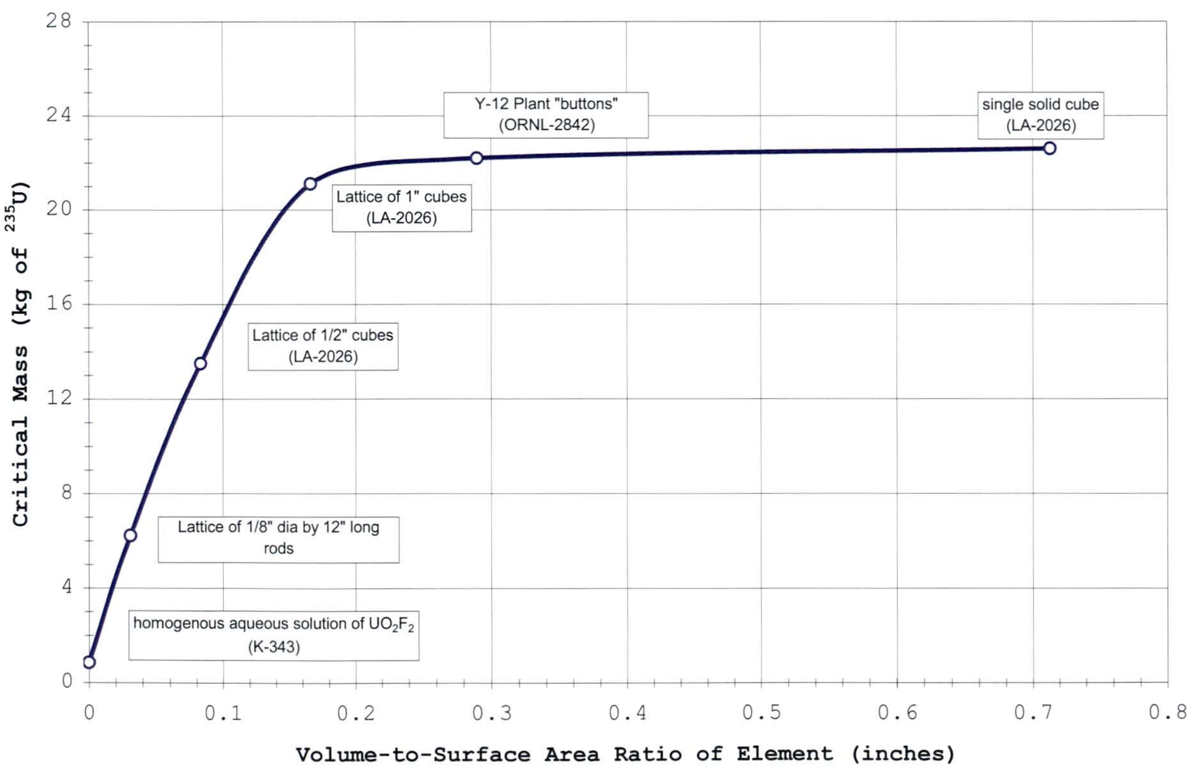

Fig. 6.9.3.1-1. Experimentally determined minimum critical mass U(~94) metal lattices immersed in water as a function of volume-to-surface area ratio of fissile material. *Source*: H. C. Paxton et al., *Critical Dimensions of Systems Containing 235U,* TID-7028, Los Alamos Scientific Lab. and Oak Ridge Natl. Lab., June 1964, Fig. 19. Y-12 data have been added.

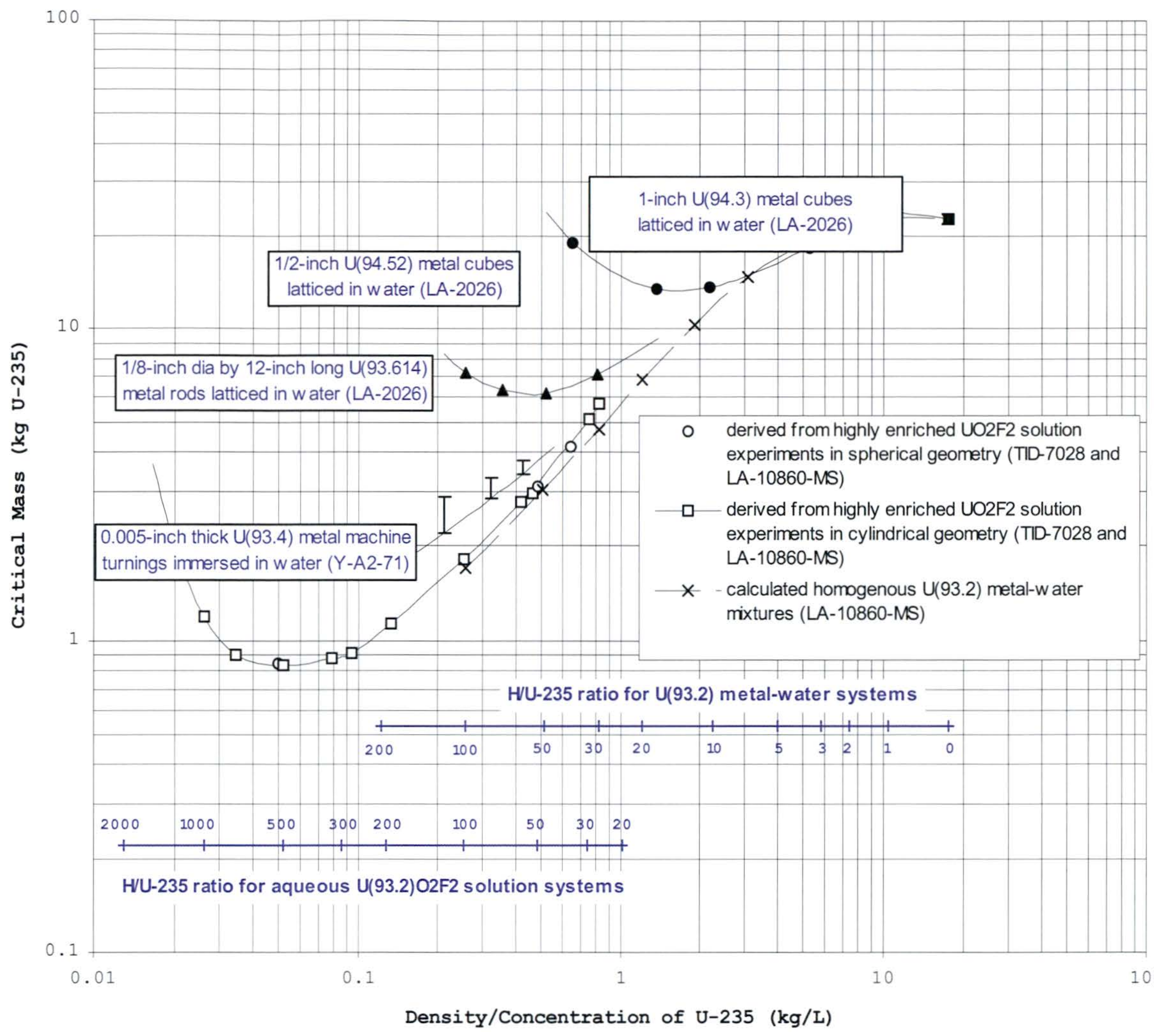

Fig. 6.9.3.1-2. Experimentally determined minimum critical mass of U(~94) metal water and solution systems as a function of the concentration of ^{235}U. *Sources*: A. W. Krass, *Survey of Experimental Data Concerning the Critical Mass of Highly Enriched Uranium–Water Systems*, CCG-365, Lockheed Martin Energy systems, Inc., Oak Ridge Y-12 Plant, July 13, 2000, Fig. 1. Y-12 data added.

Approximating broken metal as a homogenous mixture of uranium and water requires a defined space within which masses of the components are conserved. This space is generally characterized by a lattice constructed of unit cells and defined by the dimensions of the fissile material being approximated.

The broken HEU metal consists of large, irregular pieces ranging from 0.5 in. to several inches on a side as shown in Fig. 6.9.3.1-3. A lattice of cubes is chosen to represent broken metal inside the ES-3100 containment vessel. Due to the constraints of KENO V.a, an idealized configuration is defined by a square lattice circumscribed by the inner wall of the containment vessel. Water fills the truncated cylindrical regions between the inner wall of the containment vessel and the vertical faces of the lattice. Two additional models are developed to evaluate conservatism at various stages of model approximations for broken metal.

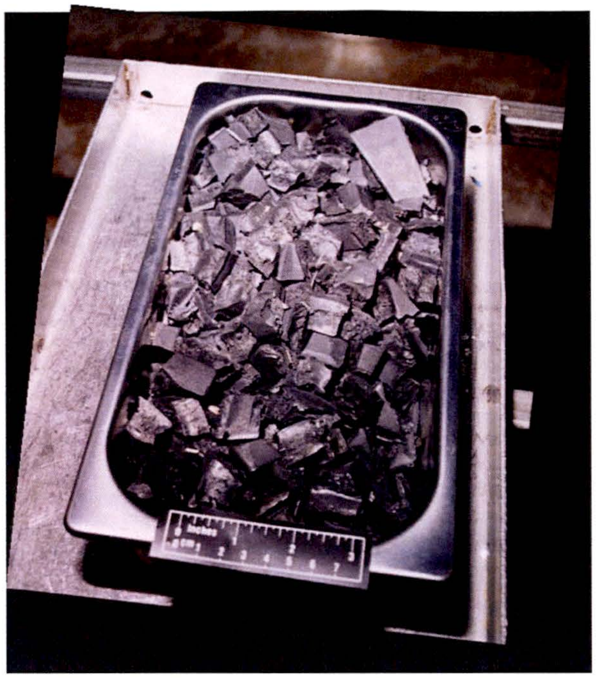

Fig. 6.9.3.1-3. Pan of HEU broken metal.

Together, these models include an explicit arrangement of HEU metal cubes forming a compact rectangular lattice inside the containment vessel, HEU metal homogeneously mixed with water within the rectangular lattice formed by the unit cells, and HEU metal homogeneously mixed with water within the volume of the containment vessel.

Parameters varied in each of these three models include (1) the cube size in the explicit model from 1.0 in. to 0.25 in. on a side, (2) water moderation inside the containment vessel from dry to the fully flooded condition, (3) enrichment from 100.0 wt % ^{235}U to 20.0 wt % ^{235}U, (4) thickness of the 277-4 canned spacers located between each convenience can, and (5) the mass of the uranium metal at each content location. One-quarter inch, 0.5-in., and 1.0-in. cubes are selected to evaluate "approach-to-homogeneity" of broken metal in this idealized form. The corresponding array configurations for 0.25-in., 0.5-in., and 1.0-in. cubes are $12 \times 12 \times N$, $6 \times 6 \times N$, and $3 \times 3 \times N$. The N-th layer of unit cells for a given mass loading may not all contain HEU metal; the empty cells are filled with water. Nevertheless, a slight variation still arises in the total mass of HEU metal between these array configurations given whole cubes are contained in the calculation models.

The results for the calculation models representing the various configurations of broken uranium metal are shown in the Table 6.9.3.1-2. As the explicitly modeled cubes become smaller in size, the calculated k_{eff} values for the explicit "sqa" models approach values for the "lha" models where HEU metal cubes are homogenized with water within the rectangular lattice formed by the unit cells of the array. A representative or converged k_{eff} value is 0.87 for increasing by smaller cubes based on calculation results for the "lha" models. The "lha" results indicate a slight difference between the k_{eff} values for the three array sizes; these differences are attributed to the difference in the HEU for the arrays of whole cubes.

Table 6.9.3.1-2. Summary for evaluation of HEU broken metal models (95 wt % ^{235}U) in a flooded containment vessel, 1.4-in. canned spacers and full water reflection of containment vessel

Array type	U (g)	^{235}U (g)	H_2O (g)	h/x	k_{eff}	σ	$k_{eff} + 2σ$
discrete array of cubes ("sqa" cases)							
3 × 3 × *n*	35,164	33,406	7,719	6.03	0.8352	0.0012	0.84
6 × 6 × *n*	35,973	34,175	7,676	5.86	0.8559	0.0011	0.86
12 × 12 × *n*	35,988	34,188	7,765	5.86	0.8603	0.0012	0.86
cubes homogenized within footprint of lattice ("lha" cases)							
3 × 3 × *n*	35,164	33,406	7,719	6.03	0.8586	0.0011	0.86
6 × 6 × *n*	35,988	34,188	7,675	5.86	0.8650	0.0012	0.87
12 × 12 × *n*	35,988	34,188	7,675	5.86	0.8677	0.0010	0.87
cubes homogenized within containment vessel ("cha" cases)							
3 × 3 × *n*	35,164	33,406	7,719	6.03	0.9427	0.0013	0.95
6 × 6 × *n*	35,973	34,175	7,676	5.86	0.9495	0.0015	0.95
12 × 12 × *n*	35,988	34,188	7,675	5.86	0.9517	0.0016	0.95

Calculation results for the "cha" models, where arrays of cubes are fully homogenized with the water for the flooded containment vessel, indicate the highest k_{eff} values. The neutron multiplication factor jumps from 0.87 to 0.95. This model is deemed to be overly conservative when applied to broken metal for the following reasons.

- HEU metal does not dissolve in water.
- HEU metal is not in an oxide or powder form that will absorb moisture or readily mix and become homogenized with the water inside the flooded containment vessel.
- Because HEU metal is much denser than water, it will not float and become distributed throughout a flooded containment vessel; instead it will gravitate toward the bottom of the containment vessel.

The calculation results for the homogeneous mixture model of HEU metal and water within a rectangular lattice bound results for the explicit model. Also, the homogenization over the entire volume of the containment vessel is deemed overly conservative. For these reasons, the "lha" model is chosen to represent HEU broken metal inside the flooded containment vessel under full water reflection. For conservatism, the "cha" model is chosen to represent broken metal in single packages and the array of packages under NCT and HAC. Details regarding the "sqa", "lha", and "cha" calculation models are presented in Appendix 6.9.1.

<u>HEU Oxide.</u> Theoretical (crystalline) densities for HEU oxide are 10.96 g/cm^3, 8.30 g/cm^3, and 7.29 g/cm^3 for UO_2, U_3O_8, and UO_3, respectively. While bulk densities of product oxides with enrichments ranging from 19 to 100 wt % ^{235}U are typically on the order of 6.54 g/cm^3, the bulk density of HEU oxides considered for shipment in the ES-3100 ranges from 2.0 to 6.54 g/cm^3. Therefore, only less-than-theoretical mass loadings would actually be achieved. Skull oxides are a mixture of graphite and U_3O_8 with densities on the order of 2.44 g/cm^3 for poured material and 2.78 g/cm^3 for tapped material. The combined water saturation and crystallization of the HEU oxide are not expected in the HAC, given that UO_2 and UO_3 are non-hygroscopic while U_3O_8 is only mildly hygroscopic. Table 6.9.3.1-3 provides summary data for 292 samples of canned skull oxide.

Table 6.9.3.1-3. Summary data for 292 samples of skull oxide

Statistic	wt % U	wt % ^{235}U	µg C/g U	µg C /g ^{235}U	Net Wt (g)	U Wt (g)	^{235}U Wt (g)
Maximum	84.52	93.19	171,000	252,861	**7,072**	5,938	4,165
Minimum	12.93	20.28	13	17	442	312	221
Median	81.66	37.62	5,590	13,910	4,448	3,541	1,414
Mean	79.64	45.02	16,968	41,333	4,419	3,532	1,563
Std Dev	6.87	16.40	24,304	59,027	745	698	606

Values of wt % U, wt % ^{235}U, µg C/g U, etc. for a given statistic (maximum, minimum, medium, or mean) do not occur simultaneously in a specific sample. Inspection of sample data reveals the following characteristics:

(1) the fissile material content is ≤221 g ^{235}U in samples with concentrations up to 252,861 µg C/g^{235}U,
(2) the enrichment is 93.2 wt % ^{235}U for samples with concentrations in the range of 12,600 to 18,600 µg C/gU,
(3) the enrichment ranges from 60 to 70.2 wt % ^{235}U for samples with concentrations in the range of 3,231 to 87,720 µg C/gU, and
(4) the enrichment ranges from 37 to 38 wt % ^{235}U for samples with concentrations in the range of 400 to 233,366 µg C/gU.

Eight skull oxide compositions representative of 292 samples of canned skull oxide were selected for establishing the bounding content calculation models. The skull oxide content is assumed to be U_3O_8 plus graphite, polyethylene, and unidentified material. Two additional compositions were derived for addressing skull oxides with an enrichment of 93.2 wt % ^{235}U where unidentified material is treated as ^{235}U and the carbon content is either maximized or minimized. Treatment of the unidentified material as fissile material in the criticality analysis assures that its presence in skull oxide does not increase reactivity beyond what is considered in the bounding analysis.

The composition of the skull oxide content is given in terms of the following parameters: the grams skull oxide content in a content can (**gramskul**), the content bulk density (**densoc**), the wt % uranium in skull oxide content (**wtpuskul**), the wt % ^{235}U in uranium (**wtpu25u**), and the grams of graphite in the content can (**gramg**). Values for the content specification parameters are provided in Table 6.9.3.1-3b.

Table 6.9.3.1-3b. Content specification parameters for skull oxide content

Content	gramskul (g)	densoc (g/cm^3)	wtpuskul (wt %)	wtpu25u (wt %)	gramg (g)
sk_01	3863	1.899	58.92	69.78	139
sk_02	4978	2.447	66.15	69.42	168
sk_03	4607	1.981	72.77	69.88	124
sk_04	5082	2.186	82.77	70.07	20
sk_05	7072	3.042	83.97	69.91	9
sk_06	5037	2.476	72.53	37.61	307
sk_07	4385	2.156	75.15	37.55	203
sk_08	4550	2.237	72.57	37.73	87
sk_09	7100	3.054	78.95	93.20	307
sk_10	7100	3.054	82.61	93.20	1.0E-05

The information in Table 6.9.3.1-3c is derived from the content specification parameters of Table 6.9.3.1-3b on the assumption that 513 g of polyethylene is present in the skull oxide content in three content locations inside the containment vessel.

The amount of skull oxide content (Column 2, Table 6.9.3.1-3c) is **gsoc** = 3.0 × **gramskul**.

The amount of uranium in the skull oxide content (Column 6, Table 6.9.3.1-3c) is **gusoc** = **gsoc** × **wtpuskul** / 100.0.

The amount of ^{235}U (Column 7, Table 6.9.3.1-3c) is **gr235** = **gusoc** × **wtpu25u** / 100.0.

The amount of graphite in the skull oxide content (Column 8, Table 6.9.3.1-3c) is **ggsoc** = 3.0 × **gramg**.

The micrograms graphite per gram uranium in skull oxide content (Column 9, Table 6.9.3.1-3c) is **mggraphgu** = **ggsoc** × 1.0e6 / **gusoc**.

The amount of U_3O_8 in the skull oxide content (**guox**) [Column 3, Table 6.9.3.1-3c] is **guox** = **gusoc** / **wtpuuox**,

where **gusoc** (Column 6, Table 6.9.3.1-3c),
wtpuuox is the weight percent uranium in uranium oxide, and
wtpuuox = **mwu** / (**mwu** + **mwo**),

where **mwu** = (3){(235.0441 × wtpu25u) + [238.0510 × (100 − wtpu25u)]} /100.0 and
mwo = (8)(15.9949).

The amount of unidentified material in skull oxide content (**gramunid**) [Column 12, Table 6.9.3.1-3c] is **gramunid** = (**gsoc** − **guox** − **ggsoc** − **grampoly**)

Skull oxide content is assumed to be saturated with water. The amount of saturation moisture (**gmsatm**) [Column 4, Table 6.9.3.1-3c] is **gmsatm** = 0.9982 × **volsatm**,

where **volsatm** is the volume of saturation moisture in the skull oxide content and
volsatm = **vsox** − **volminsox**

The volume of skull oxide (**vsox**) in the containment vessel is **vsox** = (**gsoc** / **densoc**) − (**grampoly** / **denpoly**),

where **gsoc** (Column 2, Table 6.9.3.1-3c),
densoc is the bulk density of skull oxide content,
grampoly is the 513 g of polyethylene, and
denpoly is the density of polyethylene, 0.92 g/cm^3.

The minimum volume of skull oxide (**volminsox**) in the containment vessel is **volminsox** = (**gsoc** − **grampoly** − **gramunid**) / **dnsoxtheo**,

where **gsoc** (column 2, Table 6.9.3.1-3c),
grampoly (513 g),
gramunid (column 12, Table 6.9.3.1-3c), and
dnsoxtheo is the theoretical density of skull oxide.

Table 6.9.3.1-3c. Canned skull oxide (SO) content for ES-3100 calculation models, assuming 513 g polyethylene present and can spacers absent.

Content	SO (g)	UOx (g)	Sat. H_2O (g)	SO h/x	U (g)	^{235}U (g)	C (g)	μg C/ g ^{235}U	CV H_2O (g)	CV h/x	Unident (g)
sk_01	11,589	8,063	4,468	28.09	6,828	4,765	417	87,518	4,105	50.58	2,596[a]
sk_02	14,934	11,665	4,015	17.79	9,879	6,858	504	73,492	4,105	33.41	2,252[a]
sk_03	13,821	11,876	4,893	20.62	10,058	7,028	372	52,930	3,233	32.62	1,060[a]
sk_04	15,246	14,900	4,599	15.52	12,619	8,842	60	6,786	3,235	25.07	-227[b]
sk_05	21,216	21,036	3,869	9.49	17,815	12,455	27	2,168	3,235	16.27	-360[b]
sk_06	15,111	12,933	3,765	28.02	10,960	4,122	921	223,432	4,105	54.01	744[a]
sk_07	13,155	11,666	3,989	32.68	9,886	3,712	609	164,054	4,106	61.55	367[a]
sk_08	13,650	11,689	4,068	33.01	9,906	3,737	261	69,834	4,106	61.69	1,187[a]
sk_09	21,300	19,865	3,801	7.43	16,816	15,673	921	58,764	3,235	12.82	1
sk_10	21,300	20,786	3,905	7.27	17,596	16,399	0	0	3,235	12.41	1

[a] Positive value specifies grams of miscellaneous neutron absorber elements in content, modeled as water.
[b] Negative value specifies grams of excess polyethylene included in the content model.

The theoretical density of skull oxide (**dnsoxtheo**) is
dnsoxtheo = (**ggsoc** + **guox**) / [(**ggsoc** / **dnctheo**) + (**guox** / **dnuoxtheo**)],

where **ggsoc** (Column 8, Table 6.9.3.1-3c),
guox (Column 3, Table 6.9.3.1-3c),
dnuoxtheo is the theoretical density of U_3O_8, 8.3 g/cm^3, and
dnctheo is the theoretical density of graphite, 4.2 g/cm^3.

The hydrogen to fissile uranium ratio of canned skull (Column 5, Table 6.9.3.1-3c) is
sochtox = {[(**gmsatm** × **wtphwat**) + (**grampoly** × **wtphpoly**)] × **atwu25**} / (**gr235** × **atwth** × 100.0),

where **gmsatm** (column 4, Table 6.9.3.1-3c),
wtphwat is the weight percent hydrogen in water, 11.1913%,
grampoly (513 g),
wtphpoly is the weight percent hydrogen in polyethylene, 14.3811%,
atwu25 is the atomic weight of ^{235}U, 235.0441,
gr235 (column 7, Table 6.9.3.1-3c), and
atwth is the atomic weight of hydrogen, 1.0078.

The amount of water in the voided region of the CV (column 10, Table 6.9.3.1-3c) is
gwatcv = 0.9982 × **volvcv**,

where **volvcv** is the void volume of the CV and
volvcv = (**cvarea** × **cvih**) – (**gsoc** / **densoc**),

where **cvarea** is the internal area (129.73536 cm^2) of the CV,
cvih is the internal height (78.74 cm),
gsoc (column 2, Table 6.9.3.1-3c), and
densoc (Table 6.9.3.1-3b).

The hydrogen to fissile uranium ratio inside the containment vessel (Column 11, Table 6.9.3.1-3c) is
htox = ⟨{[(**gmsatm** + **gwatcv**) × **wtphwat**] + [**grampoly** × **wtphpoly**]} × **atwu25**⟩ / (**gr235** × **atwth** × 100.0),

where **gmsatm** (column 4, Table 6.9.3.1-3c),
gwatcv is the amount of water in the voided region of CV,
wtphwat is the weight percent hydrogen in water, 11.1913%,
grampoly (513 g),
wtphpoly is the weight percent hydrogen in polyethylene, 14.3811%,
atwu25 is the atomic weight of ^{235}U, 235.0441,
gr235 (Column 7, Table 6.9.3.1-3c), and
atwth is the atomic weight of hydrogen, 1.0078.

Unirradiated TRIGA reactor fuel. TRIGA fuel is uranium zirconium hydride ($UZrH_x$), an alloy of uranium metal homogeneously dispersed as fine particles in a zirconium hydride matrix. The fuel is stable because uranium hydride does not form to any considerable extent. Moreover, uranium hydride has never been detected in the photomicrographic evaluations of TRIGA fuel.

The General Atomics catalog of stock items lists approximately 40 TRIGA fuel elements classified into four basic types: standard element, instrumented element, fuel-follower control rod, or cluster assembly. The TRIGA element active fuel region consists of three 5-in long sections "fuel meats" of $UZrH_x$. The H/Z atom ratio "x" in $UZrH_x$ equals 1.6 in all cases except for two stock items. For these cases, x = equals 1.0 and the fissile content is < 40 g ^{235}U. The unirradiated solid form TRIGA fuel is identified as either 20 % enriched or 70 % enriched, and has dimensions and material properties specific to its design function. Table 1.4 provides a summary description.

The fuel diameter for the 20 % enriched TRIGA elements is either 1.44 in., 1.41 in., 1.40 in., 1.37 in., 1.34 in., or 1.31 in. The uranium composition of the fuel is 45 wt %, 30 wt %, 20 wt %, 12 wt %, and 8.5 wt %. As illustrated in Table 6.9.3.1.4-a, the TRIGA element with a maximum fissile content of 307 g ^{235}U in 1,560 g U, 45 wt% U in $UZrH_x$, and a H/Zr atom ratio of 1.6 has a computed fuel density of ~8.66 g/cm^3. The calculated number density (N_i) for each element or isotope is also given. The TRIGA fuel element with a fuel diameter of 1.44 inches contains 3,466.7 g $UZrH_x$. Further evaluation of the manufacturers data reveals that fuel density is proportional to the uranium weight fraction. Calculated density values are: 8.6597 g/cm^3 for 45 wt% U in $UZrH_x$, 6.8995 g/cm^3 for 30 wt% U in $UZrH_x$, 6.2825 g/cm^3 for 20 wt% U in $UZrH_x$, 5.9328 g/cm^3 for 12 wt% U in $UZrH_x$, and 5.7895 g/cm^3 for 8.5 wt% U in $UZrH_x$.

The active fuel diameter for 70 % enriched TRIGA fuel is 1.44 inches in both the standard element and instrumented element, and 1.31 inches in the fuel follower control rod. The uranium composition of the fuel is 8.5 wt %. The standard element and instrumented elements contain ~136 g ^{235}U in 194 g U while the fuel follower control rod contains ~113 g ^{235}U in 162 g U. As the calculation in Table 6.9.3.1.4-b illustrates, the 70 wt % enriched TRIGA fuel has a computed density of ~5.70 g/cm^3. The TRIGA fuel element with a fuel diameter of 1.44 inches contains 2,282.4 g $UZrH_x$ while the element with a fuel diameter of 1.31 inches contains 1,888.9 g $UZrH_x$.

The clad thickness is ~0.02 inches for a TRIGA fuel element with stainless steel cladding and ~0.03 inches for an element with aluminum cladding. In preparation for shipment in the ES-3100, a TRIGA fuel element is disassembled, the fuel meats are removed from the thin cladding and packed into convenience cans.

Table 6.9.3.1-4a. Calculation of constituent weight-percentage values for 20 wt % enriched uranium-zirconium hydride content in KENO V.a calculation models

Avogadro No. (N_o) =	6.0221370e+23						
$U(ZrH_x)$							
atom	**wt %**	**x**	**mass (g)**	**at. wt.**		**calc. N_i**	**N_iA_i**
Hydrogen	0.9554	1.6		1.00780	1.6125	4.9439E+22	4.9824E+22
Zirconium	54.0447	1		91.21960	91.2196	3.0897E+22	2.8184E+24
u-235	19.6795		307.0	235.04410			
u-238	80.3205			238.05099			
uranium	45.0000		1560.0	237.45318	75.9535	9.8830E+21	2.3468E+24
	100.0001				168.7856		
summations	100.0001					9.0219E+22	5.2150E+24
At. wt molecule							
Volume (cm^3)	400.3200						
Mass (g)	3466.66667						
density (g/cm^3)	8.65974						
den.=(∑NiAi)/No							8.6597

Table 6.9.3.1-4b. Calculation of constituent weight-percentage values for 70 wt % enriched uranium-zirconium hydride content in KENO V.a calculation models

Avogadro No. (N_o) =	6.0221370e+23						
$U(ZrH_x)$							
atom	**wt %**	**x**	**mass (g)**	**at. wt**		**calc. N_i**	**N_iA_i**
Hydrogen	1.5894	1.6		1.00780	1.6125	5.4148e+22	5.4571e+22
Zirconium	89.9107	1		91.21960	91.2196	3.3841e+22	3.0870e+24
u-235	70.1031		136.0	235.04410			
u-238	29.8969			238.05099			
uranium	8.5000		194.0	235.93508	8.6237	1.2370e+21	2.9184e+23
	100.0001				101.4558		
summations	100.0001					8.9227e+22	3.4334e+24
At. wt molecule							
Volume (cm^3)	400.3200						
Mass (g)	2282.35294						
density (g/cm^3)	5.70132						
den.=(∑NiAi)/No							5.7013

The TRIGA fuel may also be configured as clad fuel rods. Each clad fuel rod will be derived from a single TRIGA fuel element by removal of the stainless steel or aluminum clad extending beyond the plenum adjacent to the axial ends of the active fuel section. Each ~15 inch long rod consists of the 3 fuel pellets and an exterior sheath of stainless steel or aluminum clad, where the protruding clad at each end has been crimped in. The fuel rods will be packed into stainless steel or tin-plated carbon steel convenience cans, with a maximum of three fuel rods per loaded convenience can. This shipping configuration requires a minimum of two convenience cans; where only one convenience can is loaded with clad fuel rods. The loaded can is 17.5 inches tall while the empty one is 8.75 inches tall. Although can spacers are not required for criticality control, can spacers or stainless steel pads may be used to take up free volume over the 31 in. internal height of the containment vessel. The maximum quantity of fissile material per package is 408 g ^{235}U.

The clad fuel rod with 1.44 inch diameter fuel pellets contains 2,282.4 g $UZrH_x$ while rod with the 1.31 inch diameter fuel pellets contains 1,888.9 g $UZrH_x$. The 0.02 in thick sheath of stainless steel clad adds ~179 g to the mass of the active fuel for the 1.48 in. diameter standard element or instrumented element, and ~163 g to active fuel mass for the 1.35 in. diameter fuel follower control rod. Allowance for 1/2 in. of residual stainless steel crimped on each end of the clad fuel rod adds ~11 - 12 g stainless steel to these amounts. Likewise, the 0.03 in thick sheath of aluminum clad adds ~90 g to the mass of the active fuel for the 1.47 in. diameter standard element or instrumented element. Allowance for 1/2 in. of residual aluminum crimped on each end of the clad fuel rod adds ~6 g aluminum.

6.9.3.2 TYPE 304 STAINLESS STEEL

The metallic components of the ES-3100 package are composed of type 304 stainless steel. These include the containment vessel, the convenience cans, the drum liner, and the drum. Type 304 stainless steel with a density of 7.9400 g/cm^3 is included as a material in the SCALE Standard Composition Library.

6.9.3.3 277-4 NEUTRON ABSORBER

Catalog No. 277 dry mix is a proprietary mixture of Thermo Electron Corporation for producing a heat-resistant shielding material which combines the most effective shielding components into a single homogeneous composite. The shielding composite material is designed to maximize the hydrogen content necessary for thermalizing fast neutrons for capture in the boron constituent. Widely used in nuclear power plant applications, the heat-resistant shielding material is capable of retaining a significant portion of its shielding properties up to 230°C (450°F). The recommended operating limit is 350°F, which is well above HAC temperatures expected inside the body weldment liner inner cavity and canned spacers.

The 277-4 neutron absorber material used in the ES-3100 is a formulation of Cat 277-0 dry mix, a boron carbide additive, and water. 277-4 is produced through a quality-controlled batch process of dry blending, wet mixing, vibration casting, and timed cure. (Equipment Specification JS-YMN3-801580-A005, Appendix 1.4.5*)* "Loss On Drying" (LOD) tests are used to measure the amount of water in the as-manufactured 277-4 casting. The as-manufactured 277-4 at 100 lb/ft^3 and 31.8 % LOD has a hydrogen concentration of 3.56 wt % and a natural boron concentration of 4.359 wt %. (DAC-PKG-801624-A001, Table 5)

The ability of 277-4 to perform its function depends upon the masses of hydrogen and ^{10}B locked inside the high alumina borated cement cast into the body weldment liner inner cavity and the spacer

cans. A calculated amount of boron carbide is added to Cat 277-0 dry mix for producing as-manufactured 277-4 material with a volumetric isotopic concentration >7.621 × 10^{20} at/cm^3 of ^{10}B. The additive is boron carbide (B_4C) with small amount of a frit-like compound and trace amounts of unaccounted elements (0.17 wt %). Boron carbide has a theoretical density from 2.45 to 2.52 g/cm^3. The boron carbide grit partical sizes used are also small after passing through mesh sizes of 200 and 40 (63 to 355 μm). 277-4 contains a large amount of hydrated alumina, also known as aluminum trihydrate [$Al(OH)_3$]. It is a nonabrasive powder with a specific gravity of 2.42. Given that both materials are of like density and similar partial size, separation and in homogeneity of 277-4 material is not expected during the controlled vibration casting process.

Table 6.9.3.3-1 provides detailed elemental composition data derived for as-manufactured neutron absorber material at 100 lb/ft^3 and 31.8% LOD. This material description allows for clear specification of reduced boron and water contents required in the evaluation of NCT and HAC. As shown in Table 6.9.3.3-1, both the water and boron components are extracted from the material specification for the neutron absorber, and the constituent weight percents are recalculated accordingly (green box). 277-4 is specified in KENO V.a as three arbitrary materials: **arbmnpmx** with a density of 1.02276 g/cm^3, **arbmnph2o** with a density of 0.509253 g/cm^3, and **arbmboron** with a density of 6.98257e-02 g/cm^3. Model densities for 277-4 inside the body weldment liner inner cavity are reduced by a factor of 0.966893 to account for a material gap at the top of the liner. This material description allows for clear specification of reduced boron and water contents required in the evaluation of NCT and HAC.

The testing of 277-4 reveals that the material will dehydrate at elevated temperatures. Test specimens were dried at 250°F for 168 hours to reach the NCT state, and weight measurements were taken. These specimens where subsequently heated to 320°F for 4 hours to reach the HAC state, and weight measurements were again taken. The compositions of 277 at NCT and HAC states were derived by adjustment of the formulation specification for measured losses taking into account the statistical variations in the data. Conservation of mass for nonvolatile materials was observed in the derivation of material specifications based upon testing. Given that hydrogen must be present for the neutron absorber to be effective, conservative material specifications were derived for minimum hydrogen content and minimum material density.

Tables 6.9.3.3-2 and 6.9.3.3-3 respectively provide NCT and HAC composition data for as-manufactured 277-4 material at minimum density and hydrogen content. Respectively, Tables 6.9.3.3-4 and 6.9.3.3-5 provide NCT and HAC composition data or as-manufactured neutron absorber material at minimum density and boron content. Because the amount of ^{10}B present in the neutron absorber material is near saturation, a change in the hydrogen concentration has a major effect on the neutron multiplication factor, while a change in the amount of boron has a minor effect.

The neutron absorbing material used in the ES-3100 Shipping Package will perform as analyzed. The analysis of 277-4 with criticality calculations is adequate in lieu of neutron transmission testing for the demonstration of acceptable performance by experimental means. Criticality calculations show boron content is adequate and k_{eff} is not dependent on absolute (microscopic) homogeneity. Geometry characteristics of the ES-3100 system preclude the need for uniformity in boron areal density as a prerequisite for criticality safety control. The neutron absorbing material will be fabricated under strict quality control and accepted for use under an NQA-1 compliant quality assurance (QA) program. A QA-approved mixing process provides a method for creating an exact mix for the neutron absorber during ES-3100 fabrication. An important part of this QA-approved process is a 277-4 material verification and acceptance testing program. The following discussion elaborates on these key points:

Table 6.9.3.3-1. **Calculation of constituent weight-percentage values used in KENO V.a calculation models for as-manufactured 277-4 at minimum acceptable density and boron content** [a]

			arbmboron	arbmnpmx	arbmnph2o			arbmboron	arbmnpmx	arbmnph2o
31.8% LOD	**At. wt**	**lb/ft³**	**lb/ft³**	**lb/ft³**	**lb/ft³**		**NID**	**Wt %**	**Wt %**	**Wt %**
H	1.0078	3.5579			3.5579	**H**	1001			11.1913%
B10	10.0129	0.7911	0.7911			**B10**	5010	18.1482%		
B11	11.0093	3.5680	3.5680			**B11**	5011	81.8518%		
C	12.0000	1.2251		1.2251		**C**	6012		1.9187%	
N	14.0031	0.0090		0.0090		**N**	7014		0.0141%	
O	15.9949	55.9620		27.7281	28.2339	**O**	8016		43.4275%	88.8087%
Na	22.9895	0.0750		0.0750		**Na**	11023		0.1175%	
Mg	24.3051	0.2156		0.2156		**Mg**	12000		0.3377%	
Al	26.9818	24.9306		24.9306		**Al**	13027		39.0461%	
Si	28.0853	1.5752		1.5752		**Si**	14000		2.4671%	
S	32.0636	0.1969		0.1969		**S**	16000		0.3084%	
Ca	40.0803	7.5553		7.5553		**Ca**	20000		11.8331%	
Fe	55.8447	0.3383		0.3383		**Fe**	24000		0.5298%	
Totals		100.0000	4.3591	63.8491	31.7918			100.00%	100.00%	100.00%
H_2O	18.0105									
density (g/cm³)		1.601838e+00	6.982572e-02	1.022759e+00	5.092532e-01	spacer density (g/cm³)	1.601838e+00	6.98257e-02	1.02276e+00	5.09253e-01
						liner density (g/cm³)	1.548806e+00	6.75140e-02	9.88899e-01	4.92393e-01
						liner den. multiplier	0.966893			

a *Source*: G. A. Byington, *Mixing Weights and Elemental Composition of 277-4 Neutron Poison Used in the ES-3100*, DAC-PKG-801624-A001, BWXT Y-12, Y-12 National Security Complex, Jan. 25, 2006, Table 5.

Table 6.9.3.3-2. Calculation of constituent weight-percentage values used in KENO V.a calculation models for NCT as-manufactured 277-4 at minimum density and hydrogen content[a]

			arbmboron	arbmnpmx	arbmnph2o			arbmboron	arbmnpmx	arbmnph2o
	At. wt	lb/ft³	lb/ft³	lb/ft³	lb/ft³		NID	Wt %	Wt %	Wt %
H	1.0078	2.6840			2.6840	**H**	1001			11.1913%
B10	10.0129	0.8282	0.8282			**B10**	5010	18.1479%		
B11	11.0093	3.7354	3.7354			**B11**	5011	81.8520%		
C	12.0000	1.2826		1.2826		**C**	6012		1.9189%	
N	14.0031	0.0094		0.0094		**N**	7014		0.0141%	
O	15.9949	50.3252		29.0262		**O**	8016		43.4251%	
O	15.9949				21.2990	**O**	8016			88.8087%
Na	22.9895	0.0785		0.0785		**Na**	11023		0.1174%	
Mg	24.3051	0.2258		0.2258		**Mg**	12000		0.3378%	
Al	26.9818	26.1004		26.1004		**Al**	13027		39.0479%	
Si	28.0853	1.6491		1.6491		**Si**	14000		2.4672%	
S	32.0636	0.2061		0.2061		**S**	16000		0.3083%	
Ca	40.0803	7.9098		7.9098		**Ca**	20000		11.8336%	
Fe	55.8447	0.3541		0.3541		**Fe**	24000		0.5298%	
Totals		95.3886	4.5636	66.8420	23.9830			100.00%	100.00%	100.00%
H_2O	18.0105									
density (g/cm³)		1.527971e+00	7.310148e-02	1.070700e+00	3.841692e-01	spacer density (g/cm³)	1.527971e+00	7.31015e-02	1.07070e+00	3.84169e-01
						liner density (g/cm³)	1.477385e+00	7.06813e-02	1.03525e+00	3.71451e-01
						liner den. multiplier	0.966893			

a *Source*: G. A. Byington, *Mixing Weights and Elemental Composition of 277-4 Neutron Poison Used in the ES-3100*, DAC-PKG-801624-A001, BWXT Y-12, Y-12 National Security Complex, Jan. 25, 2006, Table 11.

Table 6.9.3.3-3. Calculation of constituent weight-percentage values used in KENO V.a calculation models for HAC as-manufactured 277-4 at minimum density and hydrogen content [a]

			arbmboron	arbmnpmx	arbmnph2o			arbmboron	arbmnpmx	arbmnph2o
	At. wt	lb/ft³	lb/ft³	lb/ft³	lb/ft³		NID	Wt %	Wt %	Wt %
H	1.0078	2.6758			2.6758	H	1001			11.1913%
B10	10.0129	0.8282	0.8282			N10	5010	18.1479%		
B11	11.0093	3.7354	3.7354			N11	5011	81.8520%		
C	12.0000	1.2826		1.2826		V	6012		1.9188%	
N	14.0031	0.0094		0.0094		N	7014		0.0141%	
O	15.9949	50.2605		29.0265		O	8016		43.4254%	
O	15.9949				21.2340	O	8016			88.8087%
Na	22.9895	0.0785		0.0785		Na	11023		0.1174%	
Mg	24.3051	0.2258		0.2258		Mg	12000		0.3378%	
Al	26.9818	26.1004		26.1004		Al	13027		39.0477%	
Si	28.0853	1.6491		1.6491		Si	14000		2.4671%	
S	32.0636	0.2061		0.2061		S	16000		0.3083%	
Ca	40.0803	7.9098		7.9098		Ca	20000		11.8335%	
Fe	55.8447	0.3541		0.3541		Fe	24000		0.5298%	
Totals		95.3157	4.5636	66.8423	23.9098			100.00%	100.00%	100.00%
H_2O	18.0105									
density (g/cm³)		1.52680e+00	7.31015e-02	1.07071e+00	3.82995e-01	spacer density (g/cm³)	1.52680e+00	7.31015e-02	1.07071e+00	3.82995e-01
						liner density (g/cm³)	1.47626e+00	7.06813e-02	1.03526e+00	3.70316e-01
						liner den. multiplier	0.966893			

a *Source*: G. A. Byington, *Mixing Weights and Elemental Composition of 277-4 Neutron Poison Used in the ES-3100*, DAC-PKG-801624-A001, BWXT Y-12, Y-12 National Security Complex, Jan. 25, 2006, Table 12.

Table 6.9.3.3-4. Calculation of constituent weight-percentage values used in KENO V.a calculation models for NCT as-manufactured 277-4 at minimum density and boron content[a]

			arbmboron	arbmnpmx	arbmnph2o			arbmboron	arbmnpmx	arbmnph2o
	At. wt	lb/ft^3	lb/ft^3	lb/ft^3	lb/ft^3		NID	Wt %	Wt %	Wt %
H	1.0078	2.9617			2.9617	**H**	1001			11.1913%
B10	10.0129	0.7911	0.7911			**B10**	5010	18.1482%		
B11	11.0093	3.5680	3.5680			**B11**	5011	81.8517%		
C	12.0000	1.2251		1.2251		**C**	6012		1.9188%	
N	14.0031	0.0090		0.0090		**N**	7014		0.0141%	
O	15.9949	51.2291		27.7264		**O**	8016		43.4260%	
O	15.9949				23.5027	**O**	8016			88.8087%
Na	22.9895	0.0750		0.0750		**Na**	11023		0.1175%	
Mg	24.3051	0.2156		0.2156		**Mg**	12000		0.3377%	
Al	26.9818	24.9306		24.9306		**Al**	13027		39.0472%	
Si	28.0853	1.5752		1.5752		**Si**	14000		2.4671%	
S	32.0636	0.1969		0.1969		**S**	16000		0.3084%	
Ca	40.0803	7.5553		7.5553		**Ca**	20000		11.8334%	
Fe	55.8447	0.3383		0.3383		**Fe**	24000		0.5299%	
Totals		94.6709	4.3591	63.8474	26.4644			100.00%	100.00%	100.00%
H_2O	18.0105									
density (g/cm^3)		1.516474e+00	6.982572e-02	1.022731e+00	4.239172e-01	spacer density (g/cm^3)	1.516474e+00	6.98257e-02	1.02273e+00	4.23917e-01
						liner density (g/cm^3)	1.466269e+00	6.75140e-02	9.88872e-01	4.09883e-01
						liner den. multiplier	0.966893			

a *Source*: G. A. Byington, *Mixing Weights and Elemental Composition of 277-4 Neutron Poison Used in the ES-3100*, DAC-PKG-801624-A001, BWXT Y-12, Y-12 National Security Complex, Jan. 25, 2006, Table 13.

Table 6.9.3.3-5. Calculation of constituent weight-percentage values used in KENO V.a calculation models for HAC as-manufactured 277-4 at minimum density and boron content[a]

			arbmboron	arbmnpmx	arbmnph2o			arbmboron	arbmnpmx	arbmnph2o
	At. wt	lb/ft³	lb/ft³	lb/ft³	lb/ft³		NID	Wt %	Wt %	Wt %
H	1.0078	2.9524			2.9524	**H**	1001			11.1913%
B10	10.0129	0.7911	0.7911			**B10**	5010	18.1482%		
B11	11.0093	3.5680	3.5680			**B11**	5011	81.8517%		
C	12.0000	1.2251		1.2251		**C**	6012		1.9188%	
N	14.0031	0.0090		0.0090		**N**	7014		0.0141%	
O	15.9949	51.1551		27.7262		**O**	8016		43.4258%	
O	15.9949				23.4289	**O**	8016			88.8087%
Na	22.9895	0.0750		0.0750		**Na**	11023		0.1175%	
Mg	24.3051	0.2156		0.2156		**Mg**	12000		0.3377%	
Al	26.9818	24.9306		24.9306		**Al**	13027		39.0473%	
Si	28.0853	1.5752		1.5752		**Si**	14000		2.4671%	
S	32.0636	0.1969		0.1969		**S**	16000		0.3084%	
Ca	40.0803	7.5553		7.5553		**Ca**	20000		11.8334%	
Fe	55.8447	0.3383		0.3383		**Fe**	24000		0.5299%	
Totals		94.5876	4.3591	63.8472	26.3813			100.00%	100.00%	100.00%
H_2O	18.0105									
density (g/cm³)		1.515140e+00	6.982572e-02	1.022728e+00	4.225861e-01	spacer density (g/cm³)	1.515140e+00	6.98257e-02	1.02273e+00	4.22586e-01
						liner density (g/cm³)	1.464979e+00	6.75140e-02	9.88869e-01	4.08596e-01
						liner den. multiplier	0.966893			

a *Source*: G. A. Byington, *Mixing Weights and Elemental Composition of 277-4 Neutron Poison Used in the ES-3100*, DAC-PKG-801624-A001, BWXT Y-12, Y-12 National Security Complex, Jan. 25, 2006, Table 14.

The analysis of 277-4 with criticality calculations is adequate in lieu of neutron transmission testing for the demonstration of acceptable performance. Early on in the licensing process, Borobond 4 was selected as the neutron absorber material for use in the ES-3100 package. The decision to use Borobond 4 in the ES-3100 was made because of favorable experience with its use in the Highly Enriched Uranium (HEU) Rackable Can Storage Box (RCSB), an element of the new state-of-the art HEU storage facility at the Y-12 National Security Complex (Y-12). From an economic standpoint, however, Borobond 4 proved not to be a viable option for the small quantities needed for the ES-3100 project. 277-4 neutron absorber material, which has very similar nuclear material properties to Borobond 4, was then selected as an alternative.

Both the RCSB and the ES-3100 are fast systems in the normal condition when the HEU fissile material is essentially unmoderated. A key factor for an effective neutron absorber is that hydrogen should be present for moderation, and it should be interspersed with boron-10 (^{10}B), thus promoting neutron capture. The potential for neutron streaming through an absorber is significant when a hydrogenous moderator is absent, as in the case of an aluminum boron-carbide matrix (a Boral alloy).

Borobond 4 is a ceramicrete material with slightly greater than 4 wt % boron carbide (B_4C). The boron carbide powder is micro encapsulated by the crystalline matrix of the ceramic; therefore, leaching out the boron is not feasible. In Borobond 4, 100 wt % of the B_4C has a particle size <500 μm; 90 wt % of the other constituents range from <164 μm to <36 μm. Given the differences in particle size, the potential for separation in the mixing process is real.

Some of the questions regarding the use of 277-4 as a neutron poison in the ES-3100 were previously addressed regarding the use of Borobond 4 in the RCSB. Radiography was performed on Borobond 4 samples ranging in thickness from 1.0 to 1.5 in. Inspections revealed little or no visual differences, indicating uniformity of the Borobond 4. For 277-4 where the B_4C grit is on the order of 200 μm, the potential for separation is reduced.

Measurements from neutron transmission tests on Borobond 4 for determination of areal density indicated greater boron content than was physically present. This is due to the presence of elements besides the aluminum and boron (principally hydrogen, oxygen and other low and intermediate-Z elements). From these measurements, credit for 90 wt % boron in a criticality calculation was established as an adequate adjustment. Given the similarity of 277-4 to Borobond 4 (a ceramic-cement composite shielding material, with a similar elemental composition, more uniform particle size, and the same boron content), the 75% credit for boron content applied in the ES-3100 criticality calculations is an adequate enough correction for the efficiency of the material.

Criticality calculations show boron content is adequate and k_{eff} is not dependent on absolute (microscopic) homogeneity. The boron concentration calculations presented here model an infinite array of ES-3100 packages with the boron concentration of Cat 277-4 uniformly varied inside the body weldment inner liner. While the Cat 277-4 described herein is an earlier formulation of the neutron absorber material, the behavior characteristics being demonstrated for Cat 277-4 apply to the revised formulation, 277-4.

Credit for only 75% of the boron is taken in the specification of Cat 277-4. Each package in the array contains 2.774 kg of ^{235}U in broken metal form uniformly distributed inside the containment vessel. The presence of just the hydrogenous cement matrix in the inner liner reduces k_{eff} to 1.132 from a value of 1.35 without the cement matrix. As an initial 1 wt % natural boron is added to the high alumina cement system (Table 6.9.3.3-6), the calculated k_{eff} based on 75% of the boron present drops significantly. Cat 277-4 with 4.2284 wt % natural boron in the minimum cast density of 100 lb/ft^3 (1.60 g/cc) has an acceptable mixture concentration, generating a k_{eff} of 0.88. The saturation value for boron content is reached at ~8 wt %. This near doubling of the boron content results in ~4% decrease in k_{eff} to an asymptotic value of ~0.85.

The density of Cat 277-4 is the sum of constituent densities: the boron density, the base-material density, and the water density. In the calculation model, the density of water in Cat 277-4 is 0.48210 g/cm^3 (not shown in Table 6.9.3.3-6). Canned spacers are omitted from the calculation model. Credit for only 75% of the boron is taken in each parametric calculation. The volume of the 277-4 in the body weldment inner liner cavity is 1.32708×10^4 cm^3.

Table 6.9.3.3-6. Effect of boron concentration on array neutron multiplication

100%B (wt %)	Boron density (g/cm^3)	Base material density (g/cm^3)	NP277-4 mass (g)	Case name	$k_{eff} \pm 2\sigma$ (@75% B)
0.01	0.00016	1.11775	21232.6	nbiabm_kvsb_1	1.13199 +/- 0.00138
0.1	0.0016	1.11631	2.12279E+04	nbiabm_kvsb_2	1.07944 +/- 0.00145
1	0.016	1.10191	2.11801E+04	nbiabm_kvsb_3	0.95564 +/- 0.00129
2	0.032	1.08591	2.11270E+04	nbiabm_kvsb_4	0.91708 +/- 0.00135
3	0.048	1.06991	2.10739E+04	nbiabm_kvsb_5	0.89396 +/- 0.00117
4.2284	0.068614	1.04930	2.10056E+04	nbiabm_kvsb_6	0.87985 +/- 0.00145
6	9.6000E-02	1.02191	2.09147E+04	nbiabm_kvsb_7	0.86029 +/- 0.00151
8	1.2800E-01	0.98991	2.08085E+04	nbiabm_kvsb_8	0.84769 +/- 0.00150
10	0.16	0.95791	2.07024E+04	nbiabm_kvsb_9	0.84086 +/- 0.00142

NUREG-1609 recommended that only 75% of the minimum boron density be credited in criticality evaluation in order to address the issue of non-homogeneity of ^{10}B in the neutron absorber material. The boron non-homogenity calculations presented here model an infinite array of ES-3100 packages with the boron concentration of Cat 277-4 varying along the vertical height of the body weldment inner liner. However, the total amount of boron in each package is fixed. Each package in the array contains 2.774 kg of ^{235}U in broken metal form uniformly distributed inside the containment vessel. Two sets of calculations are evaluated with this model to address the effects of boron distribution in the ES-3100 inner liner.

In one set of cases, the inner cavity is divided vertically into three equal-volume regions. The density in one region is increased to 95% of the minimum boron density, while the boron density in the

other two regions is decreased to 65%, thus preserving the amount of neutron absorber material in the package. In the other set of cases, the inner cavity is divided vertically into four equal volume regions, but two regions are combined. This creates two quarter-sized regions and one half-size region. The density in the half-size region is increased to 95% of the minimum boron density, while the density in the quarter-sized regions is decreased to 55%, thus preserving the amount of neutron absorber in the package. In both sets of calculations, the high-density region was shifted upward in the package to examine the effect of boron distribution.

As shown in Figures 6.9.3.3-2 and 6.9.3.3-3, the effect of non-homogeneity of boron in the ES-3100 liner on k_{eff} is not statistically significant. The "65% - 95% - 65%" nonhomogeneous boron distribution represents a relative standard deviation of 23.1% in boron concentration. Given the controls on method of manufacture and installation of the neutron absorber material, these calculated conditions bound the expected physical distribution of boron with a large degree of conservatism.

Geometry characteristics of the ES-3100 system preclude the need for uniformity in boron areal density as a prerequisite for criticality safety control. The ISG-15 provides crucial guidance for controlling areal density in a geometry configuration where one-dimensional effects are significant, such as a distributed source separated by thin Boral sheets (aluminum and boron carbide) which range in thickness from 0.075 to 0.4 in. In this example, Boral aluminum sheets are placed between fissile fuel rods just a few inches away and only become efficient when the low-enriched fissile material is placed in a sea of hydrogenous moderator. The cylindrical thickness of the ES-3100 cast neutron absorber material (Cat 277-4) is 1.12 in., which is about three times thicker than the largest Boral sheet. Its purpose in the ES-3100 is to provide criticality safety control for arrays of packages.

In the ES-3100, the proposed fissile mass loads are separated by at least one drum diameter (19.36 in.). Drawing M2E801580A031 in Appendix 1.4.8 shows the cross-section view of the many different layers of materials that are between the fissile mass loads in adjacent packages in an array. The direct neutron transport path between dispersed fissile material (assuming a neutron passes through the following thickness of materials at a normal angle to the closest neighboring package) is:

- fissile material,
- 0.100 in. 304 stainless-steel containment vessel wall,
- air gap,
- 0.06 in. 304 stainless-steel inner liner wall,
- 1.12 in. of 277-4 neutron absorber material,
- 0.06 in. 304 stainless-steel outer liner wall,
- 4.77 in. of Kaolite,
- 0.06 in. 304 stainless-steel outer drum wall, and
- air gap,

followed by the reverse:

- 0.06 in. stainless-steel outer drum wall,
- 4.77 in. of Kaolite,
- 0.06 in. 304 stainless-steel outer liner wall,
- 1.12 in. of 277-4 neutron absorber material,
- 0.06 in. 304 stainless-steel inner liner wall,
- air gap,
- 0.100 in. 304 stainless-steel containment vessel wall, and
- back into a fissile material.

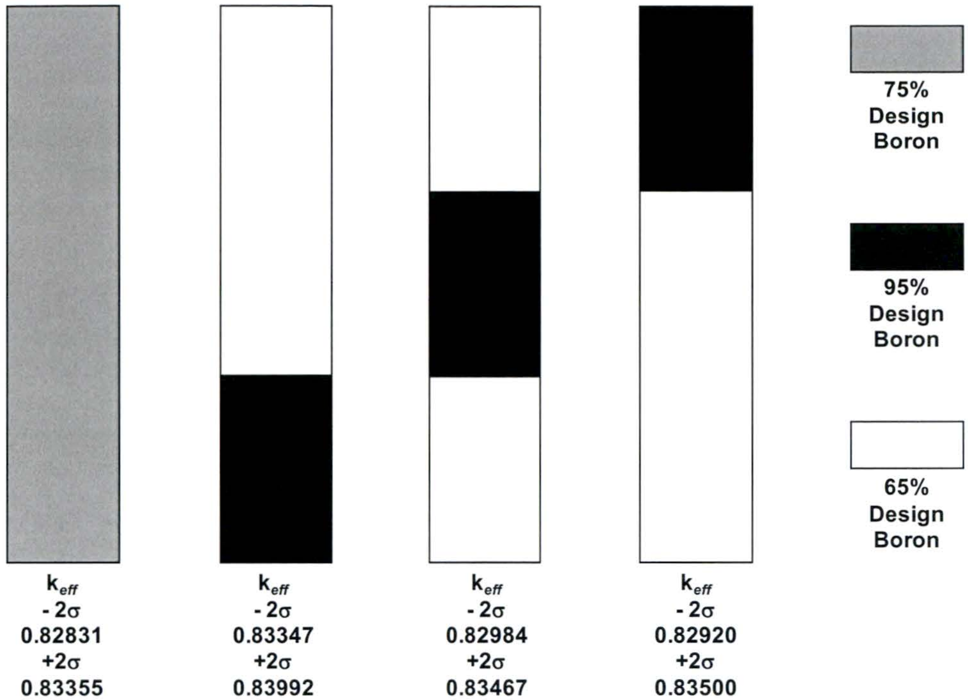

Fig. 6.9.3.3-2. Three equal-region models for evaluation of non-homogeneity in the boron distribution.

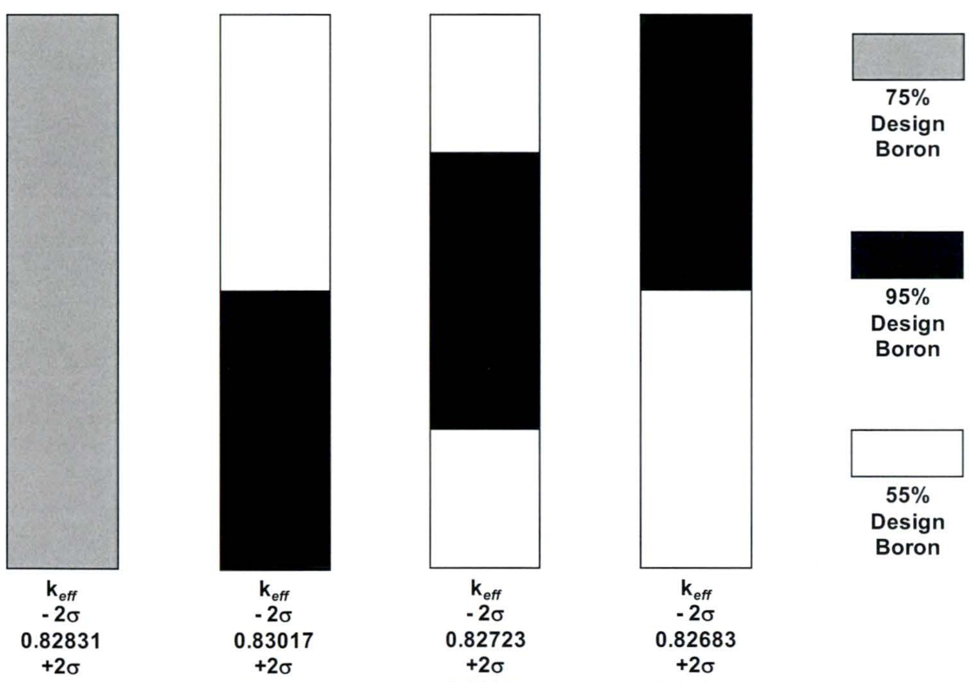

Fig. 6.9.3.3-3. Non-uniform region model for evaluation of non-homogeneity in the boron distribution.

At the shortest distance between fissile materials, neutrons travel through the 1.12 in. (2.8448 cm) of 277-4 neutron absorber material and 0.28 in. (0.7112 cm) of 304 stainless steel at least twice, with the high probability of several neutron scattering collisions along the way. Thus, the mean free path in the package is much smaller than the separation between the fissile material of adjacent packages.

In contrast to a Boral sheet application, the neutron absorber component of the ES-3100 package physically represents a significant fraction of the total container volume and is large in comparison to the potential fissile material volume. Furthermore, the neutron absorber component consists of boron dispersed throughout a hydraulic cement matrix with a high neutron scattering potential. The net result is that sensitivity to angular and spatial variations in the areal density of ^{10}B in the neutron absorber volume is eliminated.

The neutron absorbing material will be fabricated under strict quality control and accepted for use under an NQA-1 compliant QA program. The original equipment specification for the production of 277-4 neutron absorber material used a proprietary mixture from the Thermo Electron Corporation that combined high alumina cement and a boron grit (Cat 277-4). The manufacturing process for the neutron absorber was revised in order to obtain details necessary for material characterization and to achieve process control for ensuring consistency of absorber material among lots.

A two-part system of dry-blend components is now employed rather than relying on a single base material (a premixed powder of high alumina cement and boron grit). Thermo Electron Corporation's proprietary high-alumina cement without boron grit (Cat 277-0) is mixed on-site with boron carbide by the ES-3100 manufacturer under strict quality controls. A single batch is mixed on a per package basis. The boron carbide used in this process is strictly controlled. Boron carbide is specified per ASTM C 750-03, "Nuclear-Grade Boron Carbide Powder," in the Type 1 category. The grit size is controlled to ≤ 100 µm or a grit size of 120 per ANSI B74-12, with 100% passing a 120USS mesh.

The new formulation designated "277-4" is produced through a quality-controlled batch process of dry blending, wet mixing, vibration casting, and timed cure. (Equipment Specification JS-YMN3-801580-A005, Appendix 1.4.5) The plan is to control the purity, boron carbide particle size, chemistry, measurements, weights, mixing, recording, casting, and testing using one batch per each shipping package (and its two companion spacer cans). A design analysis calculation shows all of the calculations used in mixing and determines (from the minimum acceptable chemical purities) the volumetric densities in g/cm^3 and an areal density in g/cm^3 of ^{10}B. (DAC-PKG-801624-A001) These values will prove the acceptability of the mixing specifications.

An important part of this approach is a QA-approved 277-4 material verification and acceptance testing program. The applicant plans on performing 100% acceptance testing on the criticality safety significant properties of density, ^{10}B interaction (neutron absorption), and hydrogen content. The acceptance density shall be the as cast density in the drum to 105-5+10 lb/ft^3 and shall be determined as shown in Appendix 1.4.5. To test the other properties, two companion sample cans shall be cast from each batch used to cast a shipping container (the manufacturer will cast a fresh batch for each shipping container). The companion sample cans shall also have their density verified. The ^{10}B interaction will be tested in the manner described in Appendix A of the 277-4 specification (Appendix 1.4.5). Initially, a new set of 277-4–certified cans will be cast using the newly proposed casting specification with the QA plan described previously. Then, on a companion sample can for each batch pour, a Prompt Gamma-ray Neutron Activation Analysis (PGNAA) test will be used to neutronically test the ^{10}B for absorption. To pass the PGNAA test, the sample can results must be within the results obtained for the 277-4 certified standards, in units of Average Net Count rate (ANC/second) ±4 standard deviations. The second companion sample can will be used to test for hydrogen content using an LOD test as described in

Appendix 1.4.5. Upon successful completion of the density, PGNAA, and LOD testing, the ES-3100 neutron absorber material will be accepted for use.

6.9.3.4 KAOLITE 1600

Kaolite 1600, manufactured by Thermal Ceramics of Augusta, Georgia [telephone number (404) 796-4200], is a super-lightweight, low thermal conductivity, castable material designed for backup insulation up to 1600°F. The material is obtained as a dry powder with the chemical composition given in Table 6.9.3.4-1. The powder is mixed with water in a water-to-powder ratio of 14.5 qt per 20-lb bag. The mixture is poured into the drum body weldment or top plug, vibrated to eliminate voids, and then dried and fired to form the finished product. (Rowland, 2001) The density of the fired material is ~25 lb/ft³. It is assumed that the wet mixture contains the maximum water possible. This value (14.5 qt per 20 lb) is therefore used to determine the maximum water content of the fired product,

$$S.G._{max} = \frac{14.5\ \text{qt}}{20\ \text{lb dry}} \times \frac{25\ \text{lb}}{\text{ft}^3} \times \frac{0.946\ \ell}{1\ \text{qt}} \times \frac{998.2\ \text{g}}{\ell} \times \frac{35.32\ \text{ft}^3}{10^6\ \text{cm}^3} = \frac{0.6045\ \text{g}}{\text{cm}^3}$$

Table 6.9.3.4-1. Kaolite 1600 chemical composition, percent fired basis

Component	Weight percent	Component	Weight percent
Al_2O_3	9.6	CaO	30.7
SiO_2	36.7	MgO	13.1
Fe_2O_3	6.7	Na_2O	2.0
TiO_2	1.2		

Tables 6.9.3.4-2 and 6.9.3.4-3 provide detailed information regarding the weight measurements taken during the casting of Kaolite 1600 for the production of a series of drum body weldment and top plug parts for a similar package (the BWXT Y-12 Model ES-2100). The mean values for the amount of Kaolite and water present after baking are 107.08 lb of Kaolite and 4.8 lb of water in the drum body weldment, and 16.99 lb of Kaolite and 0.58 lb of water in the top plug. An ES-2100 package contains, on the average, 124.07 lb (56,276.91 g) of Kaolite and 5.38 lb (2,440.32 g) of water. Given that the average volume is 5.72 ft³, the average density of Kaolite is 22.63 lb/ft³ (0.3625 g/cm³).

The volume of the Kaolite region in the KENO models is 1.63417 × 5 cm³. For NCT, the density of Kaolite is 0.34438 g/cm³, and the density of water is 0.01493 g/cm³. The data in Tables 6.9.3.4-2 and 6.9.3.4-3 indicate that the Kaolite may have as little as 1.90 lb (861.82 g) of water after baking (Part Serial Number 97) such that the corresponding density of water is 0.00527 g/cm³. For the water-flooded HAC, the amount of water is assumed not to exceed the amount present before baking. The package would contain on the average 186.10 lb (84,413.1 g) of water such that the corresponding density is 0.51655 g/cm³. The full range of NCT and HAC conditions would be covered by a variation of water in the Kaolite from 0 g/cm³ to 0.51655 g/cm³ in a calculation model.

Table 6.9.3.4-2. Fabrication data, before and after baking the drum body weldment parts of the ES-2100 shipping package

								before baking			after baking		
Part Serial Number	clean & empty (lb)	filled with water (lb)	before baking (lb)	after baking (lb)	density after baking (lb/ft³)	water conditions (lb)	volume (ft³)	Kaolite and water (lb)	Kaolite (lb)	water (lb)	Kaolite and water (lb)	Kaolite (lb)	water (lb)
97	87.5	393.5	356.5	197.0	22.29	306.00	4.91	269.00	107.60	161.40	109.50	107.60	1.90
98	87.5	393.5	356.5	198.5	22.60	306.00	4.91	269.00	107.60	161.40	111.00	107.60	3.40
54	87.5	395.0	356.5	199.0	22.59	307.50	4.94	269.00	107.60	161.40	111.50	107.60	3.90
87	87.5	394.0	353.5	196.5	22.16	306.50	4.92	266.00	106.40	159.60	109.00	106.40	2.60
2	88.0	394.0	360.0	202.5	23.31	306.00	4.91	272.00	108.80	163.20	114.50	108.80	5.70
4	88.0	395.5	360.0	203.0	23.30	307.50	4.94	272.00	108.80	163.20	115.00	108.80	6.20
42	88.0	394.5	356.5	199.5	22.66	306.50	4.92	268.50	107.40	161.10	111.50	107.40	4.10
43	88.0	396.0	357.5	198.0	22.25	308.00	4.94	269.50	107.80	161.70	110.00	107.80	2.20
94	87.0	393.5	361.5	205.0	23.98	306.50	4.92	274.50	109.80	164.70	118.00	109.80	8.20
35	88.0	394.5	363.5	208.0	24.39	306.50	4.92	275.50	110.20	165.30	120.00	110.20	9.80
3	87.0	393.0	364.0	206.0	24.23	306.00	4.91	277.00	110.80	166.20	119.00	110.80	8.20
44	88.0	394.0	356.5	204.5	23.72	306.00	4.91	268.50	107.40	161.10	116.50	107.40	9.10
32	88.0	396.0	355.0	198.5	22.35	308.00	4.94	267.00	106.80	160.20	110.50	106.80	3.70
33	87.5	394.0	351.0	197.5	22.36	306.50	4.92	263.50	105.40	158.10	110.00	105.40	4.60
58	87.5	394.5	351.5	196.5	22.12	307.00	4.93	264.00	105.60	158.40	109.00	105.60	3.40
4	87.5	394.0	343.0	192.5	21.34	306.50	4.92	255.50	102.20	153.30	105.00	102.20	2.80
22	87.5	394.5	352.0	196.0	22.02	307.00	4.93	264.50	105.80	158.70	108.50	105.80	2.70
27	88.0	395.5	352.5	196.5	21.98	307.50	4.94	264.50	105.80	158.70	108.50	105.80	2.70
28	87.5	394.5	350.5	199.0	22.63	307.00	4.93	263.00	105.20	157.80	111.50	105.20	6.30
30	87.5	395.0	352.0	200.0	22.79	307.50	4.94	264.50	105.80	158.70	112.50	105.80	6.70
27	88.0	395.5	352.5	196.5	21.98	307.50	4.94	264.50	105.80	158.70	108.50	105.80	2.70
mean	87.67	394.50	355.36	199.55	22.72	306.83	4.93	267.69	107.08	160.61	111.88	107.08	4.80
std. dev.					0.8132						100%	95.71%	4.29%
computed on means					22.72	306.83	4.93	267.69	107.08	160.61	111.88	107.08	4.80

Table 6.9.3.4-3. Fabrication data, before and after baking the top plug parts of the ES-2100 shipping package

								before baking			after baking		
Part Serial Number	clean & empty (lb)	filled with water (lb)	before baking (lb)	after baking (lb)	density after baking (lb/ft³)	water conditions (lb)	volume (ft³)	Kaolite and water (lb)	Kaolite (lb)	water (lb)	Kaolite and water (lb)	Kaolite (lb)	water (lb)
97	10.5	60.0	53.5	28.5	22.65	49.50	0.79	43.00	17.20	25.80	18.00	17.20	0.80
83	10.5	59.0	50.5	27.0	50.50	27.00	50.50	27.00	16.00	24.00	16.00	24.00	16.00
86	10.5	60.0	50.5	27.5	21.40	49.50	0.79	40.00	16.00	24.00	17.00	16.00	1.00
87	10.5	59.0	53.0	28.5	23.12	48.50	0.78	42.50	17.00	25.50	18.00	17.00	1.00
28	11.0	59.0	53.0	28.5	22.71	48.00	0.77	42.00	16.80	25.20	17.50	16.80	0.70
23	10.5	59.5	52.5	28.0	22.25	49.00	0.79	42.00	16.80	25.20	17.50	16.80	0.70
24	10.5	59.0	53.5	28.5	23.12	48.50	0.78	43.00	17.20	25.80	18.00	17.20	0.80
25	10.5	58.5	54.0	29.0	24.01	48.00	0.77	43.50	17.40	26.10	18.50	17.40	1.10
26	10.5	59.0	54.0	29.0	23.76	48.50	0.78	43.50	17.40	26.10	18.50	17.40	1.10
27	10.5	60.0	54.5	29.0	23.28	49.50	0.79	44.00	17.60	26.40	18.50	17.60	0.90
0	10.5	60.0	52.0	27.0	20.77	49.50	0.79	41.50	16.60	24.90	16.50	16.60	-0.10[a]
20	10.5	60.0	53.5	28.0	22.03	49.50	0.79	43.00	17.20	25.80	17.50	17.20	0.30
22	10.5	60.0	54.0	28.5	22.65	49.50	0.79	43.50	17.40	26.10	18.00	17.40	0.60
21	10.5	61.0	53.0	28.0	21.59	50.50	0.81	42.50	17.00	25.50	17.50	17.00	0.50
19	10.5	60.0	53.0	27.5	21.40	49.50	0.79	42.50	17.00	25.50	17.00	17.00	0.00
11	10.5	60.0	52.5	28.0	22.03	49.50	0.79	42.00	16.80	25.20	17.50	16.80	0.70
14	10.5	60.0	52.5	27.5	21.40	49.50	0.79	42.00	16.80	25.20	17.00	16.80	0.20
15	10.5	60.5	54.0	28.0	21.80	50.00	0.80	43.50	17.40	26.10	17.50	17.40	0.10
16	10.5	59.0	52.0	27.5	21.84	48.50	0.78	41.50	16.60	24.90	17.00	16.60	0.40
17	10.5	60.5	54.5	28.5	22.43	50.00	0.80	44.00	17.60	26.40	18.00	17.60	0.40
mean	10.52	59.70	53.00	28.10	23.74	48.10	3.28	42.48	16.99	25.48	17.58	16.99	0.58
std. dev.					6.3565						100%	96.67%	3.33%
computed on means					22.27	49.18	0.79	42.48	16.99	25.48	17.58	16.99	0.58

[a] No explanation is given for the negative amount of water in Part 0. Also, the smaller percentage of water present in the top plug compared with to the drum body weldment is attributed to the larger surface-to-volume ratio, which results in better drying of the parts.

The Kaolite components of ES-3100 shipping package had not been manufactured at the time this criticality safety evaluation was performed. Given the lack of production data for ES-3100 Kaolite, a material specification (mass and density) was derived from data for ES-2100 production units. This specification, denoted "as-manufactured" (AM) Kaolite, was used for the ES-3100 criticality calculations. This ES-2100 shipping package is similar in design to the ES-3100 currently being evaluated.

The Kaolite production process was re-evaluated and improved following the production of ES-3100 units. (Y/DW-1890) Test samples were produced. These were classified into three groups: high density, medium density, and low density. The predominate number of samples fell into the medium density category (22.04 lb/ft^3), representing the expected, improved Kaolite production process. (Y/DW-1890, Appendix 2.10.4, Table 5) A material specification for use in criticality calculations was derived from the medium density "test sample" (TS) Kaolite data. However, the TS data are based on small sample volumes, whereas the AM data represents the entire package. Taking into consideration both the potential for scaling error and the uncertainty of how representative the test samples are of the manufactured ES-2100 units, the criticality safety packaging analysts chose to utilize the material specification derived from AM data rather than TS data in the criticality calculations for the ES-3100 safety analysis report.

A set of criticality calculations was performed for each of the packaging material specifications (i.e., the TS and the AM Kaolite) using three package water contents to represent the range of NCT and HAC. Y-12 statisticians were asked to determine whether or not the observed differences in neutronic performance are statistically significant for a package modeled with the TS specification versus one modeled with the AM specification. The purpose of this discussion is to summarize this comparison (DAC-FS-900000-A014) and draw conclusions.

Criticality Calculations. Each case is rerun using a different starting random number in order to produce computed k_{eff} values that are statistically independent. Table 6.9.3.4-4 presents the random starting number, the mean value (k_{eff}) and corresponding standard error (s_i) computed for 10 individual runs of each case.

Three sets of criticality calculations were run for both the AM Kaolite and TS Kaolite. One set of calculaitons is for dry Kaolite (i.e., low water content, IS = 1e-04 sp gr water); another set is for normal moisture Kaolite (i.e., NCT water content); and the third set is for flooded Kaolite (i.e., high water content, IS = 1.0 sp gr water). These conditions span the range of NCT and HAC addressed in the criticality evaluation. An infinite array of packages was evaluated in order to eliminate any biases arising from spectral leakage effects in the reflector of the finite array. Each package was modeled having 36 kg of 100% enriched uranium in the form of 3.24-in. diameter cylinder content. The k_{eff} values for each KENO V.a case are based on 500,000 neutron histories produced by running for 215 generations with 2,500 neutrons per generation and truncating the first 15 generations of data.

Statistical evaluation. A review of KENO V.a calculation results was made to determine if a statistically significant difference exists between the mean k_{eff} for the TS Kaolite specification and the AM Kaolite material specifications used in the criticality evaluation of the ES-3100 shipping package. Case results were classified into three groups (i.e., low water content, medium water content, or high water content) depending on the amount of water present in the ES-3100 shipping package. The symbol "I" is used to specify the group. The mean difference and standard deviation for each of the three (3) sets of pair-wise differences was defined as follows:

(a) $d_i = (k_{effBi} - k_{effAi})/n$ and
(b) $s_{di} = \sqrt{[\,[\,n\Sigma d_i^{\,2} - (\,\Sigma d_i\,)^2\,] / n(n-1)\,]}$ (conservatively defined for the t-test appropriate for small sample sizes)

Table 6.9.3.4-4. Data for the statistical evaluation of "as-manufactured"and "test sample" Kaolite

As-Manufactured Kaolite				Test Sample Kaolite			
Case name	Random number	k_{eff}	s_i	Case name	Random number	k_{eff}	s_i
Group 1 – Low water content							
esrandnum_01_01_in	109E77866CF	1.00274	0.00138	mdrandnum_01_01_in	109E77866CF	1.00170	0.00125
esrandnum_01_02_in	16AA4A58735	1.00224	0.00120	mdrandnum_01_02_in	16AA4A58735	1.00416	0.00116
esrandnum_01_03_in	1814171B652	1.00121	0.00107	mdrandnum_01_03_in	1814171B652	1.00208	0.00125
esrandnum_01_04_in	1A423B9472C	1.00367	0.00118	mdrandnum_01_04_in	1A423B9472C	1.00271	0.00131
esrandnum_01_05_in	20E876D8224	1.00290	0.00133	mdrandnum_01_05_in	20E876D8224	1.00406	0.00125
esrandnum_01_06_in	3F6E65CA744	1.00266	0.00137	mdrandnum_01_06_in	3F6E65CA744	1.00418	0.00124
esrandnum_01_07_in	479D21DB750	1.00393	0.00108	mdrandnum_01_07_in	479D21DB750	1.00193	0.00133
esrandnum_01_08_in	55D4371D3A2	1.00313	0.00113	mdrandnum_01_08_in	55D4371D3A2	1.00196	0.00105
esrandnum_01_09_in	6E1A14672B8	1.00343	0.00119	mdrandnum_01_09_in	6E1A14672B8	1.00503	0.00118
esrandnum_01_10_in	77A0308C0E4	1.00229	0.00113	mdrandnum_01_10_in	77A0308C0E4	1.00358	0.00108
Group 2 – NCT medium density							
esrandnum_06_01_in	109E77866CF	0.99025	0.00119	mdrandnum_06_01_in	109E77866CF	0.98323	0.00118
esrandnum_06_02_in	16AA4A58735	0.98863	0.00128	mdrandnum_06_02_in	16AA4A58735	0.98630	0.00108
esrandnum_06_03_in	1814171B652	0.98811	0.00120	mdrandnum_06_03_in	1814171B652	0.98328	0.00125
esrandnum_06_04_in	1A423B9472C	0.98933	0.00114	mdrandnum_06_04_in	1A423B9472C	0.98487	0.00112
esrandnum_06_05_in	20E876D8224	0.98869	0.00103	mdrandnum_06_05_in	20E876D8224	0.98559	0.00109
esrandnum_06_06_in	3F6E65CA744	0.98854	0.00117	mdrandnum_06_06_in	3F6E65CA744	0.98412	0.00106
esrandnum_06_07_in	479D21DB750	0.98900	0.00119	mdrandnum_06_07_in	479D21DB750	0.98395	0.00118
esrandnum_06_08_in	55D4371D3A2	0.98844	0.00113	mdrandnum_06_08_in	55D4371D3A2	0.98546	0.00114
esrandnum_06_09_in	6E1A14672B8	0.99007	0.00126	mdrandnum_06_09_in	6E1A14672B8	0.98424	0.00121
esrandnum_06_10_in	77A0308C0E4	0.99028	0.00122	mdrandnum_06_10_in	77A0308C0E4	0.98465	0.00118
Group 3 – High water content							
esrandnum_09_01_in	109E77866CF	0.92872	0.00118	mdrandnum_09_01_in	109E77866CF	0.92800	0.00123
esrandnum_09_02_in	16AA4A58735	0.92800	0.00110	mdrandnum_09_02_in	16AA4A58735	0.92817	0.00107
esrandnum_09_03_in	1814171B652	0.92844	0.00118	mdrandnum_09_03_in	1814171B652	0.92770	0.00115
esrandnum_09_04_in	1A423B9472C	0.92780	0.00123	mdrandnum_09_04_in	1A423B9472C	0.92763	0.00126
esrandnum_09_05_in	20E876D8224	0.92783	0.00134	mdrandnum_09_05_in	20E876D8224	0.92584	0.00105
esrandnum_09_06_in	3F6E65CA744	0.92809	0.00128	mdrandnum_09_06_in	3F6E65CA744	0.92853	0.00112
esrandnum_09_07_in	479D21DB750	0.92725	0.00111	mdrandnum_09_07_in	479D21DB750	0.92682	0.00111
esrandnum_09_08_in	55D4371D3A2	0.92622	0.00126	mdrandnum_09_08_in	55D4371D3A2	0.92706	0.00116
esrandnum_09_09_in	6E1A14672B8	0.92925	0.00132	mdrandnum_09_09_in	6E1A14672B8	0.92733	0.00110
esrandnum_09_10_in	77A0308C0E4	0.92757	0.00114	mdrandnum_09_10_in	77A0308C0E4	0.92886	0.00132

where A_i denotes the TS by group classification, B_i the AM by group classification, and n the sample size of ten (10). It is reasonable to assume that the paired differences have been randomly selected from a normally distributed population of paired differences with mean μ_d and standard deviation σ_d. Therefore, the sampling distribution of

$$(d - \mu_d) / (s_d/\sqrt{n})$$

is a *t*-distribution having n-1 degrees of freedom.

The evaluation of the mean differences (d_i) for the 10 set of cases is accomplished through hypothesis testing, a statistical tool used to provide evidence that a difference exists or does not exist. The t_i values are 0.70, 10.0 and 0.95 for dry Kaolite, for NCT Kaolite, and for flooded Kaolite, respectively. A value of 3.25 is obtained from the standard table for critical values for the t distribution, from which the decision to accept or reject the null hypothesis H_0 is made with a Type I error probability (α) of 0.01. For $t < 3.25$, the H_o hypothesis is not rejected. Acceptance of the null hypothesis is the result of insufficient evidence to reject it. Thus, it can be concluded that the mean estimate of the difference of the AM Kaolite is not significantly different from the mean of the TS Kaolite for both dry and flooded Kaolite. For $t > 3.25$, the H_o hypothesis is rejected. Therefore, it can be concluded that the mean estimate of the difference of the AM Kaolite is significantly different from the mean of the TS Kaolite for the normal moisture Kaolite. The mean k_{eff} for AM Kaolite is significantly greater than the mean k_{eff} of the TS Kaolite; therefore, the use of the AM specification in the ES-3100 criticality calculations is conservative and bounding. Details of the statistical evaluation are documented in Reference DAC-FS-900000-A014.

6.9.3.5 WATER

Water is used in various regions of the models to simulate HAC as an interstitial moderator and as a reflector. When used at full density, the density of water is 0.9982 g/cm^3. (SCALE, Vol. 3, Sect. M8)

6.9.3.6 CALCULATION OF EQUIVALENT WATER MASS FOR POLYETHYLENE

In the calculation models for evaluation of NCT, water may be substituted for the polyethylene composition of bags present in the package. Based on hydrogen density, 1285.14 g of water are equivalent to 1000 g of polyethylene for nuclear criticality safety calculations. The equivalent water mass is calculated as follows:
Hydrogen in 1 kg of polyethylene [$(CH_2)_2$, molecular weight = 28.0312; density = 0.92]:

$$\text{1 kg polyethylene} = \frac{1000 \text{ g}}{0.92 \text{ g/cm}^3} = 1087.0197 \text{ cm}^3$$

$$\text{H number density} = \frac{(0.92)(4)(6.02252\times10^{23})}{(28.0312)(10^{24})} = 7.906502\times10^{-2}\text{at/bn-cm}$$

$$\text{H in 1 kg} = (1087.0197\text{cm}^3)(7.906502\times10^{-2}) = 85.945234 \text{ at-cm}^2\text{/bn}$$

Grams of water [H_2O, molecular weight = 18.0110; density = 0.9982] with hydrogen content equivalent to 1 kg of polyethylene:

$$\text{equivalent g of } H_2O = \frac{(85.945234)(18.0110)(10^{24})}{(2)(6.02252\times10^{23})} = 1285.1427 \text{ g}$$

THIS PAGE INTENTIOANLLY LEFT BLANK.

Appendix 6.9.4

QUALIFICATION OF A NEUTRON ABSORBER MATERIAL FOR THE ES-3100

THIS PAGE INTENTIONALLY LEFT BLANK.

Appendix 6.9.4

QUALIFICATION OF A NEUTRON ABSORBER MATERIAL FOR THE ES-3100

6.9.4.1 INTRODUCTION

277-4 is a formulation of Thermo Electron Corporation's Cat. 277-0, a boron carbide additive and water. 277-4 is a neutron radiation shielding product and is one of several materials in its class that have been evaluated as a candidate neutron absorber system for a variety of nuclear criticality safety applications by the Y-12 National Security Complex (Y-12). This class of materials is characterized as a dispersion of $^{nat}B_4C$ particulate* throughout a hardened hydraulic cement or binder, resulting in a high-hydrogen, borated material system. It offers many advantages for typical Y-12 applications over other classes of materials such as borated aluminum because a neutron moderator and neutron absorber are both integral to the solid material system itself. The separate addition of another neutron moderating material such as water or polyethylene is not required in order for it to function effectively.

Computational methods of analysis in simple geometry permit direct comparison of neutron absorber system performance for nuclear criticality safety applications. The measure of comparison is the neutron interaction potential between two parallel 0.745-cm-thick slabs of infinite extent of ^{235}U metal at a density of 18.81 g/cm^3. The slabs are separated by a variable thickness of material and reflected by a 60-cm thickness of the same material (Fig. 6.9.4.1-1). Each material is modeled as an idealized homogenous mixture of elements based on nominal density and constituent proportions (Table 6.9.4.1-1). The result is expressed in terms of calculated k_{eff}† as influenced by the thickness of the candidate material between the two parallel slabs (see Fig. 6.9.4.1-2).

The least effective neutron absorber material systems are those with low hydrogen content and low neutron absorption cross section (e.g., ordinary concrete). The performance of concrete that contains $^{nat}B_4C$ particulate (e.g., borated concrete) is improved, but it is still hindered by its low hydrogen content. This is a function of the proportion and type of cement in the typical concrete mixture (i.e., a low proportion of lime- and silica-based Portland cement). Ordinary water is also included for comparison because of its high hydrogen content, but its performance is also limited by a low total mass density and low neutron absorption cross section.

As expected, materials with high hydrogen content and high boron content (e.g., 277-4, borated ceramics, and borated polymers) are predicted to be the most effective neutron absorber systems. Although the mechanical and thermal properties of such systems can vary significantly, their nuclear properties are dictated almost exclusively by the relative proportion and content of ^{10}B and H and the total mass density of the material system. These things being equal, the nuclear performance of any material in this class (i.e., 277-4, borated ceramics, and borated polymers) is representative of the others.

---

*277-4 is an improved variant of the Cat 277 product ca. 2000 which was originally formulated as a dispersion of ^{nat}Borosilicate glass granules rather than the current practice of using $^{nat}B_4C$ particulate.

†SCALE 4.4a, CSAS25 code sequence for KENO V.a with the 238-group ENDF B-IV neutron cross-section library on the Y-12 SAE Hewlett-Packard J5600 workstation (CMODB).

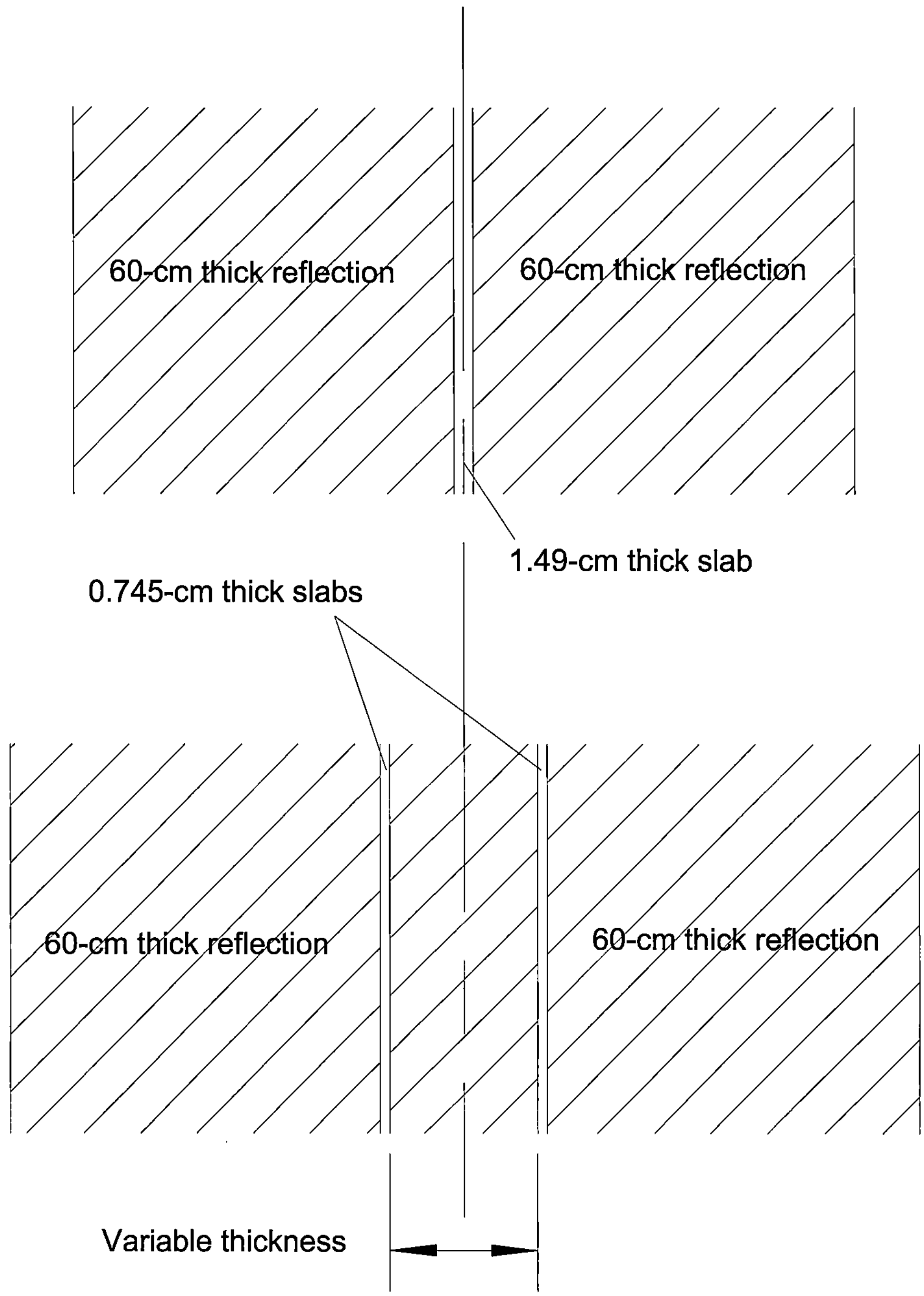

Fig. 6.9.4.1-1. Physical model of parallel ^{235}U metal slabs of infinite extent reflected and separated by various candidate neutron absorber materials.

Table 6.9.4.1-1. Nominal elemental and isotopic compositions of idealized material models for comparison of various neutron absorbers (atoms/barn·cm)

	Ordinary Concrete A 2.147 g/cm^3	Ordinary Concrete B 2.299 g/cm^3	Water 0.9982 g/cm^3	Borated Concrete 2.563 g/cm^3	Cat 277[a] 1.68 g/cm^3	Borated Ceramic 1.91 g/cm^3	Borated Polymer 1.717 g/cm^3	^{235}U Metal 18.81 g/cm^3
H	4.2581e-03	8.5010e-03	6.6751e-02	4.2900e-03	3.3800e-02	2.7200e-02	5.7600e-02	
B-10				1.7600e-04	2.8400e-04	2.6500e-03	9.4600e-04	
B-11				6.8100e-04	1.1800e-03	1.1000e-02	3.9200e-03	
C	1.1348e-02	2.0217e-02		9.0000e-04		4.2600e-03	2.3500e-02	
N							1.3800e-03	
O	4.0370e-02	3.5511e-02	3.3376e-02	4.2400e-02	3.7100e-02	3.2900e-02	2.5900e-02	
Na	7.9356e-05	1.6299e-05		6.7100e-05	2.6000e-04	7.9200e-05		
Mg	5.0111e-03	1.8602e-03		2.3000e-04	2.0800e-04	2.3300e-03		
Al	3.7660e-04	5.5580e-04		2.2900e-03	8.9700e-03	1.7400e-03	7.7000e-03	
Si	1.9382e-03	1.7000e-03		1.1800e-02	7.6700e-04	3.2300e-03		
P						2.1200e-03		
S	1.0013e-04			9.6300e-05	6.0000e-05	7.7800e-05		
Cl	1.9074e-05							
K	3.1231e-04	4.0300e-05		3.1600e-04		2.3100e-03		
Ca	7.3008e-03	1.1101e-02		3.1200e-03	2.2300e-03	2.4600e-04		
Ti	4.0183e-05					7.0800e-05		
Mn	1.2050e-05			1.4000e-04				
Fe	1.2954e-04	1.9301e-04		4.6200e-03	4.8900e-05	5.2000e-04		
U-235								4.8200e-02

[a] The ^{10}B content of this material model for Cat 277 is based on its ca. 2000 formulation using crushed borosilicate glass rather than the current practice of using $^{nat}B_4C$ particulate. This particular formulation is roughly equivalent to ~2% $^{nat}B_4C$ particulate (i.e., equivalent ^{10}B content, by weight). For otherwise identical H and B-10 content, this difference is unimportant relative to its nuclear performance as an idealized homogeneous mixture of elements. However, the current use of more than 5% $^{nat}B_4C$ particulate (by weight) is preferred due to reasons relating to the method of preparation, chemical reaction, and placement of 277-4 and uniformity of ^{10}B distribution in the cured product. As with all the materials in this class, the amount of H and ^{10}B in the finished product is determined by the relative proportions of its major constituents, which are tailored to the requirements of the specific application.

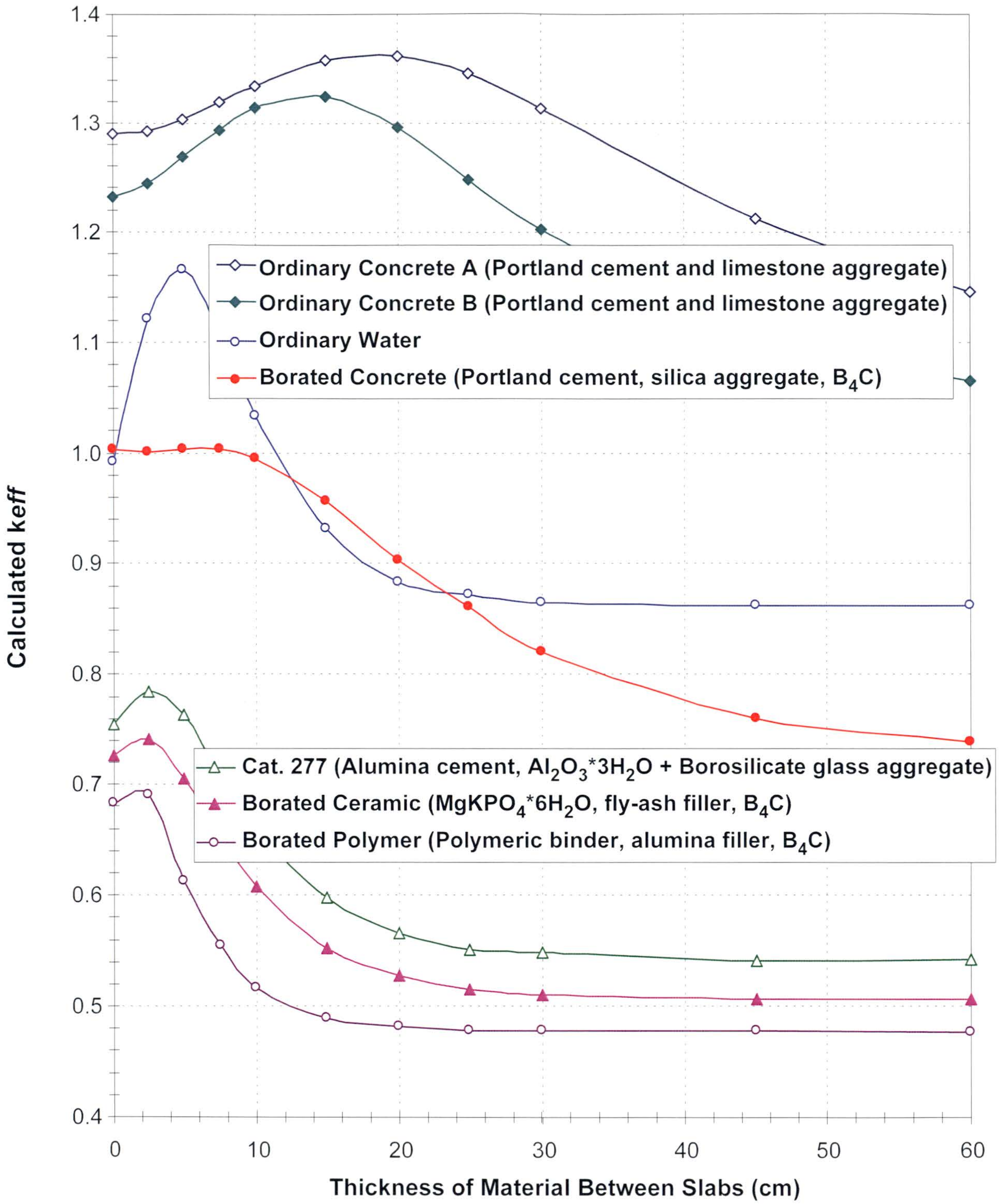

Fig. 6.9.4.1-2. The effect of various materials on neutron interaction between parallel slabs of ^{235}U metal of infinite extent.

6.9.4.2 PERFORMANCE TESTING

To investigate the performance of this class of neutron absorbing materials further, Y-12 has studied neutron radiography and neutron transmission measurements on several samples of a borated ceramic. Like 277-4, the borated ceramic is also a dispersion of ${}^{nat}B_4C$ particulate throughout a hardened hydraulic crystalline solid material matrix for which the binder phase is $MgKPO_4{\cdot}6H_2O$ rather than the hydrates of CaO and Al_2O_3. In fact, the more finely divided ${}^{nat}B_4C$ particulate specified for 277-4 is a slight advantage over the modestly coarser particulate in the borated ceramic. As shown below in Table 6.9.4.2-1, the relative proportion and content of H and ${}^{10}B$ and their total mass density are very similar. The small differences between the nuclear properties of their associated low- and intermediate-Z elements (i.e., oxides of Mg, Al, P, K, and Ca) are negligible. Thus, performance and the most significant factors affecting performance are nearly identical for both materials, so the results of neutron radiography and neutron transmission for the borated ceramic samples are judged applicable to 277-4 specimens of similar dimension.

Table 6.9.4.2-1. Comparison of nominal values for 277-4 and borated ceramic samples subjected to neutron radiography and neutron transmission testing.

Attribute	Cat 277 Original Formulation ca. 2000	277-4 ES-3100 Formulation as Cured	Borated Ceramic Samples for Testing
Principal Binder Phase(s)	Hydrates of CaO and Al_2O_3	Hydrates of CaO and Al_2O_3	$MgKPO_4{\cdot}6H_2O$
Neutron Absorber Particle Size	^{nat}Borosilicate glass granules 90 wt % <2360 μm 65 wt % <1180 μm 40 wt % <600 μm 15 wt % <102 μm 0 wt % <150 μm	${}^{nat}B_4C$ particulate 100 wt % <102 μm	${}^{nat}B_4C$ particulate 100 wt % <559 μm 90 wt % <356 μm 40 wt % <254 μm 3 wt % <122 μm 0 wt % <63 μm
Filler Material(s)	$Al_2O_3{\cdot}3H_2O$	$Al_2O_3{\cdot}3H_2O$	Class F Coal Fly-ash
Total Mass Density	1.68 g/cm^3	1.60 g/cm^3	1.91 g/cm^3
Total H_2O content	0.51 g/cm^3	0.51 g/cm^3	0.49 g/cm^3
Total ${}^{10}B$ content	0.005 g/cm^3	0.013 g/cm^3	0.012 g/cm^3

Samples were prepared from sectioned pieces of a single specimen from a vertically oriented mold measuring 10 × 10 × ~30 cm tall, as illustrated in Fig. 6.9.4.2-1 (nominally 4 × 4 × 12 in. tall). One specimen was prepared by the normal method of mixing and preparation for the borated ceramic material. Sectioning the first specimen resulted in two thick samples designated "1 of 2" and "2 of 2" which each measured 10-cm wide by ~30-cm long by ~2.4-cm thick (nominally 1-in. thick). A second specimen was prepared by abnormal methods intended to produce non-homogeneity (i.e., poorly mixed using retardants followed by excessive and extended vibration of the mold after installation). Sectioning this specimen resulted in two thin samples designated "062d1bc" and "062d1bd" which each measured 10-cm wide by ~30-cm long by ~1.2-cm thick (nominally 0.5-in. thick). The samples were delivered to the Breazeale Nuclear Reactor Building at Pennsylvania State University for inspection. Upon completion of inspection for all four samples as received, a thick sample "1 of 2" and a thin sample "062d1bc" were dehydrated by heating to 140°C to eliminate interference by hydrogen, and all four samples were tested again.

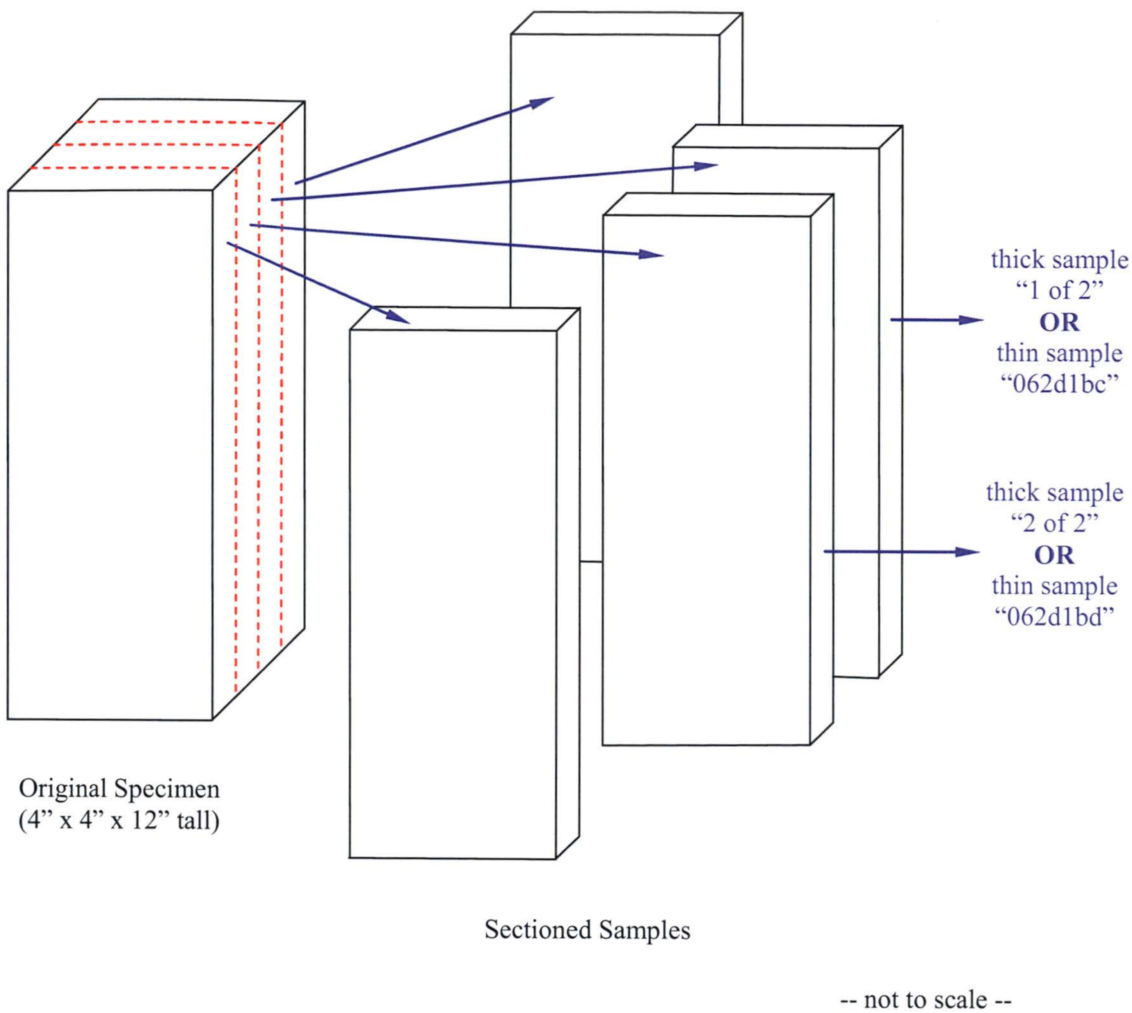

Fig. 6.9.4.2-1. Illustration of sectioning plan for borated ceramic samples for neutron radiography and neutron transmission measurements.

All four samples were qualitatively inspected for visual defects and subjected to neutron radiographic inspection. The inspections were intended to identify any variations in image luminance, which would indicate a variation in homogeneity and density. Neutron transmission measurements were calibrated to results for thin ZrB_2 reference coupons sandwiched with thick aluminum metal. The ^{10}B areal densities of the thin reference coupons ranged from 5.32 mg/cm^2 to 57.04 mg/cm^2 over a total ZrB_2 + Al reference thickness of 24.21–24.98 mm. By comparison, the thick samples contain an idealized ^{10}B areal density of 28.8 mg/cm^2 (i.e., 0.012 g/cm^3 over a 2.4-cm thickness), and the thin samples contain an idealized ^{10}B areal density of 14.4 mg/cm^2 (i.e., 0.012 g/cm^3 over a 1.2-cm thickness).

Radiographic examination of both thick samples "1 of 2" and "2 of 2" indicated uniformity of composition and density (see Fig. 6.9.4.2-2). Even after dehydration of thick sample "1 of 2," radioscopic examination indicated uniformity of composition and density. Initial neutron transmission results for both thick samples "1 of 2" and "2 of 2" indicated that neutron transmission was very low. In fact, the interference due to the hydrogen content implies an equivalent ^{10}B areal density measurement of ~67 ± 4 mg/cm^2. This is more than twice the actual physical value of 28.8 mg/cm^2. Only after thick sample of "1 of 2" is dehydrated and tested again do the results of neutron transmission measurements more accurately reflect the actual physical ^{10}B content. In fact, the average measured value of 27.419 mg/cm^2 at eleven points along the long axis of the dehydrated sample "1 of 2" is more than 95% of the actual physical value of 28.8 mg/cm^2 and varies no more than a few percent from one end to the other (see Tables 6.9.4.2-2 and 6.9.4.2-3).

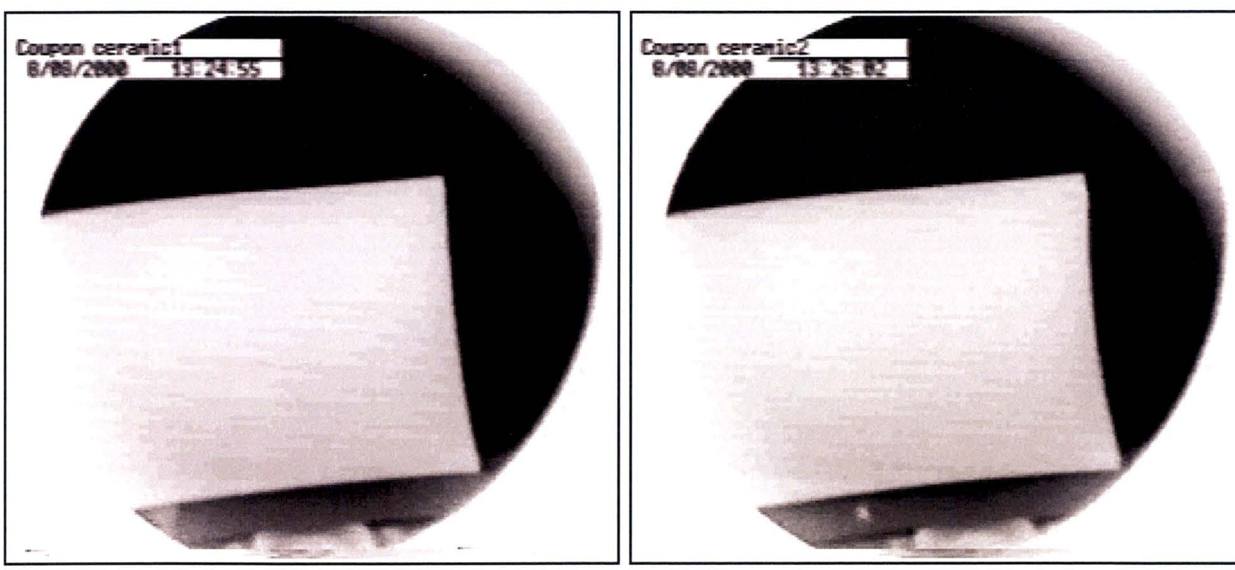

Fig. 6.9.4.2-2. Radiographic images of thick samples "1 of 2" (left) and "2 of 2" (right) indicating uniformity of composition and density.

Table 6.9.4.2-2. Results of neutron transmission measurements of thick samples

	Equivalent ^{10}B Areal Density (mg/cm^2)		
	End	**Center**	**End**
sample "1 of 2"	66.419	68.673	71.003
sample "2 of 2"	65.0	68.25	69.708
sample "1 of 2" (dehydrated)	27.586	27.191	28.555
sample "2 of 2" (re-test)	63.687	65.966	65.572

Table 6.9.4.2-3. Neutron transmission measurements of thick sample "1 of 2" after dehydration

Point of Measurement (uniform intervals from one end to the other)	Equivalent ^{10}B Areal Density (mg/cm^2)	Deviation from Average (%)
1	27.586	+0.6 %
2	26.909	-1.9 %
3	27.039	-1.4 %
4	27.358	-0.2 %
5	27.286	-0.5 %
6	27.191	-0.8 %
7	27.375	-0.2 %
8	27.179	-0.8 %
9	27.236	-0.7 %
10	27.897	-0.9 %
11	28.555	+4.1 %
Average	**27.419**	

Radiographic examination of both thin samples "062d1bc" and "062d1bd" indicates areas of nonuniformity and spots of lower neutron attenuation, along with greater dissimilarity between the samples themselves (see Fig. 6.9.4.2-3). Many of these areas and spots remained evident by radiographic examination even after dehydration of thin sample "062d1bc" and are attributed to physical voids revealed during visual inspection. Again, initial neutron transmission measurements implied a greater-than-actual equivalent ^{10}B areal density due to the interference of hydrogen (i.e., measured values averaged ~23.3 mg $^{10}B/cm^2$ rather than the actual value of 14.4 mg $^{10}B/cm^2$).

Measurements repeated after dehydration of sample "062d1bc" more correctly estimate the equivalent ^{10}B areal density to be ~11.1 mg/cm^2, which is ~77% of the actual physical ^{10}B content. Again, the relative values vary only a few percent from one end of the sample to the other (see Table 6.9.4.2-4). However, the measured values of a dehydrated sample in this case are known to be biased low. First, the total thicknesses of the ZrB_2 + Al reference coupons for calibration were ~24.21 to 24.98-mm compared to the 1.2-cm thickness of "062d1bc." Second, the total mass density of the sample is ~1.4 to 1.5 g/cm^3 after dehydration compared to an Al mass density of ~2.7 g/cm^3 for the ZrB_2 + Al reference coupons. This indicates that even the performance of the thin samples (i.e., 1.2-cm thickness) exhibiting non-uniformity of composition and density is only marginally reduced from that of the idealized, homogenous material model with respect to neutron absorber efficiency.

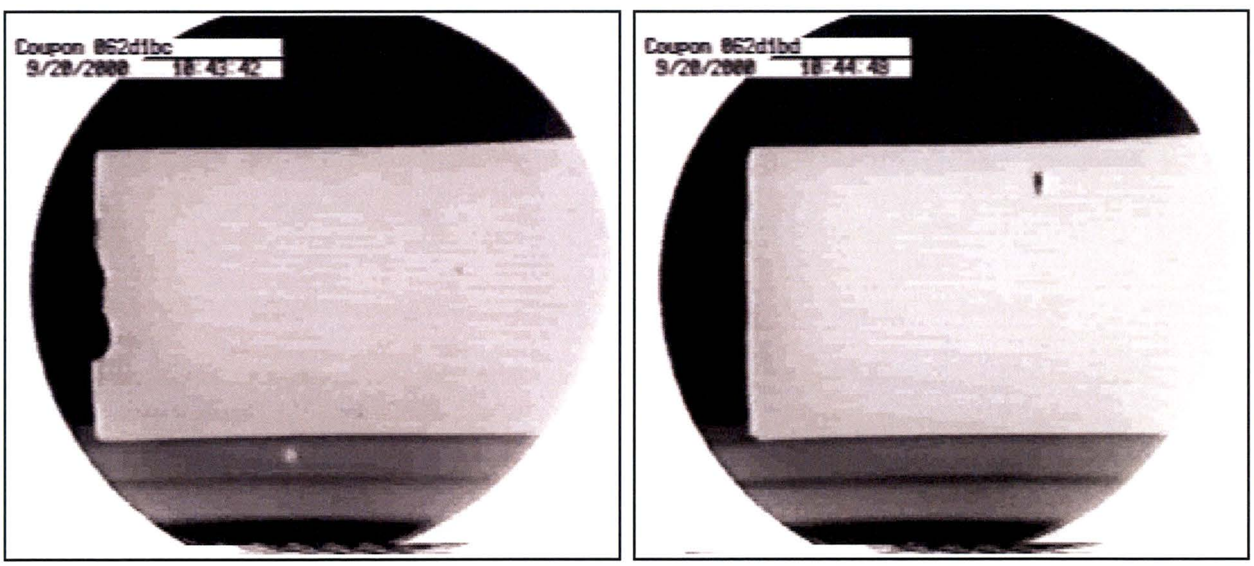

Fig. 6.9.4.2-3. Radiographic images of thin samples "062d1bc" (left) and "062d1bd" (right) indicating non-uniformity of composition and density and dissimilarity of samples.

Table 6.9.4.2-4. Neutron transmission results for dehydrated thin sample "062d1bc" and re-test of thin sample "062d1bd"

Position of Measurement (see Fig. 6.9.4.2-4)	Minimum Equivalent ^{10}B Areal Density (mg/cm^2)			
	Dehydrated Thin Sample "062d1bc"		Re-Test of Thin Sample "062d1bd"	
	Line A	Line B	Line A	Line B
1	12.227	11.781	25.909	25.154
2	11.776	11.462	24.390	25.344
3	11.388	11.252	24.257	24.645
4	10.554	10.462	25.341	24.885
5	10.432	10.528	24.646	25.483
6	10.754	11.728	25.450	25.712
7	10.396	11.534	25.761	23.063
8	11.166	10.221	24.522	25.257
9	10.875	10.459	23.113	23.882
10	11.051	10.676	25.270	23.724
11	11.258	11.214	24.922	25.355
Combined Average	11.1		24.8	

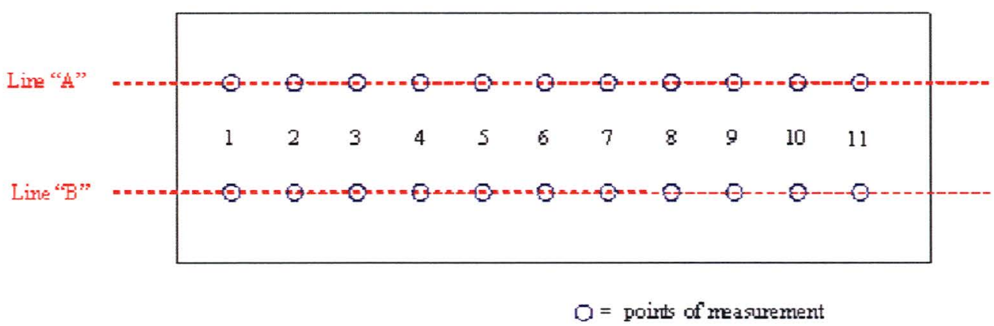

Fig. 6.9.4-6. Illustration of measurement plan for neutron transmission measurements of thin samples "062d1bc" and "062d1bd."

6.9.4.2.3 CONCLUSIONS

Provided that 277-4 is prepared in a controlled manner to ensure the proper specification and proportioning of batch constituents, thorough mixing of the wet slurry, and correct placement and installation to prevent large physical voids, a credible technical justification exists to credit no less than 75% f the $^{nat}B_4C$ particulate and its other constituents, by weight, as an idealized homogenous mixture for nuclear criticality safety analysis of the ES-3100. There is no evidence of non-homogeneity, neutron self-shielding effects, or neutron streaming effects in borated hydraulic cement or ceramic material systems for thicknesses of 2.4-cm or more. The qualification of 277-4 for use in the design and construction of the ES-3100 described herein is based on sound nuclear engineering principles and direct application of performance test results for such material systems.

Appendix 6.9.5

MISCELLANEOUS INFORMATION AND DATA

THIS PAGE INTENTIONALLY LEFT BLANK.

Appendix 6.9.5

MISCELLANEOUS INFORMATION AND DATA

Table 6.9.5.1 provides the atomic weights of the elements and isotopes of the materials used in this criticality safety evaluation. Atomic weights and isotopic weight percents of the naturally occurring materials are those taken from the Materials Information Processor in the SCALE Standard Composition Library.

Table 6.9.5.2 provides the molecular weights and weight percents of the corresponding elements and isotopes of the various compounds. The weight percents shown in this table are the input to KENO V.a. (NUREG/CR-0200, rev. 6)

Table 6.9.5.3 provides equations for determining atomic densities. These equations were derived based on the assumption that all constituents in the mixture are volume additive. Although these equations with their corresponding subscripts are for mixtures of elements, isotopes, or both, all except Equation (2) can be applied to compounds if the user substitutes certain subscript notations and meaning changes. For example, in Equations (1a) and (1b), the atomic weight becomes the molecular weight and the subscript "m" for mixture changes to the subscript "c" for compound. Likewise, in Equations (3a) and (3b), the atomic weight becomes the molecular weight, and the atom fraction (n_i) becomes the stoichiometric proportion of the elements making up the molecule. In Equations (3)–(5), the atom fraction (n_i) becomes the stoichiometric proportion (the element number subscript in the molecular formula), whose sum does not equal unity. Equation (2) is applicable only to the theoretical density of mixtures; it does not apply to the density of compounds.

Table 6.9.5.1. Atomic weights

Element or isotope	Atomic weight
H	1.0078
C	12.0000
O	15.9954
N	14.0033
Na	22.9895
Mg	24.3051
Al	26.9818
Si	28.0853
Ca	40.0803
Ti	47.8789
Cr	51.9957
Mn	54.9380
Fe	55.8447
Ni	58.6868
Zr	91.2196
^{235}U	235.0442
^{238}U	238.0510

Table 6.9.5.2. Molecular weights

Compound	Molecular or atomic weight	Weight percent in compound	Stoichiometric composition
Kaolite 1600™			
Alumina	-	9.6	Al_2O_3
Al	26.9818	52.92507	
O	15.9954	47.07493	
Silica	-	36.7	SiO_2
Si	28.0853	46.74349	
O	15.9954	53.25651	
Ferric Oxide	-	6.7	Fe_2O_3
Fe	55.8447	69.94330	
O	15.9954	30.05670	
Titanium Oxide	-	1.2	TiO_2
Ti	47.8789	59.95084	
O	15.9954	40.04916	
Calcium Oxide	-	30.7	CaO
Ca	40.0803	71.47009	
O	15.9954	28.52991	
Magnesium Oxide	-	13.1	MgO
Mg	24.3051	60.30359	
O	15.9954	39.69641	
Alkalies	-	2.0	Na_2O
Na	22.9895	74.18575	
O	15.9954	25.81425	

Table 6.9.5.3. Useful equations

N_m	=	$\rho_m N_o/A_m$.	(1a)
N_i	=	$w_i\, \rho_m N_o/A_i$.	(1b)
ρ_m	=	$1/\Sigma w_i/\rho_i$.	(2)
A_m	=	$1/\Sigma w_i/A_i$.	(3a)
	=	$\Sigma n_i A_i$	(3b)
w_i	=	m_i/m_m .	(4a)
	=	$n_i A_i/\Sigma n_i A_i$.	(4b)
n_i	=	N_i/N_m .	(5a)
	=	$(w_i/A_i)/\Sigma(w_i/A_i)$.	(5b)

where

N_o	=	0.602252×10^{24} (atoms/mole) Avogadro's number,
N	=	atom density (atoms/cm^3), $N_m = \Sigma N_i$,
ρ	=	density (g/cm^3) ,
A	=	atomic mass (g-mole) ,
w	=	weight fraction, $\Sigma w_i = 1$,
n	=	atom fraction, $\Sigma n_i = 1$,
subscript "m"	=	of the mixture ,
subscript "i"	=	i^{th} component of the mixture ,
(atoms/cm^3)($1/10^{24}$)	=	atoms/barn-cm.

Appendix 6.9.6

ABRIDGED SUMMARY TABLES OF CRITICALITY CALCULATION RESULTS

THIS PAGE INTENTIONALLY LEFT BLANK.

Appendix 6.9.6

ABRIDGED SUMMARY TABLES OF CRITICALITY CALCULATION RESULTS

This appendix contains the summary tables for calculation results identified in Sects. 6.4, 6.5, 6.6, and 6.7 of this document. The CV calculation model is a modification of the water-reflected, single-unit package calculation model where the packaging regions external to the containment vessel are replaced with full density water. The index is as follows:

CYLINDER CONTENT

Table 6.9.6-1 Results for the 3.24-in.-diam cylinder HEU content in CV calculation model.

Table 6.9.6-2 Results for the 3.24-in.-diam cylinder HEU content in bare and water reflected package calculation models.

Table 6.9.6-3 Results for the 3.24-in.-diam cylinder HEU content in package calculation models.

Table 6.9.6-3b Results for spacing of 3.24 in.-diameter cylinder HEU metal content in CV calculation model.

Table 6.9.6-3c Results for spacing of 3.24 in.-diameter cylinder HEU metal content in packaging calculation model.

SQUARE BAR CONTENT

Table 6.9.6-4 Results for the 2.29-in square bar HEU content in CV calculation model.

Table 6.9.6-5 Results for the 2.29-in square bar HEU content in packaging calculation model.

CYLINDER CONTENT

Table 6.9.6-6 Results for the 4.25-in.-diam cylinder HEU content in CV calculation model.

Table 6.9.6-7 Results for the 4.25-in.-diam cylinder HEU content in packaging calculation models.

SLUGS CONTENT

Table 6.9.6-8 Results for 1.5-in.-diam × 2.0-in.-tall slug HEU metal content in CV calculation model.

Table 6.9.6-9 Results for the 1.5-in.-diam × 2.0-in.-tall slug HEU metal content in packaging calculation model.

BROKEN METAL CONTENT

Table 6.9.6-10 Results for HEU broken metal content in CV calculation model.

Table 6.9.6-11 Results for HEU broken metal content in packaging calculation model.

Table 6.9.6-11b Comparison of NCT results for HEU broken metal content in ES-3100 NCT packaging calculation models

Table 6.9.6-11c Comparison of HAC results for HEU broken metal content in ES-3100 HAC packaging calculation models

HEU PRODUCT OXIDE CONTENT

Table 6.9.6-12 Results for HEU oxide content in CV calculation model.

Table 6.9.6-13 Results for HEU product oxide content at 6.54 g/cm^3 in single-unit packaging calculation model.

Table 6.9.6-13a Results for HEU oxide content in single-unit packaging calculation model.

Table 6.9.6-13b Results for HEU oxide content in array packaging calculation model.

UNX CRYSTAL CONTENT

Table 6.9.6-14 Results for UNX crystal content in CV calculation model.

Table 6.9.6-15 Results for UNX crystal content in packaging calculation model.

Table 6.9.6-16 Results for leakage of UNX crystal content out of containment vessel.

HEU SKULL OXIDE CONTENT

Table 6.9.6-17 Results for skull oxide (SO) content in CV calculation model.

Table 6.9.6-18a NCT results for SO content in packaging calculation model.

Table 6.9.6-18b HAC results for SO content in packaging calculation model.

UNIRRADIATED TRIGA REACTOR FUEL ELEMENT CONTENT

Table 6.9.6-19a Results for $UZrH_x$ content in CV calculation model.

Table 6.9.6-19b Results for $UZrH_x$ content spacing in CV calculation model.

Table 6.9.6-19c Results for $UZrH_x$ content uranium weight fraction in CV calculation model.

Table 6.9.6-20a Results for $UZrH_x$ content at 19.7 wt % ^{235}U in packaging calculation model.

Table 6.9.6-20b Results for $UZrH_x$ content at 70.1 wt % ^{235}U in packaging calculation model.

Table 6.9.6-20c Results for 1.31 in. Smaller diameter $UZrH_x$ at 70.1 wt % ^{235}U content in packaging calculation model.

Table 6.9.6-20d Results for 1.31 in. smaller diameter $UZrH_x$ at 19.7 wt % ^{235}U content in packaging calculation model.

AIR TRANSPORT CONTENT

Table 6.9.6-21	Results for solid HEU metal content for air transportation.
Table 6.9.6-22a	Results for TRIGA ($UZrH_x$) fuel element content at 19.7 wt % ^{235}U for air transportation.
Table 6.9.6-22b	Results for TRIGA ($UZrH_x$) fuel element content at 70.1 wt % ^{235}U for air transportation.
Table 6.9.6-23	Results for HEU broken metal content for air transport.

THIS PAGE INTENTIONALLY LEFT BLANK.

Table 6.9.6-1. Results for 3.24 in.-diameter cylinder HEU metal content in CV calculation model

case name	np (in.)	U (g)	^{235}U (g)	H_2O (g)	h/x	mocfr	k_{eff}	σ	$k_{eff}+2σ$				
flooded containment vessel, reflected													
no can spacers (np thickness = 0.0 in.)													
cvcrcyt11_36_1_1	0.0	36000	36000	0	0.00	1.0e-20	0.90460	0.00107	0.90673				
cvcrcyt11_36_1_6	0.0	36000	36000	829	0.60	1.0e-01	0.90726	0.00124	0.90973				
cvcrcyt11_36_1_7	0.0	36000	36000	1657	1.20	2.0e-01	0.91182	0.00120	0.91422				
cvcrcyt11_36_1_8	0.0	36000	36000	2486	1.80	3.0e-01	0.91690	0.00139	0.91967				
cvcrcyt11_36_1_9	0.0	36000	36000	3315	2.40	4.0e-01	0.92263	0.00119	0.92500				
cvcrcyt11_36_1_10	0.0	36000	36000	4143	3.00	5.0e-01	0.92840	0.00115	0.93071				
cvcrcyt11_36_1_11	0.0	36000	36000	4972	3.60	6.0e-01	0.93827	0.00112	0.94050				
cvcrcyt11_36_1_12	0.0	36000	36000	5801	4.21	7.0e-01	0.94633	0.00127	0.94886				
cvcrcyt11_36_1_13	0.0	36000	36000	6629	4.81	8.0e-01	0.95397	0.00120	0.95636				
cvcrcyt11_36_1_14	0.0	36000	36000	7458	5.41	9.0e-01	0.96276	0.00137	0.96551				
cvcrcyt11_36_1_15	0.0	36000	36000	8287	6.01	1.0e+00	0.97121	0.00125	0.97371				
cvcrcyt11_36_1	0.0	36000	36000	8287	6.01	1.0e+00	0.97121	0.00125	0.97371				
cvcrcyt11_35_1	0.0	35000	35000	8340	6.22	1.0e+00	0.96937	0.00120	0.97177				
cvcrcyt11_34_1	0.0	34000	34000	8393	6.44	1.0e+00	0.96886	0.00120	0.97126				
cvcrcyt11_33_1	0.0	33000	33000	8446	6.68	1.0e+00	0.96531	0.00111	0.96754				
cvcrcyt11_32_1	0.0	32000	32000	8499	6.93	1.0e+00	0.96360	0.00120	0.96600				
cvcrcyt11_31_1	0.0	31000	31000	8552	7.20	1.0e+00	0.95960	0.00122	0.96205				
cvcrcyt11_30_1	0.0	30000	30000	8605	7.49	1.0e+00	0.95842	0.00128	0.96097				
cvcrcyt11_29_1	0.0	29000	29000	8658	7.79	1.0e+00	0.95488	0.00115	0.95717				
cvcrcyt11_28_1	0.0	28000	28000	8711	8.12	1.0e+00	0.95409	0.00118	0.95645				
cvcrcyt11_27_1	0.0	27000	27000	8764	8.47	1.0e+00	0.94797	0.00113	0.95023				
cvcrcyt11_26_1	0.0	26000	26000	8817	8.85	1.0e+00	0.94376	0.00124	0.94623				

Table 6.9.6-1. Results for 3.24 in.-diameter cylinder HEU metal content in CV calculation model

case name	np (in.)	U (g)	^{235}U (g)	H_2O (g)	h/x	mocfr	k_{eff}	σ	k_{eff}+2σ				
cvcrcyt11_25_1	0.0	25000	25000	8870	9.26	1.0e+00	0.94075	0.00141	0.94357				
cvcrcyt11_24_1	0.0	24000	24000	8923	9.70	1.0e+00	0.93510	0.00133	0.93776				
cvcrcyt11_23_1	0.0	23000	23000	8977	10.19	1.0e+00	0.93038	0.00130	0.93298				
cvcrcyt11_22_1	0.0	22000	22000	9030	10.71	1.0e+00	0.92658	0.00106	0.92870				
cvcrcyt11_21_1	0.0	21000	21000	9083	11.29	1.0e+00	0.92046	0.00118	0.92282				
cvcrcyt11_20_1	0.0	20000	20000	9136	11.92	1.0e+00	0.91168	0.00125	0.91418				
cvcrcyt11_19_1	0.0	19000	19000	9189	12.62	1.0e+00	0.90618	0.00128	0.90874				
cvcrcyt11_18_1	0.0	18000	18000	9242	13.40	1.0e+00	0.89978	0.00124	0.90226				
with can spacers (np thickness=1.4 in.)													
cvcrcyt11_36_2_1	1.4	36000	36000	0	0.00	1.0e-20	0.83041	0.00103	0.83248				
cvcrcyt11_36_2_6	1.4	36000	36000	767	0.56	1.0e-01	0.82885	0.00106	0.83096				
cvcrcyt11_36_2_7	1.4	36000	36000	1535	1.11	2.0e-01	0.83022	0.00104	0.83230				
cvcrcyt11_36_2_8	1.4	36000	36000	2302	1.67	3.0e-01	0.83492	0.00104	0.83699				
cvcrcyt11_36_2_9	1.4	36000	36000	3069	2.23	4.0e-01	0.84066	0.00123	0.84311				
cvcrcyt11_36_2_10	1.4	36000	36000	3837	2.78	5.0e-01	0.84789	0.00102	0.84993				
cvcrcyt11_36_2_11	1.4	36000	36000	4604	3.34	6.0e-01	0.85423	0.00101	0.85624				
cvcrcyt11_36_2_12	1.4	36000	36000	5371	3.89	7.0e-01	0.86190	0.00106	0.86403				
cvcrcyt11_36_2_13	1.4	36000	36000	6139	4.45	8.0e-01	0.86687	0.00118	0.86923				
cvcrcyt11_36_2_14	1.4	36000	36000	6906	5.01	9.0e-01	0.87589	0.00113	0.87816				
cvcrcyt11_36_2_15	1.4	36000	36000	7673	5.56	1.0e+00	0.88436	0.00111	0.88657				
cvcrcyt11_36_2	1.4	36000	36000	7673	5.56	1.0e+00	0.88436	0.00111	0.88657				
cvcrcyt11_35_2	1.4	35000	35000	7726	5.76	1.0e+00	0.88274	0.00108	0.88491				
cvcrcyt11_34_2	1.4	34000	34000	7779	5.97	1.0e+00	0.87740	0.00119	0.87977				
cvcrcyt11_33_2	1.4	33000	33000	7832	6.19	1.0e+00	0.87234	0.00112	0.87459				

Table 6.9.6-1. Results for 3.24 in.-diameter cylinder HEU metal content in CV calculation model

case name	np (in.)	U (g)	^{235}U (g)	H_2O (g)	h/x	mocfr	k_{eff}	σ	k_{eff}+2σ				
cvcrcyt11_32_2	1.4	32000	32000	7885	6.43	1.0e+00	0.86817	0.00108	0.87033				
cvcrcyt11_31_2	1.4	31000	31000	7938	6.68	1.0e+00	0.86047	0.00124	0.86295				
cvcrcyt11_30_2	1.4	30000	30000	7992	6.95	1.0e+00	0.85525	0.00117	0.85760				
flooded containment vessel, reflected, no can spacers (np thickness = 0.0 in.)													
no polyethylene													
cvcrcyt11_21_1	0.0	21000	21000	9083	11.29	1.0e+00	0.92046	0.00118	0.92282				
500 g polyethylene													
cvcrpcyt11_21_1	0.0	21000	21000	8540	11.41	1.0e+00	0.90599	0.00107	0.90814				
dry containment vessel, reflected, no can spacers (np thickness = 0.0 in.)													
500 g polyethylene													
cvdcrpcyt11_21_1	0.0	21000	21000	0.0	0.80	1.0e+00	0.84505	0.00105	0.84716				

Table 6.9.6-2. Results for 3.24 in.-diameter cylinder HEU metal content in bare and water reflected packaging calculation models

case name	U (g)	^{235}U (g)	H_2O (g)	h/x	moifr	nlf	k_{eff}	σ	k_{eff}+2σ	case name	nlf	k_{eff}	σ	k_{eff}+2σ
content in flooded CV, single package bare										**content in flooded CV, single package reflected**				
no can spacers (np thickness = 0.0 in.)										**no can spacers (np thickness = 0.0 in.)**				
ncsbcyt11_36_1_1	36000	36000	8287	6.01	1.0e-20	0.4744	0.90856	0.00115	0.91087	ncsrcyt11_36_1_1	0.0021	0.91542	0.00120	0.91782
ncsbcyt11_36_1_2	36000	36000	8287	6.01	1.0e-05	0.4749	0.90825	0.00100	0.91026	ncsrcyt11_36_1_2	0.0021	0.91477	0.00123	0.91724
ncsbcyt11_36_1_3	36000	36000	8287	6.01	1.0e-04	0.4747	0.90817	0.00121	0.91059	ncsrcyt11_36_1_3	0.0022	0.91550	0.00111	0.91772
ncsbcyt11_36_1_4	36000	36000	8287	6.01	1.0e-03	0.4744	0.90926	0.00134	0.91194	ncsrcyt11_36_1_4	0.0022	0.91636	0.00117	0.91869
ncsbcyt11_36_1_5	36000	36000	8287	6.01	1.0e-02	0.4730	0.90883	0.00108	0.91100	ncsrcyt11_36_1_5	0.0022	0.91537	0.00109	0.91755
ncsbcyt11_36_1_6	36000	36000	8287	6.01	1.0e-01	0.4510	0.91550	0.00112	0.91774	ncsrcyt11_36_1_6	0.0019	0.92121	0.00133	0.92386
ncsbcyt11_36_1_8	36000	36000	8287	6.01	3.0e-01	0.3899	0.92546	0.00134	0.92814	ncsrcyt11_36_1_8	0.0016	0.92807	0.00112	0.93032

Table 6.9.6-2. Results for 3.24 in.-diameter cylinder HEU metal content in bare and water reflected packaging calculation models

case name	U (g)	^{235}U (g)	H_2O (g)	h/x	moifr	nlf	k_{eff}	σ	$k_{eff}+2σ$	case name	nlf	k_{eff}	σ	$k_{eff}+2σ$
ncsbcyt11_36_1_15	36000	36000	8287	6.01	1.0e+00	0.1823	0.95215	0.00119	0.95454	ncsrcyt11_36_1_15	0.0007	0.95213	0.00129	0.95472
ncsbcyt11_36_1_15	36000	36000	8287	6.01	1.0e+00	0.1823	0.95215	0.00119	0.95454	ncsrcyt11_36_1_15	0.0007	0.95213	0.00129	0.95472
ncsbcyt11_35_1_15	35000	35000	8340	6.22	1.0e+00	0.1838	0.94834	0.00122	0.95077	ncsrcyt11_35_1_15	0.0008	0.94870	0.00107	0.95083
ncsbcyt11_34_1_15	34000	34000	8393	6.44	1.0e+00	0.1842	0.94748	0.00113	0.94975	ncsrcyt11_34_1_15	0.0008	0.94742	0.00124	0.94990
ncsbcyt11_33_1_15	33000	33000	8446	6.68	1.0e+00	0.1853	0.94613	0.00118	0.94850	ncsrcyt11_33_1_15	0.0008	0.94478	0.00119	0.94716
ncsbcyt11_32_1_15	32000	32000	8499	6.93	1.0e+00	0.1863	0.94237	0.00106	0.94448	ncsrcyt11_32_1_15	0.0007	0.94247	0.00111	0.94468
ncsbcyt11_31_1_15	31000	31000	8552	7.20	1.0e+00	0.1867	0.94052	0.00106	0.94264	ncsrcyt11_31_1_15	0.0008	0.94091	0.00107	0.94306
ncsbcyt11_30_1_15	30000	30000	8605	7.49	1.0e+00	0.1882	0.93819	0.00110	0.94039	ncsrcyt11_30_1_15	0.0007	0.94139	0.00137	0.94412
ncsbcyt11_29_1_15	29000	29000	8658	7.79	1.0e+00	0.1894	0.93483	0.00104	0.93692	ncsrcyt11_29_1_15	0.0007	0.93406	0.00108	0.93622
ncsbcyt11_28_1_15	28000	28000	8711	8.12	1.0e+00	0.1894	0.93339	0.00102	0.93543	ncsrcyt11_28_1_15	0.0008	0.93012	0.00124	0.93261
ncsbcyt11_27_1_15	27000	27000	8764	8.47	1.0e+00	0.1911	0.92636	0.00112	0.92860	ncsrcyt11_27_1_15	0.0008	0.92820	0.00122	0.93064
ncsbcyt11_26_1_15	26000	26000	8817	8.85	1.0e+00	0.1919	0.92366	0.00115	0.92597	ncsrcyt11_26_1_15	0.0008	0.92396	0.00141	0.92679
ncsbcyt11_25_1_15	25000	25000	8870	9.26	1.0e+00	0.1928	0.92122	0.00122	0.92366	ncsrcyt11_25_1_15	0.0008	0.91761	0.00102	0.91966
ncsbcyt11_24_1_15	24000	24000	8923	9.70	1.0e+00	0.1948	0.91432	0.00108	0.91648	ncsrcyt11_24_1_15	0.0008	0.91466	0.00107	0.91680
ncsbcyt11_23_1_15	23000	23000	8977	10.19	1.0e+00	0.1965	0.91055	0.00130	0.91314	ncsrcyt11_23_1_15	0.0008	0.91172	0.00116	0.91403
ncsbcyt11_22_1_15	22000	22000	9030	10.71	1.0e+00	0.1969	0.90695	0.00121	0.90936	ncsrcyt11_22_1_15	0.0008	0.90680	0.00153	0.90986
ncsbcyt11_21_1_15	21000	21000	9083	11.29	1.0e+00	0.1984	0.90241	0.00124	0.90490	ncsrcyt11_21_1_15	0.0009	0.90125	0.00113	0.90352
ncsbcyt11_20_1_15	20000	20000	9136	11.92	1.0e+00	0.2007	0.89477	0.00125	0.89726	ncsrcyt11_20_1_15	0.0009	0.89481	0.00109	0.89698
ncsbcyt11_19_1_15	19000	19000	9189	12.62	1.0e+00	0.2026	0.88819	0.00113	0.89044	ncsrcyt11_19_1_15	0.0008	0.88857	0.00136	0.89129
ncsbcyt11_18_1_15	18000	18000	9242	13.40	1.0e+00	0.2037	0.88255	0.00126	0.88507	ncsrcyt11_18_1_15	0.0008	0.88157	0.00127	0.88410
with can spacers (np thickness = 1.4 in.)										**with can spacers (np thickness = 1.4 in.)**				
ncsbcyt11_36_2_1	36000	36000	7673	5.56	1.0e-20	0.4882	0.83390	0.00106	0.83603	ncsrcyt11_36_2_1	0.0022	0.83904	0.00110	0.84125
ncsbcyt11_36_2_2	36000	36000	7673	5.56	1.0e-05	0.4879	0.83481	0.00142	0.83764	ncsrcyt11_36_2_2	0.0021	0.84122	0.00110	0.84342
ncsbcyt11_36_2_3	36000	36000	7673	5.56	1.0e-04	0.4883	0.83383	0.00100	0.83583	ncsrcyt11_36_2_3	0.0022	0.84013	0.00106	0.84225

Table 6.9.6-2. Results for 3.24 in.-diameter cylinder HEU metal content in bare and water reflected packaging calculation models

case name	U (g)	^{235}U (g)	H_2O (g)	h/x	moifr	nlf	k_{eff}	σ	k_{eff}+2σ	case name	nlf	k_{eff}	σ	k_{eff}+2σ
ncsbcyt11_36_2_4	36000	36000	7673	5.56	1.0e-03	0.4880	0.83530	0.00126	0.83783	ncsrcyt11_36_2_4	0.0022	0.84001	0.00112	0.84224
ncsbcyt11_36_2_5	36000	36000	7673	5.56	1.0e-02	0.4861	0.83461	0.00120	0.83702	ncsrcyt11_36_2_5	0.0021	0.84128	0.00115	0.84359
ncsbcyt11_36_2_6	36000	36000	7673	5.56	1.0e-01	0.4642	0.83979	0.00110	0.84199	ncsrcyt11_36_2_6	0.0020	0.84524	0.00116	0.84755
ncsbcyt11_36_2_8	36000	36000	7673	5.56	3.0e-01	0.4000	0.84736	0.00123	0.84982	ncsrcyt11_36_2_8	0.0016	0.84947	0.00103	0.85153
ncsbcyt11_36_2_15	36000	36000	7673	5.56	1.0e+00	0.1881	0.87048	0.00109	0.87266	ncsrcyt11_36_2_15	0.0008	0.87062	0.00122	0.87305
ncsbcyt11_36_2_15	36000	36000	7673	5.56	1.0e+00	0.1881	0.87048	0.00109	0.87266	ncsrcyt11_36_2_15	0.0008	0.87062	0.00122	0.87305
ncsbcyt11_35_2_15	35000	35000	7726	5.76	1.0e+00	0.1879	0.86609	0.00114	0.86836	ncsrcyt11_35_2_15	0.0007	0.86649	0.00118	0.86886
ncsbcyt11_34_2_15	34000	34000	7779	5.97	1.0e+00	0.1885	0.86151	0.00103	0.86358	ncsrcyt11_34_2_15	0.0008	0.86038	0.00129	0.86296
ncsbcyt11_33_2_15	33000	33000	7832	6.19	1.0e+00	0.1901	0.85729	0.00099	0.85927	ncsrcyt11_33_2_15	0.0007	0.85903	0.00106	0.86115
ncsbcyt11_32_2_15	32000	32000	7885	6.43	1.0e+00	0.1908	0.85350	0.00116	0.85582	ncsrcyt11_32_2_15	0.0007	0.85357	0.00108	0.85573
ncsbcyt11_31_2_15	31000	31000	7938	6.68	1.0e+00	0.1922	0.84914	0.00108	0.85129	ncsrcyt11_31_2_15	0.0008	0.84895	0.00123	0.85142
ncsbcyt11_30_2_15	30000	30000	7992	6.95	1.0e+00	0.1913	0.84250	0.00100	0.84450	ncsrcyt11_30_2_15	0.0008	0.84343	0.00114	0.84572

Table 6.9.6-3. Results for 3.24 in.-diameter cylinder HEU metal content in packaging calculation model

case name	np (in)	U (g)	^{235}U (g)	H_2O (g)	h/x	moifr	k_{eff}	σ	k_{eff}+2σ	case name	k_{eff}	σ	k_{eff}+2σ
content in flooded containment vessel, single package reflected													
NCT										HAC			
no can spacers (np thickness = 0.0 in.)													
ncsrcyt11_36_1_1	0.0	36000	36000	8287	6.01	1.0e-20	0.91542	0.00120	0.91782	hcsrcyt12_36_1_1	0.91636	0.00117	0.91869
ncsrcyt11_36_1_2	0.0	36000	36000	8287	6.01	1.0e-05	0.91477	0.00123	0.91724	hcsrcyt12_36_1_2	0.91593	0.00138	0.91869
ncsrcyt11_36_1_3	0.0	36000	36000	8287	6.01	1.0e-04	0.91550	0.00111	0.91772	hcsrcyt12_36_1_3	0.91660	0.00134	0.91929
ncsrcyt11_36_1_4	0.0	36000	36000	8287	6.01	1.0e-03	0.91636	0.00117	0.91869	hcsrcyt12_36_1_4	0.91565	0.00122	0.91810

Table 6.9.6-3. Results for 3.24 in.-diameter cylinder HEU metal content in packaging calculation model

case name	np (in)	U (g)	^{235}U (g)	H_2O (g)	h/x	moifr	k_{eff}	σ	k_{eff}+2σ	case name	k_{eff}	σ	k_{eff}+2σ
ncsrcyt11_36_1_5	0.0	36000	36000	8287	6.01	1.0e-02	0.91537	0.00109	0.91755	hcsrcyt12_36_1_5	0.91489	0.00120	0.91729
ncsrcyt11_36_1_6	0.0	36000	36000	8287	6.01	1.0e-01	0.92121	0.00133	0.92386	hcsrcyt12_36_1_6	0.92198	0.00104	0.92407
ncsrcyt11_36_1_8	0.0	36000	36000	8287	6.01	3.0e-01	0.92807	0.00112	0.93032	hcsrcyt12_36_1_8	0.92950	0.00125	0.93201
ncsrcyt11_36_1_15	0.0	36000	36000	8287	6.01	1.0e+00	0.95213	0.00129	0.95472	hcsrcyt12_36_1_15	0.95112	0.00120	0.95353
ncsrcyt11_36_1_15	0.0	36000	36000	8287	6.01	1.0e+00	0.95213	0.00129	0.95472	hcsrcyt12_36_1_15	0.95112	0.00120	0.95353
ncsrcyt11_35_1_15	0.0	35000	35000	8340	6.22	1.0e+00	0.94870	0.00107	0.95083	hcsrcyt12_35_1_15	0.94915	0.00120	0.95155
ncsrcyt11_34_1_15	0.0	34000	34000	8393	6.44	1.0e+00	0.94742	0.00124	0.94990	hcsrcyt12_34_1_15	0.94863	0.00113	0.95088
ncsrcyt11_33_1_15	0.0	33000	33000	8446	6.68	1.0e+00	0.94478	0.00119	0.94716	hcsrcyt12_33_1_15	0.94610	0.00123	0.94856
ncsrcyt11_32_1_15	0.0	32000	32000	8499	6.93	1.0e+00	0.94247	0.00111	0.94468	hcsrcyt12_32_1_15	0.94528	0.00141	0.94810
ncsrcyt11_31_1_15	0.0	31000	31000	8552	7.20	1.0e+00	0.94091	0.00107	0.94306	hcsrcyt12_31_1_15	0.94090	0.00107	0.94304
ncsrcyt11_30_1_15	0.0	30000	30000	8605	7.49	1.0e+00	0.94139	0.00137	0.94412	hcsrcyt12_30_1_15	0.94035	0.00120	0.94275
ncsrcyt11_29_1_15	0.0	29000	29000	8658	7.79	1.0e+00	0.93406	0.00108	0.93622	hcsrcyt12_29_1_15	0.93540	0.00112	0.93765
ncsrcyt11_28_1_15	0.0	28000	28000	8711	8.12	1.0e+00	0.93012	0.00124	0.93261	hcsrcyt12_28_1_15	0.93239	0.00118	0.93475
ncsrcyt11_27_1_15	0.0	27000	27000	8764	8.47	1.0e+00	0.92820	0.00122	0.93064	hcsrcyt12_27_1_15	0.93043	0.00144	0.93331
ncsrcyt11_26_1_15	0.0	26000	26000	8817	8.85	1.0e+00	0.92396	0.00141	0.92679	hcsrcyt12_26_1_15	0.92632	0.00119	0.92870
ncsrcyt11_25_1_15	0.0	25000	25000	8870	9.26	1.0e+00	0.91761	0.00102	0.91966	hcsrcyt12_25_1_15	0.92218	0.00109	0.92436
ncsrcyt11_24_1_15	0.0	24000	24000	8923	9.70	1.0e+00	0.91466	0.00107	0.91680	hcsrcyt12_24_1_15	0.91688	0.00117	0.91922
ncsrcyt11_23_1_15	0.0	23000	23000	8977	10.19	1.0e+00	0.91172	0.00116	0.91403	hcsrcyt12_23_1_15	0.91134	0.00119	0.91371
ncsrcyt11_22_1_15	0.0	22000	22000	9030	10.71	1.0e+00	0.90680	0.00153	0.90986	hcsrcyt12_22_1_15	0.90850	0.00113	0.91077
ncsrcyt11_21_1_15	0.0	21000	21000	9083	11.29	1.0e+00	0.90125	0.00113	0.90352	hcsrcyt12_21_1_15	0.90188	0.00124	0.90437
ncsrcyt11_20_1_15	0.0	20000	20000	9136	11.92	1.0e+00	0.89481	0.00109	0.89698	hcsrcyt12_20_1_15	0.89612	0.00115	0.89842
ncsrcyt11_19_1_15	0.0	19000	19000	9189	12.62	1.0e+00	0.88857	0.00136	0.89129	hcsrcyt12_19_1_15	0.89080	0.00122	0.89323
ncsrcyt11_18_1_15	0.0	18000	18000	9242	13.40	1.0e+00	0.88157	0.00127	0.88410	hcsrcyt12_18_1_15	0.88276	0.00128	0.88532

Table 6.9.6-3. Results for 3.24 in.-diameter cylinder HEU metal content in packaging calculation model

case name	np (in)	U (g)	^{235}U (g)	H_2O (g)	h/x	moifr	k_{eff}	σ	$k_{eff}+2σ$	case name	k_{eff}	σ	$k_{eff}+2σ$
with can spacers (np thickness = 1.4 in.)													
ncsrcyt11_36_2_1	1.4	36000	36000	7673	5.56	1.0e-20	0.83904	0.00110	0.84125	hcsrcyt12_36_2_1	0.84250	0.00103	0.84456
ncsrcyt11_36_2_2	1.4	36000	36000	7673	5.56	1.0e-05	0.84122	0.00110	0.84342	hcsrcyt12_36_2_2	0.84146	0.00118	0.84382
ncsrcyt11_36_2_3	1.4	36000	36000	7673	5.56	1.0e-04	0.84013	0.00106	0.84225	hcsrcyt12_36_2_3	0.84182	0.00105	0.84392
ncsrcyt11_36_2_4	1.4	36000	36000	7673	5.56	1.0e-03	0.84001	0.00112	0.84224	hcsrcyt12_36_2_4	0.83975	0.00103	0.84181
ncsrcyt11_36_2_5	1.4	36000	36000	7673	5.56	1.0e-02	0.84128	0.00115	0.84359	hcsrcyt12_36_2_5	0.84070	0.00129	0.84328
ncsrcyt11_36_2_6	1.4	36000	36000	7673	5.56	1.0e-01	0.84524	0.00116	0.84755	hcsrcyt12_36_2_6	0.84484	0.00127	0.84738
ncsrcyt11_36_2_8	1.4	36000	36000	7673	5.56	3.0e-01	0.84947	0.00103	0.85153	hcsrcyt12_36_2_8	0.85159	0.00102	0.85364
ncsrcyt11_36_2_15	1.4	36000	36000	7673	5.56	1.0e+00	0.87062	0.00122	0.87305	hcsrcyt12_36_2_15	0.87110	0.00117	0.87344
ncsrcyt11_36_2_15	1.4	36000	36000	7673	5.56	1.0e+00	0.87062	0.00122	0.87305	hcsrcyt12_36_2_15	0.87110	0.00117	0.87344
ncsrcyt11_35_2_15	1.4	35000	35000	7726	5.76	1.0e+00	0.86649	0.00118	0.86886	hcsrcyt12_35_2_15	0.86666	0.00110	0.86886
ncsrcyt11_34_2_15	1.4	34000	34000	7779	5.97	1.0e+00	0.86038	0.00129	0.86296	hcsrcyt12_34_2_15	0.86109	0.00117	0.86343
ncsrcyt11_33_2_15	1.4	33000	33000	7832	6.19	1.0e+00	0.85903	0.00106	0.86115	hcsrcyt12_33_2_15	0.86022	0.00123	0.86267
ncsrcyt11_32_2_15	1.4	32000	32000	7885	6.43	1.0e+00	0.85357	0.00108	0.85573	hcsrcyt12_32_2_15	0.85544	0.00096	0.85736
ncsrcyt11_31_2_15	1.4	31000	31000	7938	6.68	1.0e+00	0.84895	0.00123	0.85142	hcsrcyt12_31_2_15	0.84745	0.00105	0.84956
ncsrcyt11_30_2_15	1.4	30000	30000	7992	6.95	1.0e+00	0.84343	0.00114	0.84572	hcsrcyt12_30_2_15	0.84390	0.00112	0.84615
content in flooded containment vessel, array packaging model for CSI=0.0													
NCT										HAC			
no can spacers (np thickness = 0.0 in.)													
nciacyt11_36_1_1	0.0	36000	36000	8287	6.01	1.0e-20	1.02410	0.00125	1.02660	hciacyt12_36_1_1	1.02427	0.00120	1.02667
nciacyt11_36_1_2	0.0	36000	36000	8287	6.01	1.0e-05	1.02380	0.00124	1.02628	hciacyt12_36_1_2	1.02384	0.00130	1.02644
nciacyt11_36_1_3	0.0	36000	36000	8287	6.01	1.0e-04	1.02208	0.00111	1.02430	hciacyt12_36_1_3	1.02390	0.00135	1.02660
nciacyt11_36_1_4	0.0	36000	36000	8287	6.01	1.0e-03	1.02276	0.00134	1.02545	hciacyt12_36_1_4	1.02441	0.00122	1.02684
nciacyt11_36_1_5	0.0	36000	36000	8287	6.01	1.0e-02	1.01749	0.00124	1.01997	hciacyt12_36_1_5	1.01867	0.00114	1.02094

Table 6.9.6-3. Results for 3.24 in.-diameter cylinder HEU metal content in packaging calculation model

case name	np (in)	U (g)	^{235}U (g)	H_2O (g)	h/x	moifr	k_{eff}	σ	$k_{eff}+2σ$	case name	k_{eff}	σ	$k_{eff}+2σ$
nciacyt11_36_1_6	0.0	36000	36000	8287	6.01	1.0e-01	0.98560	0.00118	0.98797	hciacyt12_36_1_6	0.98825	0.00112	0.99048
nciacyt11_36_1_8	0.0	36000	36000	8287	6.01	3.0e-01	0.96228	0.00116	0.96461	hciacyt12_36_1_8	0.96519	0.00122	0.96763
nciacyt11_36_1_15	0.0	36000	36000	8287	6.01	1.0e+00	0.96088	0.00119	0.96326	hciacyt12_36_1_15	0.96417	0.00119	0.96655
nciacyt11_36_1_3	0.0	36000	36000	8287	6.01	1.0e-04	1.02208	0.00111	1.02430	hciacyt12_36_1_3	1.02390	0.00135	1.02660
nciacyt11_35_1_3	0.0	35000	35000	8340	6.22	1.0e-04	1.01930	0.00118	1.02166	hciacyt12_35_1_3	1.01912	0.00127	1.02165
nciacyt11_34_1_3	0.0	34000	34000	8393	6.44	1.0e-04	1.01654	0.00130	1.01914	hciacyt12_34_1_3	1.01860	0.00104	1.02068
nciacyt11_33_1_3	0.0	33000	33000	8446	6.68	1.0e-04	1.01121	0.00116	1.01353	hciacyt12_33_1_3	1.01077	0.00142	1.01361
nciacyt11_32_1_3	0.0	32000	32000	8499	6.93	1.0e-04	1.00876	0.00134	1.01144	hciacyt12_32_1_3	1.00943	0.00114	1.01171
nciacyt11_31_1_3	0.0	31000	31000	8552	7.20	1.0e-04	1.00544	0.00116	1.00777	hciacyt12_31_1_3	1.00148	0.00102	1.00353
nciacyt11_30_1_3	0.0	30000	30000	8605	7.49	1.0e-04	0.99921	0.00131	1.00182	hciacyt12_30_1_3	0.99963	0.00138	1.00238
nciacyt11_29_1_3	0.0	29000	29000	8658	7.79	1.0e-04	0.99494	0.00121	0.99736	hciacyt12_29_1_3	0.99453	0.00117	0.99687
nciacyt11_28_1_3	0.0	28000	28000	8711	8.12	1.0e-04	0.98905	0.00124	0.99152	hciacyt12_28_1_3	0.99159	0.00123	0.99405
nciacyt11_27_1_3	0.0	27000	27000	8764	8.47	1.0e-04	0.98520	0.00115	0.98750	hciacyt12_27_1_3	0.98720	0.00122	0.98963
nciacyt11_26_1_3	0.0	26000	26000	8817	8.85	1.0e-04	0.97887	0.00117	0.98120	hciacyt12_26_1_3	0.97870	0.00130	0.98129
nciacyt11_25_1_3	0.0	25000	25000	8870	9.26	1.0e-04	0.97441	0.00118	0.97676	hciacyt12_25_1_3	0.97501	0.00106	0.97713
nciacyt11_24_1_3	0.0	24000	24000	8923	9.70	1.0e-04	0.96997	0.00115	0.97228	hciacyt12_24_1_3	0.96945	0.00122	0.97188
nciacyt11_23_1_3	0.0	23000	23000	8977	10.19	1.0e-04	0.96203	0.00122	0.96447	hciacyt12_23_1_3	0.96228	0.00121	0.96469
nciacyt11_22_1_3	0.0	22000	22000	9030	10.71	1.0e-04	0.95256	0.00110	0.95475	hciacyt12_22_1_3	0.95313	0.00138	0.95589
nciacyt11_21_1_3	0.0	21000	21000	9083	11.29	1.0e-04	0.94755	0.00114	0.94982	hciacyt12_21_1_3	0.94735	0.00121	0.94976
nciacyt11_20_1_3	0.0	20000	20000	9136	11.92	1.0e-04	0.93967	0.00124	0.94215	hciacyt12_20_1_3	0.94131	0.00113	0.94357
nciacyt11_19_1_3	0.0	19000	19000	9189	12.62	1.0e-04	0.93107	0.00113	0.93334	hciacyt12_19_1_3	0.92967	0.00120	0.93207
nciacyt11_18_1_3	0.0	18000	18000	9242	13.40	1.0e-04	0.92165	0.00100	0.92366	hciacyt12_18_1_3	0.92083	0.00110	0.92302
nciacyt11_15_1_3	0.0	15000	15000	9401	16.36	1.0e-04	0.88925	0.00111	0.89146	hciacyt12_15_1_3	0.88802	0.00116	0.89034
nciacyt11_12_1_3	0.0	12000	12000	9560	20.79	1.0e-04	0.84430	0.00103	0.84636	hciacyt12_12_1_3	0.84558	0.00110	0.84777

Table 6.9.6-3. Results for 3.24 in.-diameter cylinder HEU metal content in packaging calculation model

case name	np (in)	U (g)	^{235}U (g)	H_2O (g)	h/x	moifr	k_{eff}	σ	$k_{eff}+2σ$	case name	k_{eff}	σ	$k_{eff}+2σ$
hciacyt11_9_1_3	0.0	9000	9000	9719	28.19	1.0e-04	0.78552	0.00116	0.78784	hciacyt12_9_1_3	0.78464	0.00132	0.78728
hciacyt11_6_1_3	0.0	6000	6000	9879	42.97	1.0e-04	0.69176	0.00119	0.69414	hciacyt12_6_1_3	0.69169	0.00122	0.69413
hciacyt11_3_1_3	0.0	3000	3000	10038	87.33	1.0e-04	0.53217	0.00084	0.53385	hciacyt12_3_1_3	0.53298	0.00091	0.53481
with can spacers (np thickness = 1.4 in.)													
hciacyt11_36_2_1	1.4	36000	36000	7673	5.56	1.0e-20	0.95474	0.00109	0.95693	hciacyt12_36_2_1	0.95429	0.00106	0.95641
hciacyt11_36_2_2	1.4	36000	36000	7673	5.56	1.0e-05	0.95402	0.00119	0.95640	hciacyt12_36_2_2	0.95522	0.00105	0.95732
hciacyt11_36_2_3	1.4	36000	36000	7673	5.56	1.0e-04	0.95362	0.00105	0.95571	hciacyt12_36_2_3	0.95319	0.00139	0.95596
hciacyt11_36_2_4	1.4	36000	36000	7673	5.56	1.0e-03	0.95222	0.00128	0.95478	hciacyt12_36_2_4	0.95333	0.00116	0.95564
hciacyt11_36_2_5	1.4	36000	36000	7673	5.56	1.0e-02	0.94649	0.00110	0.94869	hciacyt12_36_2_5	0.94837	0.00124	0.95084
hciacyt11_36_2_6	1.4	36000	36000	7673	5.56	1.0e-01	0.91268	0.00128	0.91524	hciacyt12_36_2_6	0.91591	0.00121	0.91834
hciacyt11_36_2_8	1.4	36000	36000	7673	5.56	3.0e-01	0.88453	0.00140	0.88733	hciacyt12_36_2_8	0.89062	0.00119	0.89300
hciacyt11_36_2_15	1.4	36000	36000	7673	5.56	1.0e+00	0.87822	0.00106	0.88034	hciacyt12_36_2_15	0.88152	0.00135	0.88423
hciacyt11_36_2_3	1.4	36000	36000	7673	5.56	1.0e-04	0.95362	0.00105	0.95571	hciacyt12_36_2_3	0.95319	0.00139	0.95596
hciacyt11_35_2_3	1.4	35000	35000	7726	5.76	1.0e-04	0.94906	0.00125	0.95156	hciacyt12_35_2_3	0.94788	0.00129	0.95046
hciacyt11_34_2_3	1.4	34000	34000	7779	5.97	1.0e-04	0.94393	0.00136	0.94664	hciacyt12_34_2_3	0.94428	0.00130	0.94687
hciacyt11_33_2_3	1.4	33000	33000	7832	6.19	1.0e-04	0.93703	0.00114	0.93930	hciacyt12_33_2_3	0.93708	0.00122	0.93952
hciacyt11_32_2_3	1.4	32000	32000	7885	6.43	1.0e-04	0.92940	0.00125	0.93191	hciacyt12_32_2_3	0.93065	0.00109	0.93283
hciacyt11_31_2_3	1.4	31000	31000	7938	6.68	1.0e-04	0.92483	0.00119	0.92721	hciacyt12_31_2_3	0.92625	0.00125	0.92874
hciacyt11_30_2_3	1.4	30000	30000	7992	6.95	1.0e-04	0.91737	0.00106	0.91949	hciacyt12_30_2_3	0.91983	0.00107	0.92198
hciacyt11_29_2_3	1.4	29000	29000	8045	7.24	1.0e-04	0.91253	0.00116	0.91484	hciacyt12_29_2_3	0.91204	0.00107	0.91419
hciacyt11_28_2_3	1.4	28000	28000	8098	7.55	1.0e-04	0.90504	0.00117	0.90737	hciacyt12_28_2_3	0.90515	0.00100	0.90716
hciacyt11_27_2_3	1.4	27000	27000	8151	7.88	1.0e-04	0.89967	0.00121	0.90208	hciacyt12_27_2_3	0.89749	0.00097	0.89942
hciacyt11_26_2_3	1.4	26000	26000	8204	8.24	1.0e-04	0.89129	0.00107	0.89343	hciacyt12_26_2_3	0.88997	0.00124	0.89246
hciacyt11_25_2_3	1.4	25000	25000	8257	8.62	1.0e-04	0.88183	0.00104	0.88391	hciacyt12_25_2_3	0.88253	0.00129	0.88511

Table 6.9.6-3. Results for 3.24 in.-diameter cylinder HEU metal content in packaging calculation model

case name	np (in)	U (g)	^{235}U (g)	H_2O (g)	h/x	moifr	k_{eff}	σ	k_{eff}+2σ	case name	k_{eff}	σ	k_{eff}+2σ
nciacyt11_24_2_3	1.4	24000	24000	8310	9.04	1.0e-04	0.87406	0.00117	0.87640	hciacyt12_24_2_3	0.87448	0.00117	0.87681
nciacyt11_23_2_3	1.4	23000	23000	8363	9.49	1.0e-04	0.86345	0.00109	0.86564	hciacyt12_23_2_3	0.86388	0.00119	0.86626
nciacyt11_22_2_3	1.4	22000	22000	8416	9.98	1.0e-04	0.85413	0.00107	0.85627	hciacyt12_22_2_3	0.85333	0.00109	0.85551
nciacyt11_21_2_3	1.4	21000	21000	8469	10.53	1.0e-04	0.84424	0.00109	0.84642	hciacyt12_21_2_3	0.84414	0.00111	0.84636
nciacyt11_20_2_3	1.4	20000	20000	8522	11.12	1.0e-04	0.83545	0.00106	0.83756	hciacyt12_20_2_3	0.83388	0.00099	0.83585
nciacyt11_19_2_3	1.4	19000	19000	8575	11.78	1.0e-04	0.82051	0.00130	0.82311	hciacyt12_19_2_3	0.82263	0.00109	0.82480
nciacyt11_18_2_3	1.4	18000	18000	8628	12.51	1.0e-04	0.81105	0.00122	0.81350	hciacyt12_18_2_3	0.81076	0.00113	0.81301
nciacyt11_15_2_3	1.4	15000	15000	8787	15.29	1.0e-04	0.76734	0.00107	0.76948	hciacyt12_15_2_3	0.76757	0.00102	0.76960
nciacyt11_12_2_3	1.4	12000	12000	8947	19.46	1.0e-04	0.71377	0.00097	0.71571	hciacyt12_12_2_3	0.71466	0.00102	0.71669
nciacyt11_9_2_3	1.4	9000	9000	9106	26.41	1.0e-04	0.64515	0.00110	0.64734	hciacyt12_9_2_3	0.64486	0.00103	0.64692
nciacyt11_6_2_3	1.4	6000	6000	9265	40.30	1.0e-04	0.54772	0.00094	0.54960	hciacyt12_6_2_3	0.54697	0.00098	0.54893
nciacyt11_3_2_3	1.4	3000	3000	9424	81.99	1.0e-04	0.39773	0.00080	0.39933	hciacyt12_3_2_3	0.39723	0.00087	0.39896

Table 6.9.6-3b. Results for spacing of 3.24 in.-diameter cylinder HEU metal content in CV calculation model

case name	np (in.)	^{235}U (g)	H_2O (g)	h/x	separation (cm)	moifr	k_{eff}	σ	k_{eff}+2σ				
content in flooded containment vessel, reflected													
NCT													
separation is the distance between the 3.24 in.-diameter cylinders (an additional 1.4 in. is provided by the can spacer)													
cvcrcyat11_1_2	1.4	30000	7992	6.95	0.000	1.0e+00	0.85525	0.00117	0.85760				
cvcrcyat11_2_2	1.4	30000	7992	6.95	0.254	1.0e+00	0.85568	0.00100	0.85768				
cvcrcyat11_3_2	1.4	30000	7992	6.95	0.762	1.0e+00	0.85058	0.00110	0.85278				
cvcrcyat11_4_2	1.4	30000	7992	6.95	1.270	1.0e+00	0.84834	0.00124	0.85082				
cvcrcyat11_5_2	1.4	30000	7992	6.95	1.778	1.0e+00	0.84241	0.00123	0.84488				

Table 6.9.6-3b. Results for spacing of 3.24 in.-diameter cylinder HEU metal content in CV calculation model

case name	np (in.)	^{235}U (g)	H_2O (g)	h/x	separation (cm)	moifr	k_{eff}	σ	k_{eff}+2σ				
cvcrcyat11_6_2	1.4	30000	7992	6.95	2.286	1.0e+00	0.83866	0.00099	0.84063				
cvcrcyat11_7_2	1.4	30000	7992	6.95	2.794	1.0e+00	0.83549	0.00117	0.83782				
cvcrcyat11_8_2	1.4	30000	7992	6.95	3.302	1.0e+00	0.83213	0.00126	0.83465				
cvcrcyat11_9_2	1.4	30000	7992	6.95	3.810	1.0e+00	0.82984	0.00125	0.83233				
cvcrcyat11_10_2	1.4	30000	7992	6.95	4.318	1.0e+00	0.82777	0.00105	0.82986				
cvcrcyat11_11_2	1.4	30000	7992	6.95	4.826	1.0e+00	0.82499	0.00116	0.82731				
cvcrcyat11_12_2	1.4	30000	7992	6.95	12.230	1.0e+00	0.80870	0.00121	0.81113				

Table 6.9.6-3c. Results for spacing of 3.24 in.-diameter cylinder HEU metal content in packaging calculation model

case name	np (in.)	^{235}U (g)	H_2O (g)	h/x	separation (cm)	moifr	k_{eff}	σ	k_{eff}+2σ				
content in flooded containment vessel, single package reflected													
NCT													
separation is the distance between the 3.24 in.-diameter cylinders (an additional 1.4 in. is provided by the canned spacer)													
ncsrcyat11_1_2_15	1.4	30000	7992	6.95	0.000	1.0e+00	0.84343	0.00114	0.84572				
ncsrcyat11_2_2_15	1.4	30000	7992	6.95	0.254	1.0e+00	0.84249	0.00111	0.84472				
ncsrcyat11_3_2_15	1.4	30000	7992	6.95	0.762	1.0e+00	0.83638	0.00103	0.83845				
ncsrcyat11_4_2_15	1.4	30000	7992	6.95	1.270	1.0e+00	0.83416	0.00110	0.83636				
ncsrcyat11_5_2_15	1.4	30000	7992	6.95	1.778	1.0e+00	0.82786	0.00128	0.83043				
ncsrcyat11_6_2_15	1.4	30000	7992	6.95	2.286	1.0e+00	0.82516	0.00113	0.82743				
ncsrcyat11_7_2_15	1.4	30000	7992	6.95	2.794	1.0e+00	0.82161	0.00116	0.82393				
ncsrcyat11_8_2_15	1.4	30000	7992	6.95	3.302	1.0e+00	0.82004	0.00114	0.82232				
ncsrcyat11_9_2_15	1.4	30000	7992	6.95	3.810	1.0e+00	0.81641	0.00101	0.81843				
ncsrcyat11_10_2_15	1.4	30000	7992	6.95	4.318	1.0e+00	0.81362	0.00109	0.81581				

Table 6.9.6-3c. Results for spacing of 3.24 in.-diameter cylinder HEU metal content in packaging calculation model

case name	np (in.)	^{235}U (g)	H_2O (g)	h/x	separation (cm)	moifr	k_{eff}	σ	$k_{eff}+2σ$				
ncsrcyat11_11_2_15	1.4	30000	7992	6.95	4.826	1.0e+00	0.81218	0.00104	0.81426				
ncsrcyat11_12_2_15	1.4	30000	7992	6.95	12.230	1.0e+00	0.79592	0.00100	0.79793				

Table 6.9.6-4. Results for 2.29 in.-square bar HEU metal content in CV calculation model

case name	np (in)	U (g)	^{235}U (g)	H_2O (g)	h/x	mocfr	k_{eff}	σ	$k_{eff}+2σ$				
flooded containment vessel, reflected													
no can spacers (np thickness = 0.0 in.)													
cvcrsqt11_36_1	0.0	36000	36000	8287	6.01	1.0e+00	0.87614	0.00128	0.87869				
cvcrsqt11_35_1	0.0	35000	35000	8340	6.22	1.0e+00	0.87560	0.00111	0.87781				
cvcrsqt11_34_1	0.0	34000	34000	8393	6.44	1.0e+00	0.87541	0.00126	0.87794				
cvcrsqt11_33_1	0.0	33000	33000	8446	6.68	1.0e+00	0.87396	0.00108	0.87612				
cvcrsqt11_32_1	0.0	32000	32000	8499	6.93	1.0e+00	0.87319	0.00119	0.87556				
cvcrsqt11_31_1	0.0	31000	31000	8552	7.20	1.0e+00	0.86993	0.00116	0.87225				
cvcrsqt11_30_1	0.0	30000	30000	8605	7.49	1.0e+00	0.87046	0.00120	0.87286				
cvcrsqt11_29_1	0.0	29000	29000	8658	7.79	1.0e+00	0.86852	0.00107	0.87067				
cvcrsqt11_28_1	0.0	28000	28000	8711	8.12	1.0e+00	0.86740	0.00113	0.86966				
cvcrsqt11_27_1	0.0	27000	27000	8764	8.47	1.0e+00	0.86366	0.00116	0.86597				
cvcrsqt11_26_1	0.0	26000	26000	8817	8.85	1.0e+00	0.86498	0.00138	0.86773				
cvcrsqt11_25_1	0.0	25000	25000	8870	9.26	1.0e+00	0.86077	0.00121	0.86319				
cvcrsqt11_24_1	0.0	24000	24000	8923	9.70	1.0e+00	0.85955	0.00138	0.86231				
cvcrsqt11_23_1	0.0	23000	23000	8977	10.19	1.0e+00	0.85604	0.00106	0.85816				
cvcrsqt11_22_1	0.0	22000	22000	9030	10.71	1.0e+00	0.85211	0.00103	0.85417				
cvcrsqt11_21_1	0.0	21000	21000	9083	11.29	1.0e+00	0.84970	0.00118	0.85206				

Table 6.9.6-4. Results for 2.29 in.-square bar HEU metal content in CV calculation model

case name	np (in)	U (g)	^{235}U (g)	H_2O (g)	h/x	mocfr	k_{eff}	σ	k_{eff}+2σ				
cvcrsqt11_20_1	0.0	20000	20000	9136	11.92	1.0e+00	0.84694	0.00119	0.84931				
cvcrsqt11_19_1	0.0	19000	19000	9189	12.62	1.0e+00	0.84285	0.00109	0.84503				
cvcrsqt11_18_1	0.0	18000	18000	9242	13.40	1.0e+00	0.83888	0.00115	0.84117				
with can spacers (np thickness=1.4 in.)													
cvcrsqt11_36_2	1.4	36000	36000	7673	5.56	1.0e+00	0.82217	0.00098	0.82414				
cvcrsqt11_35_2	1.4	35000	35000	7726	5.76	1.0e+00	0.81622	0.00130	0.81881				
cvcrsqt11_34_2	1.4	34000	34000	7779	5.97	1.0e+00	0.81548	0.00103	0.81755				
cvcrsqt11_33_2	1.4	33000	33000	7832	6.19	1.0e+00	0.81272	0.00118	0.81508				
cvcrsqt11_32_2	1.4	32000	32000	7885	6.43	1.0e+00	0.80782	0.00120	0.81022				
cvcrsqt11_31_2	1.4	31000	31000	7938	6.68	1.0e+00	0.80495	0.00109	0.80712				
cvcrsqt11_30_2	1.4	30000	30000	7992	6.95	1.0e+00	0.80163	0.00117	0.80397				

Table 6.9.6-5. Results for 2.29 in.-square bar HEU metal content in packaging calculation model

case name	np (in)	U (g)	^{235}U (g)	H_2O (g)	h/x	moifr	k_{eff}	σ	k_{eff}+2σ	case name	k_{eff}	σ	k_{eff}+2σ
content in flooded containment vessel, single package reflected													
NCT										HAC			
no can spacers (np thickness = 0.0 in.)													
ncsrsqt11_36_1_1	0.0	36000	36000	8287	6.01	1.0e-20	0.82940	0.00124	0.83189	hcsrsqt12_36_1_1	0.83133	0.00125	0.83384
ncsrsqt11_36_1_2	0.0	36000	36000	8287	6.01	1.0e-05	0.83107	0.00107	0.83320	hcsrsqt12_36_1_2	0.83168	0.00121	0.83409
ncsrsqt11_36_1_3	0.0	36000	36000	8287	6.01	1.0e-04	0.83051	0.00120	0.83292	hcsrsqt12_36_1_3	0.83088	0.00103	0.83293
ncsrsqt11_36_1_4	0.0	36000	36000	8287	6.01	1.0e-03	0.82981	0.00116	0.83213	hcsrsqt12_36_1_4	0.83030	0.00122	0.83273
ncsrsqt11_36_1_5	0.0	36000	36000	8287	6.01	1.0e-02	0.82859	0.00123	0.83105	hcsrsqt12_36_1_5	0.83244	0.00126	0.83496
ncsrsqt11_36_1_6	0.0	36000	36000	8287	6.01	1.0e-01	0.83608	0.00123	0.83853	hcsrsqt12_36_1_6	0.83502	0.00119	0.83739

Table 6.9.6-5. Results for 2.29 in.-square bar HEU metal content in packaging calculation model

case name	np (in)	U (g)	^{235}U (g)	H_2O (g)	h/x	moifr	k_{eff}	σ	$k_{eff}+2σ$	case name	k_{eff}	σ	$k_{eff}+2σ$
ncsrsqt11_36_1_8	0.0	36000	36000	8287	6.01	3.0e-01	0.84146	0.00118	0.84382	hcsrsqt12_36_1_8	0.84236	0.00115	0.84465
ncsrsqt11_36_1_15	0.0	36000	36000	8287	6.01	1.0e+00	0.86253	0.00131	0.86516	hcsrsqt12_36_1_15	0.86198	0.00112	0.86422
ncsrsqt11_36_1_15	0.0	36000	36000	8287	6.01	1.0e+00	0.86253	0.00131	0.86516	hcsrsqt12_36_1_15	0.86198	0.00112	0.86422
ncsrsqt11_35_1_15	0.0	35000	35000	8340	6.22	1.0e+00	0.86041	0.00112	0.86265	hcsrsqt12_35_1_15	0.86067	0.00121	0.86309
ncsrsqt11_34_1_15	0.0	34000	34000	8393	6.44	1.0e+00	0.85820	0.00129	0.86078	hcsrsqt12_34_1_15	0.85896	0.00102	0.86101
ncsrsqt11_33_1_15	0.0	33000	33000	8446	6.68	1.0e+00	0.85708	0.00106	0.85920	hcsrsqt12_33_1_15	0.86064	0.00110	0.86285
ncsrsqt11_32_1_15	0.0	32000	32000	8499	6.93	1.0e+00	0.85769	0.00107	0.85983	hcsrsqt12_32_1_15	0.85800	0.00110	0.86020
ncsrsqt11_31_1_15	0.0	31000	31000	8552	7.20	1.0e+00	0.85495	0.00127	0.85749	hcsrsqt12_31_1_15	0.85333	0.00123	0.85580
ncsrsqt11_30_1_15	0.0	30000	30000	8605	7.49	1.0e+00	0.85270	0.00120	0.85510	hcsrsqt12_30_1_15	0.85520	0.00132	0.85784
ncsrsqt11_29_1_15	0.0	29000	29000	8658	7.79	1.0e+00	0.85067	0.00119	0.85305	hcsrsqt12_29_1_15	0.85348	0.00114	0.85575
ncsrsqt11_28_1_15	0.0	28000	28000	8711	8.12	1.0e+00	0.85223	0.00111	0.85446	hcsrsqt12_28_1_15	0.85043	0.00101	0.85246
ncsrsqt11_27_1_15	0.0	27000	27000	8764	8.47	1.0e+00	0.84973	0.00121	0.85214	hcsrsqt12_27_1_15	0.85029	0.00111	0.85250
ncsrsqt11_26_1_15	0.0	26000	26000	8817	8.85	1.0e+00	0.84838	0.00127	0.85091	hcsrsqt12_26_1_15	0.84829	0.00115	0.85058
ncsrsqt11_25_1_15	0.0	25000	25000	8870	9.26	1.0e+00	0.84598	0.00113	0.84824	hcsrsqt12_25_1_15	0.84583	0.00105	0.84792
ncsrsqt11_24_1_15	0.0	24000	24000	8923	9.70	1.0e+00	0.84390	0.00111	0.84611	hcsrsqt12_24_1_15	0.84296	0.00112	0.84521
ncsrsqt11_23_1_15	0.0	23000	23000	8977	10.19	1.0e+00	0.84101	0.00108	0.84317	hcsrsqt12_23_1_15	0.84241	0.00129	0.84499
ncsrsqt11_22_1_15	0.0	22000	22000	9030	10.71	1.0e+00	0.83888	0.00112	0.84111	hcsrsqt12_22_1_15	0.83951	0.00107	0.84164
ncsrsqt11_21_1_15	0.0	21000	21000	9083	11.29	1.0e+00	0.83473	0.00112	0.83696	hcsrsqt12_21_1_15	0.83577	0.00128	0.83832
ncsrsqt11_20_1_15	0.0	20000	20000	9136	11.92	1.0e+00	0.83029	0.00110	0.83250	hcsrsqt12_20_1_15	0.83094	0.00103	0.83300
ncsrsqt11_19_1_15	0.0	19000	19000	9189	12.62	1.0e+00	0.82676	0.00107	0.82889	hcsrsqt12_19_1_15	0.82652	0.00113	0.82879
ncsrsqt11_18_1_15	0.0	18000	18000	9242	13.40	1.0e+00	0.82247	0.00121	0.82489	hcsrsqt12_18_1_15	0.82440	0.00112	0.82664
with can spacers (np thickness = 1.4 in.)													
ncsrsqt11_36_2_1	1.4	36000	36000	7673	5.56	1.0e-20	0.78167	0.00104	0.78375	hcsrsqt12_36_2_1	0.78308	0.00128	0.78563
ncsrsqt11_36_2_2	1.4	36000	36000	7673	5.56	1.0e-05	0.78210	0.00112	0.78434	hcsrsqt12_36_2_2	0.78549	0.00112	0.78772

Table 6.9.6-5. Results for 2.29 in.-square bar HEU metal content in packaging calculation model

case name	np (in)	U (g)	^{235}U (g)	H_2O (g)	h/x	moifr	k_{eff}	σ	$k_{eff}+2σ$	case name	k_{eff}	σ	$k_{eff}+2σ$
ncsrsqt11_36_2_3	1.4	36000	36000	7673	5.56	1.0e-04	0.78209	0.00104	0.78417	hcsrsqt12_36_2_3	0.78508	0.00119	0.78746
ncsrsqt11_36_2_4	1.4	36000	36000	7673	5.56	1.0e-03	0.78414	0.00111	0.78636	hcsrsqt12_36_2_4	0.78484	0.00121	0.78727
ncsrsqt11_36_2_5	1.4	36000	36000	7673	5.56	1.0e-02	0.78141	0.00137	0.78415	hcsrsqt12_36_2_5	0.78362	0.00114	0.78591
ncsrsqt11_36_2_6	1.4	36000	36000	7673	5.56	1.0e-01	0.78591	0.00113	0.78818	hcsrsqt12_36_2_6	0.78757	0.00108	0.78972
ncsrsqt11_36_2_8	1.4	36000	36000	7673	5.56	3.0e-01	0.79206	0.00130	0.79466	hcsrsqt12_36_2_8	0.79070	0.00128	0.79327
ncsrsqt11_36_2_15	1.4	36000	36000	7673	5.56	1.0e+00	0.80894	0.00103	0.81101	hcsrsqt12_36_2_15	0.80856	0.00110	0.81077
ncsrsqt11_36_2_15	1.4	36000	36000	7673	5.56	1.0e+00	0.80894	0.00103	0.81101	hcsrsqt12_36_2_15	0.80856	0.00110	0.81077
ncsrsqt11_35_2_15	1.4	35000	35000	7726	5.76	1.0e+00	0.80583	0.00113	0.80808	hcsrsqt12_35_2_15	0.80522	0.00112	0.80747
ncsrsqt11_34_2_15	1.4	34000	34000	7779	5.97	1.0e+00	0.80341	0.00125	0.80591	hcsrsqt12_34_2_15	0.80255	0.00107	0.80469
ncsrsqt11_33_2_15	1.4	33000	33000	7832	6.19	1.0e+00	0.80213	0.00108	0.80429	hcsrsqt12_33_2_15	0.79972	0.00096	0.80164
ncsrsqt11_32_2_15	1.4	32000	32000	7885	6.43	1.0e+00	0.79784	0.00124	0.80032	hcsrsqt12_32_2_15	0.79750	0.00118	0.79985
ncsrsqt11_31_2_15	1.4	31000	31000	7938	6.68	1.0e+00	0.79226	0.00107	0.79440	hcsrsqt12_31_2_15	0.79447	0.00099	0.79646
ncsrsqt11_30_2_15	1.4	30000	30000	7992	6.95	1.0e+00	0.79192	0.00110	0.79412	hcsrsqt12_30_2_15	0.79053	0.00108	0.79268
content in flooded containment vessel, array packaging model for CSI=0.0													
NCT										HAC			
no can spacers (np thickness = 0.0 in.)													
nciasqt11_36_1_3	0.0	36000	36000	8287	6.01	1.0e-04	0.93786	0.00112	0.94011	hciasqt12_36_1_3	0.93760	0.00119	0.93998
nciasqt11_35_1_3	0.0	35000	35000	8340	6.22	1.0e-04	0.93414	0.00107	0.93629	hciasqt12_35_1_3	0.93524	0.00130	0.93785

Table 6.9.6-5. Results for 2.29 in.-square bar HEU metal content in packaging calculation model

case name	np (in)	U (g)	^{235}U (g)	H_2O (g)	h/x	moifr	k_{eff}	σ	k_{eff}+2σ	case name	k_{eff}	σ	k_{eff}+2σ
nciasqt11_34_1_3	0.0	34000	34000	8393	6.44	1.0e-04	0.93004	0.00116	0.93235	hciasqt12_34_1_3	0.92962	0.00116	0.93195
nciasqt11_33_1_3	0.0	33000	33000	8446	6.68	1.0e-04	0.92897	0.00121	0.93139	hciasqt12_33_1_3	0.92744	0.00120	0.92984
nciasqt11_32_1_3	0.0	32000	32000	8499	6.93	1.0e-04	0.92703	0.00119	0.92942	hciasqt12_32_1_3	0.92854	0.00110	0.93073
nciasqt11_31_1_3	0.0	31000	31000	8552	7.20	1.0e-04	0.92403	0.00109	0.92621	hciasqt12_31_1_3	0.92290	0.00105	0.92499
nciasqt11_30_1_3	0.0	30000	30000	8605	7.49	1.0e-04	0.91959	0.00114	0.92188	hciasqt12_30_1_3	0.91960	0.00125	0.92211
nciasqt11_29_1_3	0.0	29000	29000	8658	7.79	1.0e-04	0.91544	0.00122	0.91787	hciasqt12_29_1_3	0.91645	0.00138	0.91922
nciasqt11_28_1_3	0.0	28000	28000	8711	8.12	1.0e-04	0.91153	0.00123	0.91399	hciasqt12_28_1_3	0.91477	0.00122	0.91722
nciasqt11_27_1_3	0.0	27000	27000	8764	8.47	1.0e-04	0.90851	0.00099	0.91050	hciasqt12_27_1_3	0.91066	0.00119	0.91305
nciasqt11_26_1_3	0.0	26000	26000	8817	8.85	1.0e-04	0.90835	0.00125	0.91084	hciasqt12_26_1_3	0.90452	0.00124	0.90699
nciasqt11_25_1_3	0.0	25000	25000	8870	9.26	1.0e-04	0.90272	0.00115	0.90501	hciasqt12_25_1_3	0.90142	0.00116	0.90374
nciasqt11_24_1_3	0.0	24000	24000	8923	9.70	1.0e-04	0.89930	0.00123	0.90177	hciasqt12_24_1_3	0.89640	0.00120	0.89881
nciasqt11_23_1_3	0.0	23000	23000	8977	10.19	1.0e-04	0.89380	0.00120	0.89619	hciasqt12_23_1_3	0.89613	0.00135	0.89882
nciasqt11_22_1_3	0.0	22000	22000	9030	10.71	1.0e-04	0.88934	0.00105	0.89144	hciasqt12_22_1_3	0.88839	0.00106	0.89051
nciasqt11_21_1_3	0.0	21000	21000	9083	11.29	1.0e-04	0.88358	0.00109	0.88576	hciasqt12_21_1_3	0.88413	0.00118	0.88649
nciasqt11_20_1_3	0.0	20000	20000	9136	11.92	1.0e-04	0.87812	0.00123	0.88058	hciasqt12_20_1_3	0.87811	0.00124	0.88058
nciasqt11_19_1_3	0.0	19000	19000	9189	12.62	1.0e-04	0.87206	0.00108	0.87423	hciasqt12_19_1_3	0.87171	0.00118	0.87408
nciasqt11_18_1_3	0.0	18000	18000	9242	13.40	1.0e-04	0.86772	0.00140	0.87052	hciasqt12_18_1_3	0.86555	0.00119	0.86794
nciasqt11_15_1_3	0.0	15000	15000	9401	16.36	1.0e-04	0.84518	0.00119	0.84756	hciasqt12_15_1_3	0.84416	0.00102	0.84620
nciasqt11_12_1_3	0.0	12000	12000	9560	20.79	1.0e-04	0.81425	0.00113	0.81651	hciasqt12_12_1_3	0.81332	0.00101	0.81534
nciasqt11_9_1_3	0.0	9000	9000	9719	28.19	1.0e-04	0.76947	0.00115	0.77178	hciasqt12_9_1_3	0.77066	0.00107	0.77280
nciasqt11_6_1_3	0.0	6000	6000	9879	42.97	1.0e-04	0.69668	0.00099	0.69866	hciasqt12_6_1_3	0.69648	0.00101	0.69850
nciasqt11_3_1_3	0.0	3000	3000	10038	87.33	1.0e-04	0.55857	0.00089	0.56036	hciasqt12_3_1_3	0.55806	0.00092	0.55989
with can spacers (np thickness = 1.4 in.)													
nciasqt11_36_2_3	1.4	36000	36000	7673	5.56	1.0e-04	0.89382	0.00114	0.89610	hciasqt12_36_2_3	0.89230	0.00114	0.89458
nciasqt11_35_2_3	1.4	35000	35000	7726	5.76	1.0e-04	0.88604	0.00105	0.88813	hciasqt12_35_2_3	0.88890	0.00130	0.89150

Table 6.9.6-5. Results for 2.29 in.-square bar HEU metal content in packaging calculation model

case name	np (in)	U (g)	^{235}U (g)	H_2O (g)	h/x	moifr	k_{eff}	σ	$k_{eff}+2σ$	case name	k_{eff}	σ	$k_{eff}+2σ$
nciasqt11_34_2_3	1.4	34000	34000	7779	5.97	1.0e-04	0.88480	0.00105	0.88690	hciasqt12_34_2_3	0.88544	0.00139	0.88822
nciasqt11_33_2_3	1.4	33000	33000	7832	6.19	1.0e-04	0.87854	0.00118	0.88090	hciasqt12_33_2_3	0.87897	0.00106	0.88110
nciasqt11_32_2_3	1.4	32000	32000	7885	6.43	1.0e-04	0.87561	0.00104	0.87768	hciasqt12_32_2_3	0.87638	0.00121	0.87880
nciasqt11_31_2_3	1.4	31000	31000	7938	6.68	1.0e-04	0.86867	0.00123	0.87114	hciasqt12_31_2_3	0.87222	0.00105	0.87432
nciasqt11_30_2_3	1.4	30000	30000	7992	6.95	1.0e-04	0.86347	0.00122	0.86590	hciasqt12_30_2_3	0.86614	0.00121	0.86855
nciasqt11_29_2_3	1.4	29000	29000	8045	7.24	1.0e-04	0.85781	0.00109	0.86000	hciasqt12_29_2_3	0.85842	0.00113	0.86068
nciasqt11_28_2_3	1.4	28000	28000	8098	7.55	1.0e-04	0.85401	0.00119	0.85640	hciasqt12_28_2_3	0.85399	0.00116	0.85630
nciasqt11_27_2_3	1.4	27000	27000	8151	7.88	1.0e-04	0.84755	0.00127	0.85009	hciasqt12_27_2_3	0.84935	0.00125	0.85184
nciasqt11_26_2_3	1.4	26000	26000	8204	8.24	1.0e-04	0.84285	0.00119	0.84522	hciasqt12_26_2_3	0.84287	0.00106	0.84500
nciasqt11_25_2_3	1.4	25000	25000	8257	8.62	1.0e-04	0.83719	0.00124	0.83967	hciasqt12_25_2_3	0.83683	0.00113	0.83910
nciasqt11_24_2_3	1.4	24000	24000	8310	9.04	1.0e-04	0.82927	0.00102	0.83132	hciasqt12_24_2_3	0.83192	0.00111	0.83414
nciasqt11_23_2_3	1.4	23000	23000	8363	9.49	1.0e-04	0.82375	0.00132	0.82638	hciasqt12_23_2_3	0.82315	0.00124	0.82562
nciasqt11_22_2_3	1.4	22000	22000	8416	9.98	1.0e-04	0.81735	0.00107	0.81950	hciasqt12_22_2_3	0.81490	0.00105	0.81700
nciasqt11_21_2_3	1.4	21000	21000	8469	10.53	1.0e-04	0.80580	0.00118	0.80817	hciasqt12_21_2_3	0.81021	0.00121	0.81263
nciasqt11_20_2_3	1.4	20000	20000	8522	11.12	1.0e-04	0.79977	0.00110	0.80197	hciasqt12_20_2_3	0.80091	0.00116	0.80324
nciasqt11_19_2_3	1.4	19000	19000	8575	11.78	1.0e-04	0.79125	0.00109	0.79343	hciasqt12_19_2_3	0.79175	0.00113	0.79400
nciasqt11_18_2_3	1.4	18000	18000	8628	12.51	1.0e-04	0.78165	0.00110	0.78386	hciasqt12_18_2_3	0.78285	0.00110	0.78505
nciasqt11_15_2_3	1.4	15000	15000	8787	15.29	1.0e-04	0.74822	0.00105	0.75032	hciasqt12_15_2_3	0.74548	0.00107	0.74762
nciasqt11_12_2_3	1.4	12000	12000	8947	19.46	1.0e-04	0.70519	0.00106	0.70732	hciasqt12_12_2_3	0.70419	0.00105	0.70628
nciasqt11_9_2_3	1.4	9000	9000	9106	26.41	1.0e-04	0.64473	0.00106	0.64685	hciasqt12_9_2_3	0.64451	0.00101	0.64653
nciasqt11_6_2_3	1.4	6000	6000	9265	40.30	1.0e-04	0.55778	0.00097	0.55972	hciasqt12_6_2_3	0.55888	0.00098	0.56084
nciasqt11_3_2_3	1.4	3000	3000	9424	81.99	1.0e-04	0.41347	0.00085	0.41517	hciasqt12_3_2_3	0.41398	0.00074	0.41545

Table 6.9.6-6. Results for 4.25 in.-diameter cylinder HEU metal content in CV calculation model

case name	np (in)	U (g)	^{235}U (g)	H_2O (g)	h/x	mocfr	k_{eff}	σ	$k_{eff}+2σ$
flooded containment vessel, reflected									
no can spacers (np thickness = 0.0 in.)									
cvcrcyct11_36_1	0.0	36000	36000	8287	6.01	1.0e+00	1.06320	0.00115	1.06549
cvcrcyct11_35_1	0.0	35000	35000	8340	6.22	1.0e+00	1.06114	0.00121	1.06356
cvcrcyct11_34_1	0.0	34000	34000	8393	6.44	1.0e+00	1.05675	0.00122	1.05919
cvcrcyct11_33_1	0.0	33000	33000	8446	6.68	1.0e+00	1.04990	0.00112	1.05214
cvcrcyct11_32_1	0.0	32000	32000	8499	6.93	1.0e+00	1.04469	0.00123	1.04714
cvcrcyct11_31_1	0.0	31000	31000	8552	7.20	1.0e+00	1.04101	0.00104	1.04310
cvcrcyct11_30_1	0.0	30000	30000	8605	7.49	1.0e+00	1.03487	0.00117	1.03722
cvcrcyct11_29_1	0.0	29000	29000	8658	7.79	1.0e+00	1.02817	0.00115	1.03046
cvcrcyct11_28_1	0.0	28000	28000	8711	8.12	1.0e+00	1.02183	0.00125	1.02433
cvcrcyct11_27_1	0.0	27000	27000	8764	8.47	1.0e+00	1.01524	0.00109	1.01742
cvcrcyct11_26_1	0.0	26000	26000	8817	8.85	1.0e+00	1.00971	0.00116	1.01203
cvcrcyct11_25_1	0.0	25000	25000	8870	9.26	1.0e+00	1.00149	0.00136	1.00420
cvcrcyct11_24_1	0.0	24000	24000	8923	9.70	1.0e+00	0.99327	0.00137	0.99600
cvcrcyct11_23_1	0.0	23000	23000	8977	10.19	1.0e+00	0.98432	0.00124	0.98680
cvcrcyct11_22_1	0.0	22000	22000	9030	10.71	1.0e+00	0.97759	0.00112	0.97984
cvcrcyct11_21_1	0.0	21000	21000	9083	11.29	1.0e+00	0.96672	0.00116	0.96904
cvcrcyct11_20_1	0.0	20000	20000	9136	11.92	1.0e+00	0.95743	0.00128	0.95999
cvcrcyct11_19_1	0.0	19000	19000	9189	12.62	1.0e+00	0.94629	0.00118	0.94866
cvcrcyct11_18_1	0.0	18000	18000	9242	13.40	1.0e+00	0.93349	0.00114	0.93576
cvcrcyct11_17_1	0.0	17000	17000	9295	14.27	1.0e+00	0.91942	0.00105	0.92152
cvcrcyct11_16_1	0.0	16000	16000	9348	15.25	1.0e+00	0.90458	0.00120	0.90699
cvcrcyct11_15_1	0.0	15000	15000	9401	16.36	1.0e+00	0.88788	0.00107	0.89002

Table 6.9.6-6. Results for 4.25 in.-diameter cylinder HEU metal content in CV calculation model

case name	np (in)	U (g)	^{235}U (g)	H_2O (g)	h/x	mocfr	k_{eff}	σ	k_{eff}+2σ				
with can spacers (np thickness=1.4 in.)													
cvcrcyct11_36_2	1.4	36000	36000	7673	5.56	1.0e+00	0.94321	0.00111	0.94543				
cvcrcyct11_35_2	1.4	35000	35000	7726	5.76	1.0e+00	0.93828	0.00114	0.94056				
cvcrcyct11_34_2	1.4	34000	34000	7779	5.97	1.0e+00	0.93114	0.00129	0.93372				
cvcrcyct11_33_2	1.4	33000	33000	7832	6.19	1.0e+00	0.92558	0.00124	0.92805				
cvcrcyct11_32_2	1.4	32000	32000	7885	6.43	1.0e+00	0.91799	0.00111	0.92021				
cvcrcyct11_31_2	1.4	31000	31000	7938	6.68	1.0e+00	0.91146	0.00114	0.91375				
cvcrcyct11_30_2	1.4	30000	30000	7992	6.95	1.0e+00	0.90499	0.00117	0.90734				

Table 6.9.6-7. Results for 4.25 in.-diameter cylinder HEU metal content in packaging calculation model

case name	np (in)	U (g)	^{235}U (g)	H_2O (g)	h/x	moifr	k_{eff}	σ	k_{eff}+2σ	case name	k_{eff}	σ	k_{eff}+2σ
content in flooded containment vessel, single package reflected													
NCT										HAC			
no can spacers (np thickness = 0.0 in.)													
ncsrcyct11_36_1_1	0.0	36000	36000	8286.7	6.01	1.0e-20	0.98628	0.00107	0.98841	hcsrcyct12_36_1_1	0.98723	0.00126	0.98975
ncsrcyct11_36_1_2	0.0	36000	36000	8286.7	6.01	1.0e-05	0.98712	0.00138	0.98988	hcsrcyct12_36_1_2	0.98582	0.00120	0.98823
ncsrcyct11_36_1_3	0.0	36000	36000	8287	6.01	1.0e-04	0.98624	0.00119	0.98861	hcsrcyct12_36_1_3	0.98691	0.00113	0.98917
ncsrcyct11_36_1_4	0.0	36000	36000	8287	6.01	1.0e-03	0.98433	0.00102	0.98637	hcsrcyct12_36_1_4	0.98537	0.00111	0.98759
ncsrcyct11_36_1_5	0.0	36000	36000	8287	6.01	1.0e-02	0.98646	0.00103	0.98852	hcsrcyct12_36_1_5	0.98809	0.00110	0.99028
ncsrcyct11_36_1_6	0.0	36000	36000	8287	6.01	1.0e-01	0.99092	0.00127	0.99346	hcsrcyct12_36_1_6	0.99096	0.00099	0.99295
ncsrcyct11_36_1_8	0.0	36000	36000	8287	6.01	3.0e-01	1.00000	0.00123	1.00246	hcsrcyct12_36_1_8	1.00334	0.00119	1.00572
ncsrcyct11_36_1_15	0.0	36000	36000	8287	6.01	1.0e+00	1.03142	0.00144	1.03430	hcsrcyct12_36_1_15	1.03141	0.00116	1.03374
ncsrcyct11_36_1_15	0.0	36000	36000	8287	6.01	1.0e+00	1.03142	0.00144	1.03430	hcsrcyct12_36_1_15	1.03141	0.00116	1.03374

Table 6.9.6-7. Results for 4.25 in.-diameter cylinder HEU metal content in packaging calculation model

case name	np (in)	U (g)	^{235}U (g)	H_2O (g)	h/x	moifr	k_{eff}	σ	k_{eff}+2σ	case name	k_{eff}	σ	k_{eff}+2σ
ncsrcyct11_35_1_15	0.0	35000	35000	8340	6.22	1.0e+00	1.02816	0.00115	1.03045	hcsrcyct12_35_1_15	1.03309	0.00126	1.03561
ncsrcyct11_34_1_15	0.0	34000	34000	8393	6.44	1.0e+00	1.02658	0.00113	1.02884	hcsrcyct12_34_1_15	1.02529	0.00124	1.02776
ncsrcyct11_33_1_15	0.0	33000	33000	8446	6.68	1.0e+00	1.01975	0.00114	1.02203	hcsrcyct12_33_1_15	1.02060	0.00124	1.02308
ncsrcyct11_32_1_15	0.0	32000	32000	8499	6.93	1.0e+00	1.01647	0.00104	1.01854	hcsrcyct12_32_1_15	1.01688	0.00114	1.01916
ncsrcyct11_31_1_15	0.0	31000	31000	8552	7.20	1.0e+00	1.00952	0.00114	1.01179	hcsrcyct12_31_1_15	1.01218	0.00144	1.01505
ncsrcyct11_30_1_15	0.0	30000	30000	8605	7.49	1.0e+00	1.00434	0.00123	1.00679	hcsrcyct12_30_1_15	1.00757	0.00117	1.00992
ncsrcyct11_29_1_15	0.0	29000	29000	8658	7.79	1.0e+00	1.00074	0.00106	1.00287	hcsrcyct12_29_1_15	1.00071	0.00139	1.00348
ncsrcyct11_28_1_15	0.0	28000	28000	8711	8.12	1.0e+00	0.99381	0.00135	0.99652	hcsrcyct12_28_1_15	0.99442	0.00129	0.99700
ncsrcyct11_27_1_15	0.0	27000	27000	8764	8.47	1.0e+00	0.98595	0.00094	0.98782	hcsrcyct12_27_1_15	0.99057	0.00119	0.99296
ncsrcyct11_26_1_15	0.0	26000	26000	8817	8.85	1.0e+00	0.97783	0.00117	0.98017	hcsrcyct12_26_1_15	0.98010	0.00135	0.98281
ncsrcyct11_25_1_15	0.0	25000	25000	8870	9.26	1.0e+00	0.97189	0.00126	0.97440	hcsrcyct12_25_1_15	0.97263	0.00118	0.97499
ncsrcyct11_24_1_15	0.0	24000	24000	8923	9.70	1.0e+00	0.96439	0.00121	0.96681	hcsrcyct12_24_1_15	0.96656	0.00113	0.96881
ncsrcyct11_23_1_15	0.0	23000	23000	8977	10.19	1.0e+00	0.95375	0.00130	0.95635	hcsrcyct12_23_1_15	0.95783	0.00118	0.96018
ncsrcyct11_22_1_15	0.0	22000	22000	9030	10.71	1.0e+00	0.94744	0.00132	0.95008	hcsrcyct12_22_1_15	0.94901	0.00143	0.95187
ncsrcyct11_21_1_15	0.0	21000	21000	9083	11.29	1.0e+00	0.93842	0.00127	0.94095	hcsrcyct12_21_1_15	0.93880	0.00126	0.94132
ncsrcyct11_20_1_15	0.0	20000	20000	9136	11.92	1.0e+00	0.92684	0.00118	0.92920	hcsrcyct12_20_1_15	0.92929	0.00124	0.93176
ncsrcyct11_19_1_15	0.0	19000	19000	9189	12.62	1.0e+00	0.91527	0.00109	0.91745	hcsrcyct12_19_1_15	0.91879	0.00101	0.92081
ncsrcyct11_18_1_15	0.0	18000	18000	9242	13.40	1.0e+00	0.90374	0.00111	0.90597	hcsrcyct12_18_1_15	0.90716	0.00105	0.90927
ncsrcyct11_17_1_15	0.0	17000	17000	9295	14.27	1.0e+00	0.89147	0.00133	0.89412	hcsrcyct12_17_1_15	0.89585	0.00104	0.89794
ncsrcyct11_16_1_15	0.0	16000	16000	9348	15.25	1.0e+00	0.87788	0.00101	0.87990	hcsrcyct12_16_1_15	0.87933	0.00118	0.88168
ncsrcyct11_15_1_15	0.0	15000	15000	9401	16.36	1.0e+00	0.86209	0.00110	0.86429	hcsrcyct12_15_1_15	0.86488	0.00110	0.86708
with can spacers (np thickness = 1.4 in.)													
ncsrcyct11_36_2_1	1.4	36000	36000	7673	5.56	1.0e-20	0.87502	0.00112	0.87725	hcsrcyct12_36_2_1	0.87543	0.00107	0.87757
ncsrcyct11_36_2_2	1.4	36000	36000	7673	5.56	1.0e-05	0.87474	0.00108	0.87691	hcsrcyct12_36_2_2	0.87795	0.00117	0.88029
ncsrcyct11_36_2_3	1.4	36000	36000	7673	5.56	1.0e-04	0.87595	0.00126	0.87846	hcsrcyct12_36_2_3	0.87675	0.00112	0.87899

Table 6.9.6-7. Results for 4.25 in.-diameter cylinder HEU metal content in packaging calculation model

case name	np (in)	U (g)	^{235}U (g)	H_2O (g)	h/x	moifr	k_{eff}	σ	$k_{eff}+2σ$	case name	k_{eff}	σ	$k_{eff}+2σ$
ncsrcyct11_36_2_4	1.4	36000	36000	7673	5.56	1.0e-03	0.87655	0.00100	0.87856	hcsrcyct12_36_2_4	0.87798	0.00106	0.88011
ncsrcyct11_36_2_5	1.4	36000	36000	7673	5.56	1.0e-02	0.87634	0.00104	0.87843	hcsrcyct12_36_2_5	0.87876	0.00109	0.88094
ncsrcyct11_36_2_6	1.4	36000	36000	7673	5.56	1.0e-01	0.87971	0.00102	0.88174	hcsrcyct12_36_2_6	0.88317	0.00111	0.88539
ncsrcyct11_36_2_8	1.4	36000	36000	7673	5.56	3.0e-01	0.88865	0.00115	0.89094	hcsrcyct12_36_2_8	0.89169	0.00103	0.89375
ncsrcyct11_36_2_15	1.4	36000	36000	7673	5.56	1.0e+00	0.91608	0.00120	0.91847	hcsrcyct12_36_2_15	0.91815	0.00118	0.92050
ncsrcyct11_36_2_15	1.4	36000	36000	7673	5.56	1.0e+00	0.91608	0.00120	0.91847	hcsrcyct12_36_2_15	0.91815	0.00118	0.92050
ncsrcyct11_35_2_15	1.4	35000	35000	7726	5.76	1.0e+00	0.91190	0.00116	0.91422	hcsrcyct12_35_2_15	0.91300	0.00117	0.91534
ncsrcyct11_34_2_15	1.4	34000	34000	7779	5.97	1.0e+00	0.90497	0.00112	0.90721	hcsrcyct12_34_2_15	0.90616	0.00116	0.90848
ncsrcyct11_33_2_15	1.4	33000	33000	7832	6.19	1.0e+00	0.90032	0.00120	0.90272	hcsrcyct12_33_2_15	0.90269	0.00118	0.90506
ncsrcyct11_32_2_15	1.4	32000	32000	7885	6.43	1.0e+00	0.89251	0.00102	0.89455	hcsrcyct12_32_2_15	0.89526	0.00120	0.89766
ncsrcyct11_31_2_15	1.4	31000	31000	7938	6.68	1.0e+00	0.88531	0.00136	0.88803	hcsrcyct12_31_2_15	0.88765	0.00108	0.88981
ncsrcyct11_30_2_15	1.4	30000	30000	7992	6.95	1.0e+00	0.88012	0.00120	0.88252	hcsrcyct12_30_2_15	0.88005	0.00120	0.88246
content in flooded containment vessel, array packaging model for CSI=0.0													
NCT										**HAC**			
no can spacers (np thickness = 0.0 in.)													
nciacyct11_36_1_3	0.0	36000	36000	8287	6.01	1.0e-04	1.10334	0.00135	1.10604	hciacyct12_36_1_3	1.10722	0.00119	1.10961
nciacyct11_35_1_3	0.0	35000	35000	8340	6.22	1.0e-04	1.10128	0.00116	1.10360	hciacyct12_35_1_3	1.10067	0.00114	1.10295
nciacyct11_34_1_3	0.0	34000	34000	8393	6.44	1.0e-04	1.09399	0.00125	1.09648	hciacyct12_34_1_3	1.09477	0.00124	1.09726
nciacyct11_33_1_3	0.0	33000	33000	8446	6.68	1.0e-04	1.08794	0.00127	1.09048	hciacyct12_33_1_3	1.08942	0.00134	1.09210
nciacyct11_32_1_3	0.0	32000	32000	8499	6.93	1.0e-04	1.08183	0.00131	1.08444	hciacyct12_32_1_3	1.08089	0.00128	1.08346
nciacyct11_31_1_3	0.0	31000	31000	8552	7.20	1.0e-04	1.07391	0.00114	1.07619	hciacyct12_31_1_3	1.07627	0.00101	1.07829
nciacyct11_30_1_3	0.0	30000	30000	8605	7.49	1.0e-04	1.06840	0.00131	1.07102	hciacyct12_30_1_3	1.06781	0.00107	1.06994
nciacyct11_29_1_3	0.0	29000	29000	8658	7.79	1.0e-04	1.06070	0.00108	1.06286	hciacyct12_29_1_3	1.05946	0.00121	1.06188
nciacyct11_28_1_3	0.0	28000	28000	8711	8.12	1.0e-04	1.05398	0.00116	1.05630	hciacyct12_28_1_3	1.05253	0.00102	1.05457

Table 6.9.6-7. Results for 4.25 in.-diameter cylinder HEU metal content in packaging calculation model

case name	np (in)	U (g)	^{235}U (g)	H_2O (g)	h/x	moifr	k_{eff}	σ	$k_{eff}+2\sigma$	case name	k_{eff}	σ	$k_{eff}+2\sigma$
nciacyct11_27_1_3	0.0	27000	27000	8764	8.47	1.0e-04	1.04385	0.00142	1.04670	hciacyct12_27_1_3	1.04481	0.00121	1.04723
nciacyct11_26_1_3	0.0	26000	26000	8817	8.85	1.0e-04	1.03489	0.00124	1.03736	hciacyct12_26_1_3	1.03688	0.00118	1.03923
nciacyct11_25_1_3	0.0	25000	25000	8870	9.26	1.0e-04	1.02495	0.00128	1.02751	hciacyct12_25_1_3	1.02706	0.00120	1.02946
nciacyct11_24_1_3	0.0	24000	24000	8923	9.70	1.0e-04	1.01610	0.00120	1.01850	hciacyct12_24_1_3	1.01634	0.00118	1.01870
nciacyct11_23_1_3	0.0	23000	23000	8977	10.19	1.0e-04	1.00723	0.00108	1.00938	hciacyct12_23_1_3	1.00427	0.00110	1.00648
nciacyct11_22_1_3	0.0	22000	22000	9030	10.71	1.0e-04	0.99573	0.00122	0.99817	hciacyct12_22_1_3	0.99481	0.00112	0.99705
nciacyct11_21_1_3	0.0	21000	21000	9083	11.29	1.0e-04	0.98149	0.00122	0.98393	hciacyct12_21_1_3	0.98514	0.00127	0.98768
nciacyct11_20_1_3	0.0	20000	20000	9136	11.92	1.0e-04	0.97377	0.00104	0.97585	hciacyct12_20_1_3	0.97210	0.00120	0.97450
nciacyct11_19_1_3	0.0	19000	19000	9189	12.62	1.0e-04	0.95985	0.00127	0.96240	hciacyct12_19_1_3	0.95807	0.00143	0.96092
nciacyct11_18_1_3	0.0	18000	18000	9242	13.40	1.0e-04	0.94375	0.00137	0.94649	hciacyct12_18_1_3	0.94639	0.00124	0.94887
nciacyct11_15_1_3	0.0	15000	15000	9401	16.36	1.0e-04	0.89699	0.00109	0.89917	hciacyct12_15_1_3	0.89646	0.00108	0.89862
nciacyct11_12_1_3	0.0	12000	12000	9560	20.79	1.0e-04	0.83537	0.00118	0.83772	hciacyct12_12_1_3	0.83858	0.00118	0.84093
nciacyct11_9_1_3	0.0	9000	9000	9719	28.19	1.0e-04	0.76061	0.00121	0.76303	hciacyct12_9_1_3	0.75657	0.00112	0.75882
nciacyct11_6_1_3	0.0	6000	6000	9879	42.97	1.0e-04	0.64959	0.00106	0.65172	hciacyct12_6_1_3	0.64940	0.00109	0.65157
nciacyct11_3_1_3	0.0	3000	3000	10038	87.33	1.0e-04	0.48405	0.00103	0.48611	hciacyct12_3_1_3	0.48552	0.00096	0.48745
with can spacers (np thickness = 1.4 in.)													
nciacyct11_36_2_3	1.4	36000	36000	7673	5.56	1.0e-04	1.01018	0.00139	1.01297	hciacyct12_36_2_3	1.01024	0.00120	1.01263
nciacyct11_35_2_3	1.4	35000	35000	7726	5.76	1.0e-04	1.00029	0.00110	1.00249	hciacyct12_35_2_3	1.00083	0.00105	1.00293
nciacyct11_34_2_3	1.4	34000	34000	7779	5.97	1.0e-04	0.99523	0.00100	0.99723	hciacyct12_34_2_3	0.99499	0.00116	0.99731
nciacyct11_33_2_3	1.4	33000	33000	7832	6.19	1.0e-04	0.98713	0.00110	0.98932	hciacyct12_33_2_3	0.98922	0.00108	0.99139
nciacyct11_32_2_3	1.4	32000	32000	7885	6.43	1.0e-04	0.97809	0.00109	0.98028	hciacyct12_32_2_3	0.98046	0.00098	0.98242
nciacyct11_31_2_3	1.4	31000	31000	7938	6.68	1.0e-04	0.96968	0.00130	0.97227	hciacyct12_31_2_3	0.96951	0.00147	0.97246
nciacyct11_30_2_3	1.4	30000	30000	7992	6.95	1.0e-04	0.96031	0.00132	0.96295	hciacyct12_30_2_3	0.96156	0.00107	0.96370
nciacyct11_29_2_3	1.4	29000	29000	8045	7.24	1.0e-04	0.95128	0.00117	0.95362	hciacyct12_29_2_3	0.95414	0.00120	0.95654
nciacyct11_28_2_3	1.4	28000	28000	8098	7.55	1.0e-04	0.94378	0.00138	0.94654	hciacyct12_28_2_3	0.94376	0.00138	0.94652

Table 6.9.6-7. Results for 4.25 in.-diameter cylinder HEU metal content in packaging calculation model

case name	np (in)	U (g)	^{235}U (g)	H_2O (g)	h/x	moifr	k_{eff}	σ	k_{eff}+2σ	case name	k_{eff}	σ	k_{eff}+2σ
nciacyct11_27_2_3	1.4	27000	27000	8151	7.88	1.0e-04	0.93234	0.00111	0.93456	hciacyct12_27_2_3	0.93273	0.00132	0.93536
nciacyct11_26_2_3	1.4	26000	26000	8204	8.24	1.0e-04	0.92078	0.00104	0.92287	hciacyct12_26_2_3	0.92390	0.00128	0.92646
nciacyct11_25_2_3	1.4	25000	25000	8257	8.62	1.0e-04	0.91264	0.00100	0.91465	hciacyct12_25_2_3	0.91352	0.00105	0.91562
nciacyct11_24_2_3	1.4	24000	24000	8310	9.04	1.0e-04	0.89955	0.00124	0.90203	hciacyct12_24_2_3	0.90170	0.00109	0.90388
nciacyct11_23_2_3	1.4	23000	23000	8363	9.49	1.0e-04	0.89118	0.00128	0.89374	hciacyct12_23_2_3	0.89159	0.00128	0.89414
nciacyct11_22_2_3	1.4	22000	22000	8416	9.98	1.0e-04	0.87715	0.00098	0.87910	hciacyct12_22_2_3	0.87791	0.00103	0.87997
nciacyct11_21_2_3	1.4	21000	21000	8469	10.53	1.0e-04	0.86679	0.00109	0.86898	hciacyct12_21_2_3	0.86482	0.00106	0.86693
nciacyct11_20_2_3	1.4	20000	20000	8522	11.12	1.0e-04	0.85029	0.00131	0.85292	hciacyct12_20_2_3	0.85207	0.00119	0.85445
nciacyct11_19_2_3	1.4	19000	19000	8575	11.78	1.0e-04	0.83585	0.00110	0.83805	hciacyct12_19_2_3	0.83631	0.00101	0.83833
nciacyct11_18_2_3	1.4	18000	18000	8628	12.51	1.0e-04	0.82112	0.00105	0.82323	hciacyct12_18_2_3	0.82020	0.00108	0.82236
nciacyct11_15_2_3	1.4	15000	15000	8787	15.29	1.0e-04	0.77012	0.00102	0.77216	hciacyct12_15_2_3	0.77067	0.00099	0.77265
nciacyct11_12_2_3	1.4	12000	12000	8947	19.46	1.0e-04	0.70996	0.00113	0.71222	hciacyct12_12_2_3	0.70716	0.00100	0.70915
nciacyct11_9_2_3	1.4	9000	9000	9106	26.41	1.0e-04	0.38338	0.00093	0.38524	hciacyct12_9_2_3	0.62982	0.00097	0.63175
nciacyct11_6_2_3	1.4	6000	6000	9265	40.30	1.0e-04	0.63066	0.00100	0.63267	hciacyct12_6_2_3	0.52901	0.00100	0.53101
nciacyct11_3_2_3	1.4	3000	3000	9424	81.99	1.0e-04	0.52971	0.00101	0.53173	hciacyct12_3_2_3	0.38124	0.00075	0.38274

Table 6.9.6-8. Results for 1.5in.-diameter x 2.0 in.-tall slug HEU metal content in CV calculation model

case name	np (in)	U (g)	^{235}U (g)	H_2O (g)	h/x	mocfr	k_{eff}	σ	k_{eff}+2σ	content description
flooded containment vessel, reflected										
no can spacers (np thickness = 0.0 in.)										
cvcr5st11_1_1	0.0	18277	18277	9227	13.18	1.0e+00	0.90734	0.00123	0.90980	5 slugs in a pentagonal ring
cvcr5est11_1_1	0.0	18277	18277	9227	13.18	1.0e+00	0.90718	0.00119	0.90955	5 slugs in a pentagonal ring, extended spacing
cvcr50st11_1	0.0	18277	18277	9227	13.18	1.0e+00	0.90671	0.00120	0.90911	5 slugs in cruciform pattern

Table 6.9.6-8. Results for 1.5in.-diameter x 2.0 in.-tall slug HEU metal content in CV calculation model

case name	np (in)	U (g)	^{235}U (g)	H_2O (g)	h/x	mocfr	k_{eff}	σ	$k_{eff}+2σ$	content description
cvcr5e0st11_1	0.0	18277	18277	9227	13.18	1.0e+00	0.90690	0.00124	0.90938	5 slugs in cruciform pattern, extended spacing
cvcr5u0st11_1	0.0	18277	18277	9227	13.18	1.0e+00	0.90690	0.00122	0.90935	5 slugs in four pointed star pattern
cvcr5l0st11_1	0.0	18277	18277	9227	13.18	1.0e+00	0.90660	0.00113	0.90885	5 slugs, filled hex. Ring with 2 slugs missing
cvcr6st11_1_1	0.0	21933	21933	9033	10.75	1.0e+00	0.95173	0.00118	0.95409	6 slugs in a hexagonal ring
cvcr6e0st11_1	0.0	21933	21933	9033	10.75	1.0e+00	0.95531	0.00106	0.95742	6 slugs in pentagonal ring with center slug
cvcr70st11_1	0.0	25588	25588	8839	9.02	1.0e+00	0.99827	0.00135	1.00097	7 slugs in hexagonal ring with center slug
cvcr5st11_1_2	0.0	36555	36555	8257	5.90	1.0e+00	0.99909	0.00125	1.00158	10 slugs in stacked pentagonal rings
cvcr5est11_1_2	0.0	36555	36555	8257	5.90	1.0e+00	1.00409	0.00136	1.00681	10 slugs in stacked pent. rings, extended spacing
cvcr6e4st11_1	0.0	36555	36555	8257	5.90	1.0e+00	1.00361	0.00134	1.00630	10 slugs, lower 6 slugs in hex ring, upper 4 in square
cvcr73st11_1	0.0	36555	36555	8257	5.90	1.0e+00	1.00523	0.00127	1.00776	10 slugs, lower 7 slugs in hex ring, upper 3 in triangle
cvcr6st11_1_2	0.0	43865	43865	7869	4.68	1.0e+00	1.05336	0.00130	1.05597	12 slugs in stacked hexagonal rings
with can spacers (np thickness=1.4 in.)										
cvcr5st11_2_1	1.4	18277	18277	8613	12.30	1.0e+00	0.76864	0.00113	0.77089	5 slugs in a pentagonal ring
cvcr5est11_2_1	1.4	18277	18277	8613	12.30	1.0e+00	0.76420	0.00102	0.76624	5 slugs in a pentagonal ring, extended spacing
cvcr50st11_2	1.4	18277	18277	8613	12.30	1.0e+00	0.76929	0.00117	0.77163	5 slugs in cruciform pattern
cvcr5e0st11_2	1.4	18277	18277	8613	12.30	1.0e+00	0.76532	0.00127	0.76785	5 slugs in cruciform pattern, extended spacing
cvcr5u0st11_2	1.4	18277	18277	8613	12.30	1.0e+00	0.76953	0.00108	0.77168	5 slugs in four pointed star pattern
cvcr5l0st11_2	1.4	18277	18277	8613	12.30	1.0e+00	0.77162	0.00102	0.77366	5 slugs, filled hex. Ring with 2 slugs missing
cvcr6st11_2_1	1.4	21933	21933	8419	10.02	1.0e+00	0.81300	0.00148	0.81596	6 slugs in a hexagonal ring
cvcr6e0st11_2	1.4	21933	21933	8419	10.02	1.0e+00	0.81943	0.00116	0.82176	6 slugs in pentagonal ring with center slug
cvcr70st11_2	1.4	25588	25588	8225	8.39	1.0e+00	0.86296	0.00104	0.86503	7 slugs in hexagonal ring with center slug
cvcr5st11_2_2	1.4	36555	36555	7643	5.46	1.0e+00	0.90058	0.00115	0.90287	10 slugs in stacked pentagonal rings
cvcr5est11_2_2	1.4	36555	36555	7643	5.46	1.0e+00	0.89862	0.00121	0.90104	10 slugs in stacked pent. rings, extended spacing
cvcr6e4st11_2	1.4	36555	36555	7643	5.46	1.0e+00	0.89991	0.00109	0.90209	10 slugs, lower 6 slugs in hex ring, upper 4 in square

Table 6.9.6-8. Results for 1.5in.-diameter x 2.0 in.-tall slug HEU metal content in CV calculation model

case name	np (in)	U (g)	^{235}U (g)	H_2O (g)	h/x	mocfr	k_{eff}	σ	$k_{eff}+2σ$	content description
cvcr73st11_2	1.4	36555	36555	7643	5.46	1.0e+00	0.89922	0.00109	0.90139	10 slugs, lower 7 slugs in hex ring, upper 3 in triangle
cvcr6st11_2_2	1.4	43865	43865	7256	4.32	1.0e+00	0.94962	0.00126	0.95213	12 slugs in stacked hexagonal rings
evaluation of model approximations in no can spacer configurations (np thickness=0.0002 in.)										
cvcr6e0st11_1	0.0	21933	21933	9033	10.75	1.0e+00	0.95531	0.00106	0.95742	6 slugs in pentagonal ring with center slug
cv0r6e0s_1	0.0	21933	21933	9033	10.75	1.0e+00	0.95418	0.00135	0.95689	0.0002 cm thick spacers voided in above model
cvwr6e0s_1	0.0	21933	21933	9033	10.75	1.0e+00	0.95384	0.00117	0.95618	0.0002 cm thick spacers replaced with water in above
cvcr70st11_1	0.0	25588	25588	8839	9.02	1.0e+00	0.99827	0.00135	1.00097	7 slugs, hex ring with slug in center
cv0r70s_1	0.0	25588	25588	8839	9.02	1.0e+00	0.99814	0.00118	1.00051	0.0002 cm thick spacers voided in above model
cvwr70s_1	0.0	25588	25588	8839	9.02	1.0e+00	0.99847	0.00120	1.00088	0.0002 cm thick spacers flooded in above model
evaluation of model approximations in configurations with can spacers (np thickness=1.4 in.)										
cvcr6e0st11_2	1.4	21933	21933	8419	10.02	1.0e+00	0.81943	0.00116	0.82176	6 slugs in pentagonal ring with center slug
cv0r6e0s_2	1.4	21933	21933	8419	10.02	1.0e+00	0.84682	0.00118	0.84918	1.4 in thick spacers voided in above model
cvcr6e0st11_1	0.0	21933	21933	9033	10.75	1.0e+00	0.95531	0.00106	0.95742	6 slugs in pentagonal ring with center slug
cvwr6e0s_2	1.4	21933	21933	9033	10.75	1.0e+00	0.89988	0.00138	0.90263	1.4 in thick spacers replace with water
cvcr70st11_2	1.4	25588	25588	8225	8.39	1.0e+00	0.86296	0.00104	0.86503	7 slugs, hex ring with slug in center
cv0r70s_2	1.4	25588	25588	8225	8.39	1.0e+00	0.88250	0.00110	0.88470	1.4 in thick spacers voided in above model
cvcr70st11_1	0.0	25588	25588	8839	9.02	1.0e+00	0.99827	0.00135	1.00097	7 slugs, hex ring with slug in center
cvwr70s_2	1.4	25588	25588	8839	9.02	1.0e+00	0.93953	0.00111	0.94175	1.4 in thick spacers replace with water

Table 6.9.6-9. Results for 1.5in.-diameter x 2.0 in.-tall slug HEU metal content in packaging calculation model

case name	enr	U (g)	^{235}U (g)	H_2O (g)	h/x	moifr	k_{eff}	σ	k_{eff}+2σ	case name	k_{eff}	σ	k_{eff}+2σ
content in flooded containment vessel, single package reflected													
NCT										HAC			
no can spacers (np thickness = 0.0 in.)													
ncsr5est11_1_1_15	100	18277	18277	9227	13.18	1.0e+00	0.86857	0.00128	0.87113	hcsr5est12_1_1_15	0.87319	0.00116	0.87551
ncsr5st11_1_1_15	100	18277	18277	9227	13.18	1.0e+00	0.88102	0.00119	0.88339	hcsr5st12_1_1_15	0.88322	0.00142	0.88606
ncsr6st11_1_1_15	100	21933	21933	9033	10.75	1.0e+00	0.91461	0.00110	0.91680				
ncsr5est11_1_2_15	100	36555	36555	8257	5.90	1.0e+00	0.96511	0.00123	0.96756	hcsr5est12_1_2_15	0.96512	0.00128	0.96768
ncsr5st11_1_2_15	100	36555	36555	8257	5.90	1.0e+00	0.96727	0.00116	0.96960	hcsr5st12_1_2_15	0.97082	0.00124	0.97330
ncsr6e4st11_1_1	100	36555	36555	8257	5.90	1.0e-20	0.92156	0.00105	0.92367				
ncsr6e4st11_1_2	100	36555	36555	8257	5.90	1.0e-05	0.92051	0.00114	0.92279				
ncsr6e4st11_1_3	100	36555	36555	8257	5.90	1.0e-04	0.92239	0.00107	0.92453				
ncsr6e4st11_1_4	100	36555	36555	8257	5.90	1.0e-03	0.91834	0.00126	0.92086				
ncsr6e4st11_1_5	100	36555	36555	8257	5.90	1.0e-02	0.92233	0.00111	0.92455				
ncsr6e4st11_1_6	100	36555	36555	8257	5.90	1.0e-01	0.92584	0.00123	0.92830				
ncsr6e4st11_1_8	100	36555	36555	8257	5.90	3.0e-01	0.93741	0.00125	0.93990				
ncsr6e4st11_1_15	100	36555	36555	8257	5.90	1.0e+00	0.97010	0.00114	0.97238				
ncsr73st11_1_1	100	36555	36555	8257	5.90	1.0e-20	0.92144	0.00127	0.92399				
ncsr73st11_1_2	100	36555	36555	8257	5.90	1.0e-05	0.92591	0.00108	0.92808				
ncsr73st11_1_3	100	36555	36555	8257	5.90	1.0e-04	0.92106	0.00121	0.92348				
ncsr73st11_1_4	100	36555	36555	8257	5.90	1.0e-03	0.92326	0.00122	0.92570				
ncsr73st11_1_5	100	36555	36555	8257	5.90	1.0e-02	0.92213	0.00113	0.92439				
ncsr73st11_1_6	100	36555	36555	8257	5.90	1.0e-01	0.92784	0.00111	0.93007				

Table 6.9.6-9. Results for 1.5in.-diameter x 2.0 in.-tall slug HEU metal content in packaging calculation model

case name	enr	U (g)	^{235}U (g)	H_2O (g)	h/x	moifr	k_{eff}	σ	$k_{eff}+2\sigma$	case name	k_{eff}	σ	$k_{eff}+2\sigma$
ncsr73st11_1_8	100	36555	36555	8257	5.90	3.0e-01	0.93898	0.00115	0.94128				
ncsr73st11_1_15	100	36555	36555	8257	5.90	1.0e+00	0.96854	0.00128	0.97110				
ncsr6st11_1_2_15	100	43865	43865	7869	4.68	1.0e+00	1.01197	0.00132	1.01461				
with can spacers (np thickness = 1.4 in.)													
ncsr5est11_2_1_1	100	18277	18277	8613	12.30	1.0e-20	0.68597	0.00122	0.68841	hcsr5est12_2_1_1	0.68926	0.00101	0.69128
ncsr5est11_2_1_2	100	18277	18277	8613	12.30	1.0e-05	0.68486	0.00101	0.68688	hcsr5est12_2_1_2	0.68645	0.00110	0.68866
ncsr5est11_2_1_3	100	18277	18277	8613	12.30	1.0e-04	0.68766	0.00128	0.69022	hcsr5est12_2_1_3	0.68796	0.00105	0.69007
ncsr5est11_2_1_4	100	18277	18277	8613	12.30	1.0e-03	0.68729	0.00120	0.68969	hcsr5est12_2_1_4	0.68815	0.00098	0.69010
ncsr5est11_2_1_5	100	18277	18277	8613	12.30	1.0e-02	0.68465	0.00128	0.68720	hcsr5est12_2_1_5	0.69008	0.00097	0.69201
ncsr5est11_2_1_6	100	18277	18277	8613	12.30	1.0e-01	0.68906	0.00105	0.69117	hcsr5est12_2_1_6	0.69613	0.00117	0.69847
ncsr5est11_2_1_8	100	18277	18277	8613	12.30	3.0e-01	0.70289	0.00101	0.70491	hcsr5est12_2_1_8	0.70357	0.00107	0.70571
ncsr5est11_2_1_15	100	18277	18277	8613	12.30	1.0e+00	0.73412	0.00109	0.73629	hcsr5est12_2_1_15	0.73557	0.00101	0.73759
ncsr5st11_2_1_1	100	18277	18277	8613	12.30	1.0e-20	0.70896	0.00096	0.71087				
ncsr5st11_2_1_2	100	18277	18277	8613	12.30	1.0e-05	0.70901	0.00095	0.71092				
ncsr5st11_2_1_3	100	18277	18277	8613	12.30	1.0e-04	0.71109	0.00096	0.71300				
ncsr5st11_2_1_4	100	18277	18277	8613	12.30	1.0e-03	0.70980	0.00102	0.71184				
ncsr5st11_2_1_5	100	18277	18277	8613	12.30	1.0e-02	0.71089	0.00103	0.71294				
ncsr5st11_2_1_6	100	18277	18277	8613	12.30	1.0e-01	0.71505	0.00112	0.71729				
ncsr5st11_2_1_8	100	18277	18277	8613	12.30	3.0e-01	0.72364	0.00121	0.72605				
ncsr5st11_2_1_15	100	18277	18277	8613	12.30	1.0e+00	0.74773	0.00114	0.75001	hcsr5st12_2_1_15	0.74885	0.00101	0.75087
ncsr6st11_2_1_1	100	21933	21933	8419	10.02	1.0e-20	0.73305	0.00104	0.73514				
ncsr6st11_2_1_2	100	21933	21933	8419	10.02	1.0e-05	0.73284	0.00105	0.73494				

Table 6.9.6-9. Results for 1.5in.-diameter x 2.0 in.-tall slug HEU metal content in packaging calculation model

case name	enr	U (g)	^{235}U (g)	H_2O (g)	h/x	moifr	k_{eff}	σ	k_{eff}+2σ	case name	k_{eff}	σ	k_{eff}+2σ
ncsr6st11_2_1_3	100	21933	21933	8419	10.02	1.0e-04	0.73419	0.00111	0.73641				
ncsr6st11_2_1_4	100	21933	21933	8419	10.02	1.0e-03	0.73339	0.00106	0.73551				
ncsr6st11_2_1_5	100	21933	21933	8419	10.02	1.0e-02	0.73282	0.00101	0.73484				
ncsr6st11_2_1_6	100	21933	21933	8419	10.02	1.0e-01	0.73962	0.00104	0.74170				
ncsr6st11_2_1_8	100	21933	21933	8419	10.02	3.0e-01	0.74981	0.00112	0.75206				
ncsr6st11_2_1_15	100	21933	21933	8419	10.02	1.0e+00	0.78295	0.00118	0.78531				
ncsr5est11_2_2_1	100	36555	36555	7643	5.46	1.0e-20	0.81441	0.00102	0.81646	hcsr5est12_2_2_1	0.81949	0.00126	0.82202
ncsr5est11_2_2_2	100	36555	36555	7643	5.46	1.0e-05	0.81751	0.00107	0.81966	hcsr5est12_2_2_2	0.81765	0.00108	0.81981
ncsr5est11_2_2_3	100	36555	36555	7643	5.46	1.0e-04	0.81443	0.00110	0.81664	hcsr5est12_2_2_3	0.81691	0.00115	0.81922
ncsr5est11_2_2_4	100	36555	36555	7643	5.46	1.0e-03	0.81628	0.00124	0.81876	hcsr5est12_2_2_4	0.81854	0.00123	0.82100
ncsr5est11_2_2_5	100	36555	36555	7643	5.46	1.0e-02	0.81513	0.00118	0.81749	hcsr5est12_2_2_5	0.81898	0.00104	0.82106
ncsr5est11_2_2_6	100	36555	36555	7643	5.46	1.0e-01	0.82099	0.00114	0.82326	hcsr5est12_2_2_6	0.82414	0.00111	0.82636
ncsr5est11_2_2_8	100	36555	36555	7643	5.46	3.0e-01	0.83205	0.00109	0.83424	hcsr5est12_2_2_8	0.83469	0.00107	0.83683
ncsr5est11_2_2_15	100	36555	36555	7643	5.46	1.0e+00	0.86471	0.00124	0.86719	hcsr5est12_2_2_15	0.86591	0.00115	0.86822
ncsr5st11_2_2_1	100	36555	36555	7643	5.46	1.0e-20	0.83654	0.00109	0.83872				
ncsr5st11_2_2_2	100	36555	36555	7643	5.46	1.0e-05	0.83389	0.00104	0.83597				
ncsr5st11_2_2_3	100	36555	36555	7643	5.46	1.0e-04	0.83615	0.00113	0.83841				
ncsr5st11_2_2_4	100	36555	36555	7643	5.46	1.0e-03	0.83524	0.00141	0.83806				
ncsr5st11_2_2_5	100	36555	36555	7643	5.46	1.0e-02	0.83580	0.00109	0.83797				
ncsr5st11_2_2_6	100	36555	36555	7643	5.46	1.0e-01	0.84206	0.00110	0.84426				
ncsr5st11_2_2_8	100	36555	36555	7643	5.46	3.0e-01	0.85011	0.00135	0.85281				
ncsr5st11_2_2_15	100	36555	36555	7643	5.46	1.0e+00	0.87549	0.00131	0.87810	hcsr5st12_2_2_15	0.87483	0.00116	0.87715

Table 6.9.6-9. Results for 1.5in.-diameter x 2.0 in.-tall slug HEU metal content in packaging calculation model

case name	enr	U (g)	^{235}U (g)	H_2O (g)	h/x	moifr	k_{eff}	σ	k_{eff}+2σ	case name	k_{eff}	σ	k_{eff}+2σ
ncsr6e4st11_2_1	100	36555	36555	7643	5.46	1.0e-20	0.83636	0.00110	0.83857				
ncsr6e4st11_2_2	100	36555	36555	7643	5.46	1.0e-05	0.83532	0.00112	0.83757				
ncsr6e4st11_2_3	100	36555	36555	7643	5.46	1.0e-04	0.83689	0.00118	0.83924				
ncsr6e4st11_2_4	100	36555	36555	7643	5.46	1.0e-03	0.83744	0.00114	0.83972				
ncsr6e4st11_2_5	100	36555	36555	7643	5.46	1.0e-02	0.83615	0.00122	0.83858				
ncsr6e4st11_2_6	100	36555	36555	7643	5.46	1.0e-01	0.84173	0.00127	0.84426				
ncsr6e4st11_2_8	100	36555	36555	7643	5.46	3.0e-01	0.84987	0.00113	0.85213				
ncsr6e4st11_2_15	100	36555	36555	7643	5.46	1.0e+00	0.87722	0.00131	0.87984				
ncsr73st11_2_1	100	36555	36555	7643	5.46	1.0e-20	0.83665	0.00111	0.83887				
ncsr73st11_2_2	100	36555	36555	7643	5.46	1.0e-05	0.83570	0.00116	0.83801				
ncsr73st11_2_3	100	36555	36555	7643	5.46	1.0e-04	0.83716	0.00115	0.83946				
ncsr73st11_2_4	100	36555	36555	7643	5.46	1.0e-03	0.83728	0.00117	0.83961				
ncsr73st11_2_5	100	36555	36555	7643	5.46	1.0e-02	0.83790	0.00116	0.84023				
ncsr73st11_2_6	100	36555	36555	7643	5.46	1.0e-01	0.84068	0.00120	0.84309				
ncsr73st11_2_8	100	36555	36555	7643	5.46	3.0e-01	0.84928	0.00106	0.85139				
ncsr73st11_2_15	100	36555	36555	7643	5.46	1.0e+00	0.87257	0.00099	0.87455				
ncsr6st11_2_2_1	100	43865	43865	7256	4.32	1.0e-20	0.86427	0.00104	0.86636				
ncsr6st11_2_2_2	100	43865	43865	7256	4.32	1.0e-05	0.86386	0.00108	0.86601				
ncsr6st11_2_2_3	100	43865	43865	7256	4.32	1.0e-04	0.86637	0.00117	0.86870				
ncsr6st11_2_2_4	100	43865	43865	7256	4.32	1.0e-03	0.86498	0.00125	0.86747				
ncsr6st11_2_2_5	100	43865	43865	7256	4.32	1.0e-02	0.86541	0.00116	0.86773				
ncsr6st11_2_2_6	100	43865	43865	7256	4.32	1.0e-01	0.87070	0.00111	0.87292				

Table 6.9.6-9. Results for 1.5in.-diameter x 2.0 in.-tall slug HEU metal content in packaging calculation model

case name	enr	U (g)	^{235}U (g)	H_2O (g)	h/x	moifr	k_{eff}	σ	k_{eff}+2σ	case name	k_{eff}	σ	k_{eff}+2σ
ncsr6st11_2_2_8	100	43865	43865	7256	4.32	3.0e-01	0.88148	0.00122	0.88392				
ncsr6st11_2_2_15	100	43865	43865	7256	4.32	1.0e+00	0.91478	0.00118	0.91713				
content in flooded containment vessel, array packaging model for CSI=0.0													
NCT										HAC			
no can spacers (np thickness = 0.0 in.)													
ncia5est11_1_1_8_3	100	18277	18277	9227	13.18	1.0e-04	0.92163	0.00126	0.92414	hcia5est12_1_1_8_3	0.91941	0.00126	0.92194
ncia5est11_1_1_7_3	95	18289	17374	9227	13.86	1.0e-04	0.90412	0.00109	0.90630	hcia5est12_1_1_7_3	0.90066	0.00110	0.90285
ncia5est11_1_1_5_3	90	18324	14659	9227	16.43	1.0e-04	0.85207	0.00110	0.85427	hcia5est12_1_1_6_3	0.88401	0.00108	0.88616
ncia5est11_1_1_4_3	80	18347	12843	9227	18.75	1.0e-04	0.81402	0.00108	0.81617	hcia5est12_1_1_5_3	0.84983	0.00117	0.85217
ncia5est11_1_1_6_3	70	18300	16470	9227	14.62	1.0e-04	0.88510	0.00118	0.88746	hcia5est12_1_1_4_3	0.81368	0.00111	0.81590
ncia5est11_1_1_3_3	60	18370	11022	9227	21.85	1.0e-04	0.77131	0.00109	0.77349	hcia5est12_1_1_3_3	0.77296	0.00113	0.77523
ncia5est11_1_1_2_3	40	18417	7367	9227	32.69	1.0e-04	0.67736	0.00103	0.67943	hcia5est12_1_1_2_3	0.67968	0.00108	0.68184
ncia5est11_1_1_1_3	19	18466	3509	9227	68.64	1.0e-04	0.54780	0.00092	0.54964	hcia5est12_1_1_1_3	0.54586	0.00117	0.54819
ncia5st11_1_1_8_3	100	18277	18277	9227	13.18	1.0e-04	0.92611	0.00127	0.92865	hcia5st12_1_1_8_3	0.92609	0.00110	0.92829
ncia5st11_1_1_7_3	95	18289	17374	9227	13.86	1.0e-04	0.90538	0.00116	0.90769	hcia5st12_1_1_7_3	0.90683	0.00113	0.90909
ncia5st11_1_1_5_3	90	18324	14659	9227	16.43	1.0e-04	0.88586	0.00112	0.88811	hcia5st12_1_1_6_3	0.88827	0.00110	0.89046
ncia5st11_1_1_4_3	80	18347	12843	9227	18.75	1.0e-04	0.84871	0.00124	0.85119	hcia5st12_1_1_5_3	0.85050	0.00113	0.85276
ncia5st11_1_1_6_3	70	18300	16470	9227	14.62	1.0e-04	0.80834	0.00102	0.81037	hcia5st12_1_1_4_3	0.80870	0.00112	0.81094
ncia5st11_1_1_3_3	60	18370	11022	9227	21.85	1.0e-04	0.76467	0.00098	0.76663	hcia5st12_1_1_3_3	0.76245	0.00105	0.76454
ncia5st11_1_1_2_3	40	18417	7367	9227	32.69	1.0e-04	0.66040	0.00106	0.66252	hcia5st12_1_1_2_3	0.65955	0.00097	0.66149
ncia5st11_1_1_1_3	19	18466	3509	9227	68.64	1.0e-04	0.51929	0.00090	0.52109	hcia5st12_1_1_1_3	0.51805	0.00084	0.51973
with can spacers (np thickness = 1.4 in.)													
ncia5est11_2_1_8_3	100	18277	18277	8613	12.30	1.0e-04	0.80353	0.00113	0.80580	hcia5est12_2_1_8_3	0.80594	0.00121	0.80835
ncia5est11_2_1_7_3	95	18289	17374	8613	12.94	1.0e-04	0.78741	0.00118	0.78977	hcia5est12_2_1_7_3	0.78684	0.00107	0.78898

Table 6.9.6-9. Results for 1.5in.-diameter x 2.0 in.-tall slug HEU metal content in packaging calculation model

case name	enr	U (g)	^{235}U (g)	H_2O (g)	h/x	moifr	k_{eff}	σ	k_{eff}+2σ	case name	k_{eff}	σ	k_{eff}+2σ
ncia5est11_2_1_6_3	90	18300	16470	8613	13.65	1.0e-04	0.77061	0.00112	0.77285	hcia5est12_2_1_6_3	0.77268	0.00114	0.77496
ncia5est11_2_1_5_3	80	18324	14659	8613	15.34	1.0e-04	0.73732	0.00118	0.73969	hcia5est12_2_1_5_3	0.73645	0.00094	0.73834
ncia5est11_2_1_4_3	70	18347	12843	8613	17.51	1.0e-04	0.70261	0.00108	0.70477	hcia5est12_2_1_4_3	0.70418	0.00107	0.70631
ncia5est11_2_1_3_3	60	18370	11022	8613	20.40	1.0e-04	0.66332	0.00094	0.66520	hcia5est12_2_1_3_3	0.66396	0.00114	0.66624
ncia5est11_2_1_2_3	40	18417	7367	8613	30.52	1.0e-04	0.57466	0.00097	0.57660	hcia5est12_2_1_2_3	0.57526	0.00080	0.57687
ncia5est11_2_1_1_3	19	18466	3509	8613	64.08	1.0e-04	0.45117	0.00082	0.45280	hcia5est12_2_1_1_3	0.45114	0.00084	0.45281
ncia70st11_2_8_3	100	25588	25588	8225	8.39	1.0e-04	0.91300	0.00104	0.91507	hcia70st12_2_8_3	0.91329	0.00111	0.91551
ncia70st11_2_7_3	95	25604	24324	8225	8.83	1.0e-04	0.89143	0.00108	0.89360	hcia70st12_2_7_3	0.89210	0.00124	0.89457
ncia70st11_2_6_3	90	25621	23059	8225	9.31	1.0e-04	0.87368	0.00108	0.87585	hcia70st12_2_6_3	0.87198	0.00113	0.87425
ncia70st11_2_5_3	80	25653	20522	8225	10.46	1.0e-04	0.83357	0.00110	0.83577	hcia70st12_2_5_3	0.83150	0.00106	0.83362
ncia70st11_2_4_3	70	25686	17980	8225	11.94	1.0e-04	0.78606	0.00105	0.78816	hcia70st12_2_4_3	0.78783	0.00099	0.78981
ncia70st11_2_3_3	60	25718	15431	8225	13.91	1.0e-04	0.73820	0.00099	0.74017	hcia70st12_2_3_3	0.73745	0.00100	0.73944
ncia70st11_2_2_3	40	25784	10313	8225	20.82	1.0e-04	0.62591	0.00090	0.62771	hcia70st12_2_2_3	0.62664	0.00107	0.62878
ncia70st11_2_1_3	19	25853	4912	8225	43.71	1.0e-04	0.47179	0.00077	0.47333	hcia70st12_2_1_3	0.47178	0.00086	0.47349
ncia5est11_2_2_8_3	100	36555	36555	7643	5.46	1.0e-04	0.98202	0.00112	0.98425	hcia5est12_2_2_8_3	0.98033	0.00111	0.98254
ncia5est11_2_2_7_3	95	36578	34749	7643	5.74	1.0e-04	0.96108	0.00119	0.96346	hcia5est12_2_2_7_3	0.96166	0.00113	0.96392
ncia5est11_2_2_6_3	90	36601	32941	7643	6.06	1.0e-04	0.94424	0.00134	0.94692	hcia5est12_2_2_6_3	0.94560	0.00118	0.94796
ncia5est11_2_2_5_3	80	36647	29318	7643	6.80	1.0e-04	0.90628	0.00109	0.90846	hcia5est12_2_2_5_3	0.90763	0.00117	0.90997
ncia5est11_2_2_4_3	70	36694	25686	7643	7.77	1.0e-04	0.86606	0.00104	0.86814	hcia5est12_2_2_4_3	0.86855	0.00104	0.87064
ncia5est11_2_2_3_3	60	36740	22044	7643	9.05	1.0e-04	0.82451	0.00098	0.82647	hcia5est12_2_2_3_3	0.82536	0.00115	0.82767
ncia5est11_2_2_2_3	40	36834	14734	7643	13.54	1.0e-04	0.72349	0.00093	0.72535	hcia5est12_2_2_2_3	0.72285	0.00114	0.72513
ncia5est11_2_2_1_3	19	36932	7017	7643	28.43	1.0e-04	0.58171	0.00100	0.58370	hcia5est12_2_2_1_3	0.58235	0.00096	0.58427

Table 6.9.6-9. Results for 1.5in.-diameter x 2.0 in.-tall slug HEU metal content in packaging calculation model

case name	enr	U (g)	^{235}U (g)	H_2O (g)	h/x	moifr	k_{eff}	σ	$k_{eff}+2σ$	case name	k_{eff}	σ	$k_{eff}+2σ$
ncia5st11_2_2_8_3	100	36555	36555	7643	5.46	1.0e-04	0.97720	0.00133	0.97986	hcia5st12_2_2_8_3	0.97562	0.00123	0.97807
ncia5st11_2_2_7_3	95	36578	34749	7643	5.74	1.0e-04	0.95854	0.00105	0.96064	hcia5st12_2_2_7_3	0.95594	0.00097	0.95789
ncia5st11_2_2_6_3	90	36601	32941	7643	6.06	1.0e-04	0.93619	0.00132	0.93883	hcia5st12_2_2_6_3	0.93579	0.00110	0.93800
ncia5st11_2_2_5_3	80	36647	29318	7643	6.80	1.0e-04	0.90011	0.00117	0.90244	hcia5st12_2_2_5_3	0.89786	0.00154	0.90095
ncia5st11_2_2_4_3	70	36694	25686	7643	7.77	1.0e-04	0.85499	0.00102	0.85703	hcia5st12_2_2_4_3	0.85363	0.00119	0.85601
ncia5st11_2_2_3_3	60	36740	22044	7643	9.05	1.0e-04	0.80868	0.00116	0.81101	hcia5st12_2_2_3_3	0.80882	0.00105	0.81091
ncia5st11_2_2_2_3	40	36834	14734	7643	13.54	1.0e-04	0.70077	0.00098	0.70274	hcia5st12_2_2_2_3	0.70205	0.00105	0.70415
ncia5st11_2_2_1_3	19	36932	7017	7643	28.43	1.0e-04	0.55139	0.00095	0.55330	hcia5st12_2_2_1_3	0.55187	0.00101	0.55389
content in flooded containment vessel, array packaging model for CSI=0.4													
NCT										HAC			
no can spacers (np thickness = 0.0 in.)													
ncf15est11_1_1_8_3	100	18277	18277	9227	13.18	1.0e-04	0.87707	0.00119	0.87944	hcf25est12_1_1_8_3	0.86992	0.00106	0.87204
ncf15est11_1_1_7_3	95	18289	17374	9227	13.86	1.0e-04	0.86115	0.00120	0.86354	hcf25est12_1_1_7_3	0.85401	0.00126	0.85652
ncf15est11_1_1_6_3	90	18300	16470	9227	14.62	1.0e-04	0.84672	0.00112	0.84896	hcf25est12_1_1_6_3	0.83451	0.00102	0.83656
ncf15est11_1_1_5_3	80	18324	14659	9227	16.43	1.0e-04	0.81108	0.00109	0.81327	hcf25est12_1_1_5_3	0.80144	0.00107	0.80358
ncf15est11_1_1_4_3	70	18347	12843	9227	18.75	1.0e-04	0.77287	0.00112	0.77510	hcf25est12_1_1_4_3	0.76516	0.00111	0.76739
ncf15est11_1_1_3_3	60	18370	11022	9227	21.85	1.0e-04	0.73211	0.00114	0.73440	hcf25est12_1_1_3_3	0.72484	0.00118	0.72719
ncf15est11_1_1_2_3	40	18417	7367	9227	32.69	1.0e-04	0.64270	0.00105	0.64480	hcf25est12_1_1_2_3	0.63366	0.00107	0.63580
ncf15est11_1_1_1_3	19	18466	3509	9227	68.64	1.0e-04	0.51398	0.00088	0.51573	hcf25est12_1_1_1_3	0.51052	0.00094	0.51241
with can spacers (np thickness = 1.4 in.)													
ncf15est11_2_1_8_3	100	18277	18277	8613	12.30	1.0e-04	0.76015	0.00112	0.76239	hcf25est12_2_1_8_3	0.75353	0.00102	0.75558
ncf15est11_2_1_7_3	95	18289	17374	8613	12.94	1.0e-04	0.74428	0.00129	0.74686	hcf25est12_2_1_7_3	0.73938	0.00109	0.74156
ncf15est11_2_1_6_3	90	18300	16470	8613	13.65	1.0e-04	0.72783	0.00107	0.72998	hcf25est12_2_1_6_3	0.72401	0.00105	0.72611
ncf15est11_2_1_5_3	80	18324	14659	8613	15.34	1.0e-04	0.69813	0.00098	0.70009	hcf25est12_2_1_5_3	0.69017	0.00089	0.69195
ncf15est11_2_1_4_3	70	18347	12843	8613	17.51	1.0e-04	0.66593	0.00098	0.66789	hcf25est12_2_1_4_3	0.65691	0.00113	0.65916

Table 6.9.6-9. Results for 1.5in.-diameter x 2.0 in.-tall slug HEU metal content in packaging calculation model

case name	enr	U (g)	^{235}U (g)	H_2O (g)	h/x	moifr	k_{eff}	σ	k_{eff}+2σ	case name	k_{eff}	σ	k_{eff}+2σ
ncf15est11_2_1_3_3	60	18370	11022	8613	20.40	1.0e-04	0.62541	0.00096	0.62733	hcf25est12_2_1_3_3	0.61903	0.00111	0.62125
ncf15est11_2_1_2_3	40	18417	7367	8613	30.52	1.0e-04	0.54139	0.00091	0.54320	hcf25est12_2_1_2_3	0.53450	0.00087	0.53625
ncf15est11_2_1_1_3	19	18466	3509	8613	64.08	1.0e-04	0.42329	0.00080	0.42489	hcf25est12_2_1_1_3	0.41671	0.00077	0.41825
ncf15est11_2_2_8_3	100	36555	36555	7643	5.46	1.0e-04	0.93621	0.00109	0.93839	hcf25est12_2_2_8_3	0.92186	0.00104	0.92394
ncf15est11_2_2_7_3	95	36578	34749	7643	5.74	1.0e-04	0.91732	0.00132	0.91995	hcf25est12_2_2_7_3	0.90286	0.00137	0.90560
ncf15est11_2_2_6_3	90	36601	32941	7643	6.06	1.0e-04	0.89754	0.00118	0.89990	hcf25est12_2_2_6_3	0.88774	0.00119	0.89013
ncf15est11_2_2_5_3	80	36647	29318	7643	6.80	1.0e-04	0.86210	0.00109	0.86428	hcf25est12_2_2_5_3	0.85335	0.00111	0.85557
ncf15est11_2_2_4_3	70	36694	25686	7643	7.77	1.0e-04	0.82389	0.00121	0.82631	hcf25est12_2_2_4_3	0.81165	0.00110	0.81386
ncf15est11_2_2_3_3	60	36740	22044	7643	9.05	1.0e-04	0.78278	0.00120	0.78519	hcf25est12_2_2_3_3	0.77147	0.00114	0.77375
ncf15est11_2_2_2_3	40	36834	14734	7643	13.54	1.0e-04	0.68461	0.00116	0.68692	hcf25est12_2_2_2_3	0.67454	0.00112	0.67679
ncf15est11_2_2_1_3	19	36932	7017	7643	28.43	1.0e-04	0.54624	0.00099	0.54823	hcf25est12_2_2_1_3	0.53779	0.00105	0.53989

Table 6.9.6-10. Results for HEU broken metal content in CV calculation model

case name	np (in)	enr. (wt%)	U (g)	^{235}U (g)	H_2O (g)	h/x	mocfr	k_{eff}	σ	k_{eff}+2σ				
broken metal as 1-in. cubes, flooded containment vessel, reflected														
no can spacers (np thickness = 0.0 in.)														
cvr3sqa_36_1_8_15	0.0	100	35142	35142	8332	6.19	1.0e+00	0.93455	0.00107	0.93668				
cvr3sqa_36_1_7_15	0.0	95	35164	33406	8332	6.51	1.0e+00	0.91663	0.00128	0.91920				
cvr3sqa_36_1_6_15	0.0	90	35186	31667	8332	6.87	1.0e+00	0.90133	0.00123	0.90379				
cvr3sqa_36_1_5_15	0.0	80	35230	28184	8332	7.72	1.0e+00	0.87330	0.00119	0.87567				
cvr3sqa_36_1_4_15	0.0	70	35275	24693	8332	8.81	1.0e+00	0.84424	0.00113	0.84650				
cvr3sqa_36_1_3_15	0.0	60	35320	21192	8332	10.26	1.0e+00	0.81162	0.00124	0.81410				

Table 6.9.6-10. Results for HEU broken metal content in CV calculation model

case name	np (in)	enr. (wt%)	U (g)	^{235}U (g)	H_2O (g)	h/x	mocfr	k_{eff}	σ	$k_{eff}+2σ$				
cvr3sqa_36_1_2_15	0.0	40	35410	14164	8332	15.35	1.0e+00	0.73700	0.00098	0.73896				
cvr3sqa_36_1_1_15	0.0	19	35505	6746	8332	32.24	1.0e+00	0.63755	0.00119	0.63992				
cvr3sqa_36_1_8_1	0.0	100	35142	35142	0	0.00	1.0e-20	0.78442	0.00112	0.78667				
cvr3sqa_36_1_8_6	0.0	100	35142	35142	833	0.62	1.0e-01	0.79134	0.00116	0.79366				
cvr3sqa_36_1_8_7	0.0	100	35142	35142	1666	1.24	2.0e-01	0.80350	0.00113	0.80577				
cvr3sqa_36_1_8_8	0.0	100	35142	35142	2500	1.86	3.0e-01	0.81548	0.00107	0.81761				
cvr3sqa_36_1_8_9	0.0	100	35142	35142	3333	2.48	4.0e-01	0.83048	0.00122	0.83293				
cvr3sqa_36_1_8_10	0.0	100	35142	35142	4166	3.09	5.0e-01	0.84727	0.00122	0.84971				
cvr3sqa_36_1_8_11	0.0	100	35142	35142	4999	3.71	6.0e-01	0.86174	0.00123	0.86420				
cvr3sqa_36_1_8_12	0.0	100	35142	35142	5832	4.33	7.0e-01	0.87977	0.00118	0.88213				
cvr3sqa_36_1_8_13	0.0	100	35142	35142	6666	4.95	8.0e-01	0.89818	0.00110	0.90037				
cvr3sqa_36_1_8_14	0.0	100	35142	35142	7499	5.57	9.0e-01	0.91611	0.00118	0.91846				
cvr3sqa_36_1_8_15	0.0	100	35142	35142	8332	6.19	1.0e+00	0.93455	0.00107	0.93668				
with can spacers (np thickness = 1.4 in.)														
cvr3sqa_36_2_8_15	1.4	100	35142	35142	7719	5.73	1.0e+00	0.85151	0.00123	0.85397				
cvr3sqa_36_2_7_15	1.4	95	35164	33406	7719	6.03	1.0e+00	0.83521	0.00123	0.83766				
cvr3sqa_36_2_6_15	1.4	90	35186	31667	7719	6.36	1.0e+00	0.82166	0.00125	0.82415				
cvr3sqa_36_2_5_15	1.4	80	35230	28184	7719	7.15	1.0e+00	0.78928	0.00112	0.79152				
cvr3sqa_36_2_4_15	1.4	70	35275	24693	7719	8.16	1.0e+00	0.75994	0.00113	0.76220				
cvr3sqa_36_2_3_15	1.4	60	35320	21192	7719	9.51	1.0e+00	0.72673	0.00112	0.72898				
cvr3sqa_36_2_2_15	1.4	40	35410	14164	7719	14.22	1.0e+00	0.65008	0.00102	0.65213				
cvr3sqa_36_2_1_15	1.4	19	35505	6746	7719	29.86	1.0e+00	0.54677	0.00102	0.54881				

Table 6.9.6-10. Results for HEU broken metal content in CV calculation model

case name	np (in)	enr. (wt%)	U (g)	^{235}U (g)	H_2O (g)	h/x	mocfr	k_{eff}	σ	k_{eff}+2σ				
broken metal as lattice homogenized 1-in. cubes, flooded containment vessel, reflected														
no can spacers (np thickness = 0.0 in.)														
cvr3lha_36_1_8_1	0.0	100	35142	35142	0	0.00	1.0e-20	0.74814	0.00123	0.75060				
cvr3lha_36_1_8_6	0.0	100	35142	35142	833	0.62	1.0e-01	0.76415	0.00125	0.76665				
cvr3lha_36_1_8_7	0.0	100	35142	35142	1666	1.24	2.0e-01	0.77899	0.00102	0.78103				
cvr3lha_36_1_8_8	0.0	100	35142	35142	2500	1.86	3.0e-01	0.79660	0.00143	0.79946				
cvr3lha_36_1_8_9	0.0	100	35142	35142	3333	2.48	4.0e-01	0.81635	0.00113	0.81861				
cvr3lha_36_1_8_10	0.0	100	35142	35142	4166	3.09	5.0e-01	0.83767	0.00109	0.83986				
cvr3lha_36_1_8_11	0.0	100	35142	35142	4999	3.71	6.0e-01	0.85716	0.00116	0.85949				
cvr3lha_36_1_8_12	0.0	100	35142	35142	5832	4.33	7.0e-01	0.88187	0.00114	0.88415				
cvr3lha_36_1_8_13	0.0	100	35142	35142	6666	4.95	8.0e-01	0.90182	0.00109	0.90399				
cvr3lha_36_1_8_14	0.0	100	35142	35142	7499	5.57	9.0e-01	0.92553	0.00148	0.92849				
cvr3lha_36_1_8_15	0.0	100	35142	35142	8332	6.19	1.0e+00	0.94654	0.00126	0.94906				
cvr3lha_36_1_8_15	0.0	100	35142	35142	8332	6.19	1.0e+00	0.94654	0.00126	0.94906				
cvr3lha_36_1_7_15	0.0	95	35164	33406	8332	6.51	1.0e+00	0.93172	0.00115	0.93403				
cvr3lha_36_1_6_15	0.0	90	35186	31667	8332	6.87	1.0e+00	0.91744	0.00126	0.91995				
cvr3lha_36_1_5_15	0.0	80	35230	28184	8332	7.72	1.0e+00	0.89049	0.00113	0.89274				
cvr3lha_36_1_4_15	0.0	70	35275	24693	8332	8.81	1.0e+00	0.85930	0.00133	0.86196				
cvr3lha_36_1_3_15	0.0	60	35320	21192	8332	10.26	1.0e+00	0.82623	0.00131	0.82886				
cvr3lha_36_1_2_15	0.0	40	35410	14164	8332	15.35	1.0e+00	0.75317	0.00110	0.75536				
cvr3lha_36_1_1_15	0.0	19	35505	6746	8332	32.24	1.0e+00	0.65522	0.00102	0.65726				
cvr3lha_36_1_8_15	0.0	100	35142	35142	8332	6.19	1.0e+00	0.94654	0.00126	0.94906				
cvr3lha_35_1_8_15	0.0	100	34217	34217	8381	6.39	1.0e+00	0.94183	0.00106	0.94396				

Table 6.9.6-10. Results for HEU broken metal content in CV calculation model

case name	np (in)	enr. (wt%)	U (g)	^{235}U (g)	H_2O (g)	h/x	mocfr	k_{eff}	σ	$k_{eff}+2σ$				
cvr3lha_34_1_8_15	0.0	100	33292	33292	8430	6.61	1.0e+00	0.93673	0.00125	0.93922				
cvr3lha_33_1_8_15	0.0	100	32367	32367	8479	6.84	1.0e+00	0.95706	0.00123	0.95952				
cvr3lha_32_1_8_15	0.0	100	31442	31442	8528	7.08	1.0e+00	0.94986	0.00142	0.95271				
cvr3lha_31_1_8_15	0.0	100	30518	30518	8578	7.34	1.0e+00	0.94716	0.00118	0.94953				
cvr3lha_30_1_8_15	0.0	100	29593	29593	8627	7.61	1.0e+00	0.93908	0.00127	0.94162				
cvr3lha_29_1_8_15	0.0	100	28668	28668	8676	7.90	1.0e+00	0.93306	0.00126	0.93557				
cvr3lha_28_1_8_15	0.0	100	27743	27743	8725	8.21	1.0e+00	0.93059	0.00137	0.93333				
cvr3lha_27_1_8_15	0.0	100	26818	26818	8774	8.54	1.0e+00	0.92502	0.00139	0.92780				
cvr3lha_26_1_8_15	0.0	100	25894	25894	8823	8.89	1.0e+00	0.91519	0.00145	0.91810				
cvr3lha_25_1_8_15	0.0	100	24969	24969	8872	9.27	1.0e+00	0.91200	0.00125	0.91451				
cvr3lha_24_1_8_15	0.0	100	23119	23119	8970	10.13	1.0e+00	0.92028	0.00106	0.92241				
cvr3lha_23_1_8_15	0.0	100	22195	22195	9019	10.61	1.0e+00	0.91201	0.00115	0.91430				
cvr3lha_22_1_8_15	0.0	100	21270	21270	9068	11.13	1.0e+00	0.90500	0.00138	0.90777				
cvr3lha_21_1_8_15	0.0	100	20345	20345	9117	11.70	1.0e+00	0.89763	0.00133	0.90030				
cvr3lha_31_1_7_15	0.0	95	30537	29010	8578	7.72	1.0e+00	0.92875	0.00129	0.93134				
cvr3lha_30_1_7_15	0.0	95	29612	28131	8627	8.00	1.0e+00	0.92618	0.00111	0.92840				
cvr3lha_29_1_7_15	0.0	95	28686	27252	8676	8.31	1.0e+00	0.91841	0.00107	0.92055				
cvr3lha_28_1_7_15	0.0	95	27761	26373	8725	8.63	1.0e+00	0.91075	0.00124	0.91322				
cvr3lha_27_1_7_15	0.0	95	26835	25494	8774	8.98	1.0e+00	0.90920	0.00117	0.91153				
cvr3lha_33_1_6_15	0.0	90	32408	29167	8479	7.59	1.0e+00	0.92553	0.00126	0.92804				
cvr3lha_32_1_6_15	0.0	90	31482	28334	8528	7.86	1.0e+00	0.92000	0.00119	0.92238				
cvr3lha_31_1_6_15	0.0	90	30556	27501	8578	8.14	1.0e+00	0.91758	0.00132	0.92021				

Table 6.9.6-10. Results for HEU broken metal content in CV calculation model

case name	np (in)	enr. (wt%)	U (g)	^{235}U (g)	H_2O (g)	h/x	mocfr	k_{eff}	σ	$k_{eff}+2σ$				
cvr3lha_36_1_5_15	0.0	80	35230	28184	8332	7.72	1.0e+00	0.89049	0.00113	0.89274				
cvr3lha_35_1_5_15	0.0	80	34303	27443	8381	7.97	1.0e+00	0.88496	0.00111	0.88719				
cvr3lha_34_1_5_15	0.0	80	33376	26701	8430	8.24	1.0e+00	0.88044	0.00106	0.88256				
cvr3lha_33_1_5_15	0.0	80	32449	25959	8479	8.53	1.0e+00	0.89355	0.00112	0.89579				
cvr3lha_32_1_5_15	0.0	80	31522	25218	8528	8.83	1.0e+00	0.88961	0.00146	0.89253				
cvr3lha_31_1_5_15	0.0	80	30595	24476	8578	9.15	1.0e+00	0.88752	0.00141	0.89034				
cvr3lha_36_1_4_15	0.0	70	35275	24693	8332	8.81	1.0e+00	0.85930	0.00133	0.86196				
cvr3lha_35_1_4_15	0.0	70	34347	24043	8381	9.10	1.0e+00	0.85473	0.00113	0.85698				
cvr3lha_34_1_4_15	0.0	70	33419	23393	8430	9.41	1.0e+00	0.85237	0.00129	0.85496				
cvr3lha_33_1_4_15	0.0	70	32490	22743	8479	9.73	1.0e+00	0.86299	0.00121	0.86542				
cvr3lha_32_1_4_15	0.0	70	31562	22093	8528	10.08	1.0e+00	0.85876	0.00132	0.86140				
cvr3lha_31_1_4_15	0.0	70	30634	21444	8578	10.44	1.0e+00	0.85471	0.00125	0.85720				
cvr3lha_36_1_3_15	0.0	60	35320	21192	8332	10.26	1.0e+00	0.82623	0.00131	0.82886				
cvr3lha_36_1_2_15	0.0	40	35410	14164	8332	15.35	1.0e+00	0.75317	0.00110	0.75536				
cvr3lha_36_1_1_15	0.0	19	35505	6746	8332	32.24	1.0e+00	0.65522	0.00102	0.65726				
cvr3lha_36_2_8_15	1.4	100	35142	35142	7719	5.73	1.0e+00	0.87286	0.00134	0.87554				
cvr3lha_36_2_7_15	1.4	95	35164	33406	7719	6.03	1.0e+00	0.85858	0.00109	0.86077				
cvr3lha_36_2_6_15	1.4	90	35186	31667	7719	6.36	1.0e+00	0.84459	0.00107	0.84672				
cvr3lha_36_2_5_15	1.4	80	35230	28184	7719	7.15	1.0e+00	0.81698	0.00127	0.81952				
cvr3lha_36_2_4_15	1.4	70	35275	24693	7719	8.16	1.0e+00	0.78484	0.00122	0.78727				

Table 6.9.6-10. Results for HEU broken metal content in CV calculation model

case name	np (in)	enr. (wt%)	U (g)	^{235}U (g)	H_2O (g)	h/x	mocfr	k_{eff}	σ	$k_{eff}+2σ$				
cvr3lha_36_2_3_15	1.4	60	35320	21192	7719	9.51	1.0e+00	0.75584	0.00105	0.75795				
cvr3lha_36_2_2_15	1.4	40	35410	14164	7719	14.22	1.0e+00	0.68360	0.00131	0.68623				
cvr3lha_36_2_1_15	1.4	19	35505	6746	7719	29.86	1.0e+00	0.58144	0.00104	0.58352				
broken metal as 1-in. cubes fully homogenized with water for flooded containment vessel, reflected														
no can spacers (np thickness = 0.0 in.)														
cvr3cha_36_1_8_1	0.0	100	35142	35142	0	0.00	1.0e+00	0.61068	0.00099	0.61266				
cvr3cha_36_1_8_6	0.0	100	35142	35142	833	0.62	1.0e+00	0.64671	0.00117	0.64905				
cvr3cha_36_1_8_7	0.0	100	35142	35142	1666	1.24	1.0e+00	0.68117	0.00106	0.68329				
cvr3cha_36_1_8_8	0.0	100	35142	35142	2500	1.86	1.0e+00	0.71931	0.00121	0.72174				
cvr3cha_36_1_8_9	0.0	100	35142	35142	3333	2.48	1.0e+00	0.75910	0.00125	0.76160				
cvr3cha_36_1_8_10	0.0	100	35142	35142	4166	3.09	1.0e+00	0.79344	0.00123	0.79589				
cvr3cha_36_1_8_11	0.0	100	35142	35142	4999	3.71	1.0e+00	0.83513	0.00132	0.83777				
cvr3cha_36_1_8_12	0.0	100	35142	35142	5832	4.33	1.0e+00	0.87270	0.00117	0.87504				
cvr3cha_36_1_8_13	0.0	100	35142	35142	6666	4.95	1.0e+00	0.90988	0.00115	0.91219				
cvr3cha_36_1_8_14	0.0	100	35142	35142	7499	5.57	1.0e+00	0.94696	0.00136	0.94968				
cvr3cha_36_1_8_15	0.0	100	35142	35142	8332	6.19	1.0e+00	0.98062	0.00128	0.98318				
cvr3cha_36_1_8_15	0.0	100	35142	35142	8332	6.19	1.0e+00	0.98062	0.00128	0.98318				
cvr3cha_36_1_7_15	0.0	95	35164	33406	8332	6.51	1.0e+00	0.96729	0.00134	0.96997				
cvr3cha_36_1_6_15	0.0	90	35186	31667	8332	6.87	1.0e+00	0.95443	0.00144	0.95731				
cvr3cha_36_1_5_15	0.0	80	35230	28184	8332	7.72	1.0e+00	0.93639	0.00114	0.93867				
cvr3cha_36_1_4_15	0.0	70	35275	24693	8332	8.81	1.0e+00	0.91729	0.00125	0.91978				
cvr3cha_36_1_3_15	0.0	60	35320	21192	8332	10.26	1.0e+00	0.89768	0.00137	0.90042				

Table 6.9.6-10. Results for HEU broken metal content in CV calculation model

case name	np (in)	enr. (wt%)	U (g)	^{235}U (g)	H_2O (g)	h/x	mocfr	k_{eff}	σ	k_{eff}+2σ				
cvr3cha_36_1_2_15	0.0	40	35410	14164	8332	15.35	1.0e+00	0.85347	0.00132	0.85612				
cvr3cha_36_1_1_15	0.0	19	35505	6746	8332	32.24	1.0e+00	0.78799	0.00132	0.79064				
with can spacers (np thickness = 1.4 in.)														
cvr3cha_36_2_8_15	1.4	100	35142	35142	7719	5.73	1.0e+00	0.96066	0.00128	0.96321				
cvr3cha_36_2_7_15	1.4	95	35164	33406	7719	6.03	1.0e+00	0.94267	0.00127	0.94521				
cvr3cha_36_2_6_15	1.4	90	35186	31667	7719	6.36	1.0e+00	0.93250	0.00117	0.93484				
cvr3cha_36_2_5_15	1.4	80	35230	28184	7719	7.15	1.0e+00	0.91364	0.00126	0.91615				
cvr3cha_36_2_4_15	1.4	70	35275	24693	7719	8.16	1.0e+00	0.89707	0.00125	0.89957				
cvr3cha_36_2_3_15	1.4	60	35320	21192	7719	9.51	1.0e+00	0.87509	0.00121	0.87751				
cvr3cha_36_2_2_15	1.4	40	35410	14164	7719	14.22	1.0e+00	0.82672	0.00135	0.82943				
cvr3cha_36_2_1_15	1.4	19	35505	6746	7719	29.86	1.0e+00	0.76024	0.00148	0.76320				

Table 6.9.6-11. Results for HEU broken metal content in packaging calculation model

case name	np (in)	enr. (wt%)	U (g)	^{235}U (g)	H_2O (g)	h/x	moifr	k_{eff}	σ	k_{eff}+2σ	case name	k_{eff}	σ	k_{eff}+2σ
content in flooded containment vessel, single package reflected														
NCT											HAC			
no can spacers (np thickness = 0.0 in.)														
ncsrbmt11_36_1_1	0.0	100	35142	35142	8332	6.19	1.0e-20	0.81144	0.00127	0.81397	hcsrbmt12_36_1_1	0.81597	0.00140	0.81877
ncsrbmt11_36_1_2	0.0	100	35142	35142	8332	6.19	1.0e-05	0.81278	0.00143	0.81563	hcsrbmt12_36_1_2	0.81496	0.00123	0.81741
ncsrbmt11_36_1_3	0.0	100	35142	35142	8332	6.19	1.0e-04	0.81066	0.00124	0.81314	hcsrbmt12_36_1_3	0.81490	0.00149	0.81787
ncsrbmt11_36_1_4	0.0	100	35142	35142	8332	6.19	1.0e-03	0.81064	0.00142	0.81347	hcsrbmt12_36_1_4	0.81512	0.00157	0.81826
ncsrbmt11_36_1_5	0.0	100	35142	35142	8332	6.19	1.0e-02	0.81069	0.00138	0.81346	hcsrbmt12_36_1_5	0.81594	0.00126	0.81846
ncsrbmt11_36_1_6	0.0	100	35142	35142	8332	6.19	1.0e-01	0.81880	0.00126	0.82132	hcsrbmt12_36_1_6	0.82255	0.00126	0.82507

Table 6.9.6-11. Results for HEU broken metal content in packaging calculation model

case name	np (in)	enr. (wt%)	U (g)	^{235}U (g)	H_2O (g)	h/x	moifr	k_{eff}	σ	k_{eff}+2σ	case name	k_{eff}	σ	k_{eff}+2σ
ncsrbmt11_36_1_8	0.0	100	35142	35142	8332	6.19	3.0e-01	0.83502	0.00115	0.83732	hcsrbmt12_36_1_8	0.83846	0.00125	0.84095
ncsrbmt11_36_1_15	0.0	100	35142	35142	8332	6.19	1.0e+00	0.88830	0.00122	0.89075	hcsrbmt12_36_1_15	0.88841	0.00140	0.89122
ncsrbmt11_36_1_15	0.0	100	35142	35142	8332	6.19	1.0e+00	0.88830	0.00122	0.89075				
ncsrbmt11_35_1_15	0.0	100	34217	34217	8381	6.39	1.0e+00	0.88662	0.00129	0.88921				
ncsrbmt11_34_1_15	0.0	100	33292	33292	8430	6.61	1.0e+00	0.88622	0.00119	0.88860				
ncsrbmt11_33_1_15	0.0	100	32367	32367	8479	6.84	1.0e+00	0.88175	0.00127	0.88429				
ncsrbmt11_32_1_15	0.0	100	31442	31442	8529	7.08	1.0e+00	0.88109	0.00124	0.88357				
ncsrbmt11_31_1_15	0.0	100	30518	30518	8578	7.34	1.0e+00	0.87995	0.00126	0.88247				
ncsrbmt11_30_1_15	0.0	100	29593	29593	8627	7.61	1.0e+00	0.87410	0.00144	0.87697				
ncsrbmt11_29_1_15	0.0	100	28668	28668	8676	7.90	1.0e+00	0.87385	0.00118	0.87621				
ncsrbmt11_28_1_15	0.0	100	27743	27743	8725	8.21	1.0e+00	0.87237	0.00119	0.87474				
ncsrbmt11_27_1_15	0.0	100	26819	26819	8774	8.54	1.0e+00	0.86800	0.00126	0.87053				
ncsrbmt11_26_1_15	0.0	100	25894	25894	8823	8.89	1.0e+00	0.86869	0.00123	0.87115				
ncsrbmt11_25_1_15	0.0	100	24969	24969	8872	9.27	1.0e+00	0.86558	0.00152	0.86862				
ncsrbmt11_24_1_15	0.0	100	23119	23119	8970	10.13	1.0e+00	0.85827	0.00123	0.86074				
ncsrbmt11_23_1_15	0.0	100	22195	22195	9019	10.61	1.0e+00	0.85657	0.00134	0.85924				
ncsrbmt11_22_1_15	0.0	100	21270	21270	9068	11.13	1.0e+00	0.85373	0.00156	0.85686				
ncsrbmt11_21_1_15	0.0	100	20345	20345	9117	11.70	1.0e+00	0.85521	0.00126	0.85774				
ncsrbmt11_20_1_15	0.0	100	19420	19420	9166	12.32	1.0e+00	0.84989	0.00157	0.85303				
ncsrbmt11_19_1_15	0.0	100	18496	18496	9216	13.00	1.0e+00	0.85069	0.00155	0.85378				
ncsrbmt11_18_1_15	0.0	100	17571	17571	9265	13.76	1.0e+00	0.84676	0.00182	0.85039				
ncsrbmt11_17_1_15	0.0	100	16646	16646	9314	14.60	1.0e+00	0.84566	0.00147	0.84859				
ncsrbmt11_16_1_15	0.0	100	15721	15721	9363	15.54	1.0e+00	0.84458	0.00125	0.84708				
ncsrbmt11_15_1_15	0.0	100	14796	14796	9412	16.60	1.0e+00	0.83932	0.00148	0.84229				

Table 6.9.6-11. Results for HEU broken metal content in packaging calculation model

case name	np (in)	enr. (wt%)	U (g)	^{235}U (g)	H_2O (g)	h/x	moifr	k_{eff}	σ	$k_{eff}+2σ$	case name	k_{eff}	σ	$k_{eff}+2σ$
ncsrbmt11_14_1_15	0.0	100	13872	13872	9461	17.80	1.0e+00	0.83752	0.00133	0.84019				
ncsrbmt11_13_1_15	0.0	100	12947	12947	9510	19.17	1.0e+00	0.83532	0.00151	0.83834				
ncsrbmt11_12_1_15	0.0	100	11097	11097	9608	22.60	1.0e+00	0.82792	0.00133	0.83057				
ncsrbmt11_11_1_15	0.0	100	10173	10173	9657	24.78	1.0e+00	0.82643	0.00127	0.82898				
ncsrbmt11_10_1_15	0.0	100	9248	9248	9706	27.39	1.0e+00	0.82649	0.00160	0.82968				
ncsrbmt11_9_1_15	0.0	100	8323	8323	9755	30.59	1.0e+00	0.81840	0.00140	0.82119				
ncsrbmt11_8_1_15	0.0	100	7398	7398	9804	34.59	1.0e+00	0.81808	0.00170	0.82148				
ncsrbmt11_7_1_15	0.0	100	6473	6473	9854	39.73	1.0e+00	0.81130	0.00152	0.81434				
ncsrbmt11_6_1_15	0.0	100	5549	5549	9903	46.58	1.0e+00	0.80480	0.00140	0.80761				
ncsrbmt11_5_1_15	0.0	100	4624	4624	9952	56.17	1.0e+00	0.79723	0.00124	0.79971				
ncsrbmt11_4_1_15	0.0	100	3699	3699	10001	70.56	1.0e+00	0.78533	0.00133	0.78799				
ncsrbmt11_3_1_15	0.0	100	2774	2774	10050	94.55	1.0e+00	0.76796	0.00152	0.77099				
ncsrbmt11_2_1_15	0.0	100	1850	1850	10099	142.51	1.0e+00	0.73495	0.00142	0.73778				
ncsrbmt11_1_1_15	0.0	100	925	925	10148	286.41	1.0e+00	0.65230	0.00132	0.65494				
with can spacers (np thickness = 1.4 in.)														
ncsrbmt11_36_2_1	1.4	100	35142	35142	7719	5.73	1.0e-20	0.79252	0.00122	0.79496	hcsrbmt12_36_2_1	0.79368	0.00134	0.79636
ncsrbmt11_36_2_2	1.4	100	35142	35142	7719	5.73	1.0e-05	0.79014	0.00147	0.79309	hcsrbmt12_36_2_2	0.79487	0.00120	0.79727
ncsrbmt11_36_2_3	1.4	100	35142	35142	7719	5.73	1.0e-04	0.79182	0.00134	0.79450	hcsrbmt12_36_2_3	0.79667	0.00135	0.79938
ncsrbmt11_36_2_4	1.4	100	35142	35142	7719	5.73	1.0e-03	0.79144	0.00116	0.79376	hcsrbmt12_36_2_4	0.79705	0.00133	0.79971
ncsrbmt11_36_2_5	1.4	100	35142	35142	7719	5.73	1.0e-02	0.78918	0.00111	0.79141	hcsrbmt12_36_2_5	0.79627	0.00135	0.79898
ncsrbmt11_36_2_6	1.4	100	35142	35142	7719	5.73	1.0e-01	0.80114	0.00117	0.80348	hcsrbmt12_36_2_6	0.80431	0.00130	0.80691
ncsrbmt11_36_2_8	1.4	100	35142	35142	7719	5.73	3.0e-01	0.81416	0.00141	0.81698	hcsrbmt12_36_2_8	0.82035	0.00119	0.82273
ncsrbmt11_36_2_15	1.4	100	35142	35142	7719	5.73	1.0e+00	0.86924	0.00119	0.87162	hcsrbmt12_36_2_15	0.87124	0.00142	0.87408

Table 6.9.6-11. Results for HEU broken metal content in packaging calculation model

case name	np (in)	enr. (wt%)	U (g)	^{235}U (g)	H_2O (g)	h/x	moifr	k_{eff}	σ	$k_{eff}+2σ$	case name	k_{eff}	σ	$k_{eff}+2σ$
ncsrbmt11_36_2_15	1.4	100	35142	35142	7719	5.73	1.0e+00	0.86924	0.00119	0.87162				
ncsrbmt11_35_2_15	1.4	100	34217	34217	7768	5.93	1.0e+00	0.86697	0.00130	0.86957				
ncsrbmt11_34_2_15	1.4	100	33292	33292	7817	6.13	1.0e+00	0.86435	0.00138	0.86712				
ncsrbmt11_33_2_15	1.4	100	32367	32367	7866	6.34	1.0e+00	0.86988	0.00130	0.87249				
ncsrbmt11_32_2_15	1.4	100	31442	31442	7915	6.57	1.0e+00	0.86598	0.00145	0.86889				
ncsrbmt11_31_2_15	1.4	100	30518	30518	7964	6.81	1.0e+00	0.86432	0.00153	0.86739				
ncsrbmt11_30_2_15	1.4	100	29593	29593	8013	7.07	1.0e+00	0.85951	0.00163	0.86277				
ncsrbmt11_29_2_15	1.4	100	28668	28668	8062	7.34	1.0e+00	0.85938	0.00134	0.86206				
ncsrbmt11_28_2_15	1.4	100	27743	27743	8111	7.63	1.0e+00	0.85890	0.00133	0.86157				
ncsrbmt11_27_2_15	1.4	100	26819	26819	8160	7.94	1.0e+00	0.85736	0.00143	0.86023				
ncsrbmt11_26_2_15	1.4	100	25894	25894	8209	8.28	1.0e+00	0.85189	0.00129	0.85447				
ncsrbmt11_25_2_15	1.4	100	24969	24969	8258	8.63	1.0e+00	0.84986	0.00148	0.85281				
ncsrbmt11_24_2_15	1.4	100	23119	23119	8357	9.43	1.0e+00	0.85225	0.00131	0.85488				
ncsrbmt11_23_2_15	1.4	100	22195	22195	8406	9.89	1.0e+00	0.84824	0.00142	0.85108				
ncsrbmt11_22_2_15	1.4	100	21270	21270	8455	10.38	1.0e+00	0.84600	0.00135	0.84869				
ncsrbmt11_21_2_15	1.4	100	20345	20345	8504	10.91	1.0e+00	0.84406	0.00150	0.84706				
ncsrbmt11_20_2_15	1.4	100	19420	19420	8553	11.50	1.0e+00	0.83992	0.00126	0.84244				
ncsrbmt11_19_2_15	1.4	100	18496	18496	8602	12.14	1.0e+00	0.83869	0.00134	0.84138				
ncsrbmt11_18_2_15	1.4	100	17571	17571	8651	12.85	1.0e+00	0.83488	0.00152	0.83793				
ncsrbmt11_17_2_15	1.4	100	16646	16646	8700	13.64	1.0e+00	0.83409	0.00130	0.83669				
ncsrbmt11_16_2_15	1.4	100	15721	15721	8749	14.53	1.0e+00	0.83520	0.00135	0.83789				
ncsrbmt11_15_2_15	1.4	100	14796	14796	8798	15.52	1.0e+00	0.83427	0.00129	0.83686				
ncsrbmt11_14_2_15	1.4	100	13872	13872	8847	16.65	1.0e+00	0.83162	0.00157	0.83476				
ncsrbmt11_13_2_15	1.4	100	12947	12947	8896	17.94	1.0e+00	0.82907	0.00147	0.83201				
ncsrbmt11_12_2_15	1.4	100	11097	11097	8995	21.16	1.0e+00	0.82195	0.00149	0.82493				

Table 6.9.6-11. Results for HEU broken metal content in packaging calculation model

case name	np (in)	enr. (wt%)	U (g)	^{235}U (g)	H_2O (g)	h/x	moifr	k_{eff}	σ	$k_{eff}+2σ$	case name	k_{eff}	σ	$k_{eff}+2σ$
ncsrbmt11_11_2_15	1.4	100	10173	10173	9044	23.20	1.0e+00	0.81845	0.00120	0.82084				
ncsrbmt11_10_2_15	1.4	100	9248	9248	9093	25.66	1.0e+00	0.81508	0.00142	0.81792				
ncsrbmt11_9_2_15	1.4	100	8323	8323	9142	28.67	1.0e+00	0.81075	0.00138	0.81351				
ncsrbmt11_8_2_15	1.4	100	7398	7398	9191	32.43	1.0e+00	0.81425	0.00169	0.81764				
ncsrbmt11_7_2_15	1.4	100	6473	6473	9240	37.26	1.0e+00	0.80774	0.00155	0.81084				
ncsrbmt11_6_2_15	1.4	100	5549	5549	9289	43.70	1.0e+00	0.80060	0.00138	0.80336				
ncsrbmt11_5_2_15	1.4	100	4624	4624	9338	52.71	1.0e+00	0.79537	0.00167	0.79870				
ncsrbmt11_4_2_15	1.4	100	3699	3699	9387	66.24	1.0e+00	0.78379	0.00136	0.78651				
ncsrbmt11_3_2_15	1.4	100	2774	2774	9436	88.78	1.0e+00	0.76586	0.00130	0.76846				
ncsrbmt11_2_2_15	1.4	100	1850	1850	9485	133.86	1.0e+00	0.73246	0.00135	0.73516				
ncsrbmt11_1_2_15	1.4	100	925	925	9534	269.10	1.0e+00	0.65664	0.00150	0.65963				
content in flooded containment vessel, array packaging model for CSI=0.0														
NCT											**HAC**			
no can spacers (np thickness = 0.0 in.)														
nciabmt11_36_1_8_1	0.0	100	35142	35142	8332	6.19	1.0e-20	1.13613	0.00121	1.13855	hciabmt12_36_1_8_1	1.13721	0.00124	1.13969
nciabmt11_36_1_8_2	0.0	100	35142	35142	8332	6.19	1.0e-05	1.13830	0.00153	1.14135	hciabmt12_36_1_8_2	1.13634	0.00114	1.13862
nciabmt11_36_1_8_3	0.0	100	35142	35142	8332	6.19	1.0e-04	1.13709	0.00121	1.13952	hciabmt12_36_1_8_3	1.13700	0.00127	1.13954
nciabmt11_36_1_8_4	0.0	100	35142	35142	8332	6.19	1.0e-03	1.13450	0.00115	1.13679	hciabmt12_36_1_8_4	1.13567	0.00121	1.13809
nciabmt11_36_1_8_5	0.0	100	35142	35142	8332	6.19	1.0e-02	1.11154	0.00120	1.11394	hciabmt12_36_1_8_5	1.12232	0.00129	1.12490
nciabmt11_36_1_8_6	0.0	100	35142	35142	8332	6.19	1.0e-01	0.98653	0.00121	0.98894	hciabmt12_36_1_8_6	1.03049	0.00115	1.03278
nciabmt11_36_1_8_8	0.0	100	35142	35142	8332	6.19	3.0e-01	0.91622	0.00135	0.91892	hciabmt12_36_1_8_8	0.95566	0.00126	0.95818
nciabmt11_36_1_8_15	0.0	100	35142	35142	8332	6.19	1.0e+00	0.91008	0.00124	0.91255	hciabmt12_36_1_8_15	0.93645	0.00120	0.93884
nciabmt11_7_1_5_3	0.0	80	6490	5192	9854	49.54	1.0e-04	0.96163	0.00130	0.96423	hciabmt12_7_1_5_3	0.96193	0.00149	0.96490
nciabmt11_6_1_5_3	0.0	80	5563	4450	9903	58.08	1.0e-04	0.95210	0.00130	0.95471	hciabmt12_6_1_5_3	0.95164	0.00139	0.95442

Table 6.9.6-11. Results for HEU broken metal content in packaging calculation model

case name	np (in)	enr. (wt%)	U (g)	^{235}U (g)	H_2O (g)	h/x	moifr	k_{eff}	σ	k_{eff}+2σ	case name	k_{eff}	σ	k_{eff}+2σ
nciabmt11_5_1_5_3	0.0	80	4636	3709	9952	70.04	1.0e-04	0.93892	0.00161	0.94215	hciabmt12_5_1_5_3	0.93880	0.00141	0.94162
nciabmt11_4_1_5_3	0.0	80	3709	2967	10001	87.98	1.0e-04	0.91835	0.00149	0.92133	hciabmt12_4_1_5_3	0.92156	0.00160	0.92476
nciabmt11_3_1_5_3	0.0	80	2781	2225	10050	117.89	1.0e-04	0.89262	0.00129	0.89520	hciabmt12_3_1_5_3	0.89109	0.00160	0.89430
nciabmt11_9_1_4_3	0.0	70	8355	5848	9755	43.54	1.0e-04	0.95952	0.00130	0.96213	hciabmt12_9_1_4_3	0.95495	0.00150	0.95795
nciabmt11_8_1_4_3	0.0	70	7426	5198	9804	49.23	1.0e-04	0.94887	0.00152	0.95191	hciabmt12_8_1_4_3	0.95267	0.00156	0.95578
nciabmt11_7_1_4_3	0.0	70	6498	4549	9854	56.54	1.0e-04	0.94082	0.00132	0.94346	hciabmt12_7_1_4_3	0.94409	0.00125	0.94659
nciabmt11_6_1_4_3	0.0	70	5570	3899	9903	66.29	1.0e-04	0.92987	0.00119	0.93225	hciabmt12_6_1_4_3	0.93280	0.00123	0.93526
nciabmt11_5_1_4_3	0.0	70	4642	3249	9952	79.95	1.0e-04	0.91799	0.00136	0.92070	hciabmt12_5_1_4_3	0.92053	0.00147	0.92347
nciabmt11_10_1_3_3	0.0	60	9295	5577	9706	45.43	1.0e-04	0.94106	0.00152	0.94409	hciabmt12_10_1_3_3	0.94167	0.00126	0.94419
nciabmt11_9_1_3_3	0.0	60	8365	5019	9755	50.73	1.0e-04	0.93671	0.00123	0.93918	hciabmt12_9_1_3_3	0.93973	0.00135	0.94242
nciabmt11_8_1_3_3	0.0	60	7436	4462	9804	57.36	1.0e-04	0.92907	0.00129	0.93166	hciabmt12_8_1_3_3	0.93016	0.00128	0.93273
nciabmt11_7_1_3_3	0.0	60	6506	3904	9854	65.88	1.0e-04	0.92171	0.00118	0.92407	hciabmt12_7_1_3_3	0.92300	0.00130	0.92560
nciabmt11_6_1_3_3	0.0	60	5577	3346	9903	77.24	1.0e-04	0.91221	0.00147	0.91515	hciabmt12_6_1_3_3	0.91017	0.00128	0.91274
with can spacers (np thickness = 1.4 in.)														
nciabmt11_36_2_8_1	1.4	100	35142	35142	7719	5.73	1.0e-20	1.11012	0.00118	1.11249	hciabmt12_36_2_8_1	1.11021	0.00115	1.11250
nciabmt11_36_2_8_2	1.4	100	35142	35142	7719	5.73	1.0e-05	1.10934	0.00103	1.11141	hciabmt12_36_2_8_2	1.10929	0.00137	1.11202
nciabmt11_36_2_8_3	1.4	100	35142	35142	7719	5.73	1.0e-04	1.10991	0.00131	1.11252	hciabmt12_36_2_8_3	1.10922	0.00112	1.11145
nciabmt11_36_2_8_4	1.4	100	35142	35142	7719	5.73	1.0e-03	1.10774	0.00123	1.11020	hciabmt12_36_2_8_4	1.10732	0.00115	1.10963
nciabmt11_36_2_8_5	1.4	100	35142	35142	7719	5.73	1.0e-02	1.08309	0.00140	1.08589	hciabmt12_36_2_8_5	1.09559	0.00114	1.09786
nciabmt11_36_2_8_6	1.4	100	35142	35142	7719	5.73	1.0e-01	0.95955	0.00128	0.96212	hciabmt12_36_2_8_6	1.00216	0.00124	1.00463
nciabmt11_36_2_8_8	1.4	100	35142	35142	7719	5.73	3.0e-01	0.88829	0.00112	0.89053	hciabmt12_36_2_8_8	0.92859	0.00158	0.93175
nciabmt11_36_2_8_15	1.4	100	35142	35142	7719	5.73	1.0e+00	0.88638	0.00158	0.88953	hciabmt12_36_2_8_15	0.91405	0.00147	0.91698

Table 6.9.6-11. Results for HEU broken metal content in packaging calculation model

case name	np (in)	enr. (wt%)	U (g)	^{235}U (g)	H_2O (g)	h/x	moifr	k_{eff}	σ	$k_{eff}+2σ$	case name	k_{eff}	σ	$k_{eff}+2σ$
nciabmt11_5_2_8_3	1.4	100	4624	4624	9338	52.71	1.0e-04	0.94785	0.00147	0.95079	hciabmt12_5_2_8_3	0.95226	0.00143	0.95511
nciabmt11_4_2_8_3	1.4	100	3699	3699	9387	66.24	1.0e-04	0.92504	0.00170	0.92845	hciabmt12_4_2_8_3	0.93069	0.00142	0.93352
nciabmt11_3_2_8_3	1.4	100	2774	2774	9436	88.78	1.0e-04	0.90131	0.00139	0.90409	hciabmt12_3_2_8_3	0.90243	0.00127	0.90497
nciabmt11_2_2_8_3	1.4	100	1850	1850	9485	133.86	1.0e-04	0.85414	0.00141	0.85696	hciabmt12_2_2_8_3	0.85600	0.00123	0.85846
nciabmt11_1_2_8_3	1.4	100	925	925	9534	269.10	1.0e-04	0.74985	0.00124	0.75232	hciabmt12_1_2_8_3	0.75078	0.00135	0.75347
nciabmt11_6_2_7_3	1.4	95	5552	5275	9289	45.97	1.0e-04	0.95078	0.00124	0.95327	hciabmt12_6_2_7_3	0.95399	0.00153	0.95704
nciabmt11_5_2_7_3	1.4	95	4627	4396	9338	55.45	1.0e-04	0.93742	0.00130	0.94002	hciabmt12_5_2_7_3	0.93696	0.00142	0.93981
nciabmt11_4_2_7_3	1.4	95	3701	3516	9387	69.68	1.0e-04	0.91690	0.00149	0.91987	hciabmt12_4_2_7_3	0.92094	0.00140	0.92374
nciabmt11_3_2_7_3	1.4	95	2776	2637	9436	93.39	1.0e-04	0.89089	0.00127	0.89343	hciabmt12_3_2_7_3	0.89250	0.00144	0.89537
nciabmt11_2_2_7_3	1.4	95	1851	1758	9485	140.81	1.0e-04	0.84225	0.00143	0.84510	hciabmt12_2_2_7_3	0.84604	0.00135	0.84875
nciabmt11_6_2_6_3	1.4	90	5556	5000	9289	48.49	1.0e-04	0.93703	0.00127	0.93956	hciabmt12_6_2_6_3	0.93967	0.00130	0.94227
nciabmt11_5_2_6_3	1.4	90	4630	4167	9338	58.49	1.0e-04	0.92640	0.00142	0.92925	hciabmt12_5_2_6_3	0.92390	0.00155	0.92700
nciabmt11_4_2_6_3	1.4	90	3704	3333	9387	73.50	1.0e-04	0.90541	0.00147	0.90835	hciabmt12_4_2_6_3	0.90643	0.00133	0.90909
nciabmt11_3_2_6_3	1.4	90	2778	2500	9436	98.52	1.0e-04	0.87970	0.00157	0.88283	hciabmt12_3_2_6_3	0.87916	0.00154	0.88224
nciabmt11_2_2_6_3	1.4	90	1852	1667	9485	148.54	1.0e-04	0.83371	0.00129	0.83628	hciabmt12_2_2_6_3	0.83414	0.00130	0.83674
nciabmt11_8_2_5_3	1.4	80	7417	5934	9191	40.43	1.0e-04	0.94131	0.00162	0.94455	hciabmt12_8_2_5_3	0.93963	0.00149	0.94261
nciabmt11_7_2_5_3	1.4	80	6490	5192	9240	46.45	1.0e-04	0.92939	0.00127	0.93193	hciabmt12_7_2_5_3	0.93070	0.00160	0.93391
nciabmt11_6_2_5_3	1.4	80	5563	4450	9289	54.48	1.0e-04	0.91981	0.00127	0.92235	hciabmt12_6_2_5_3	0.91987	0.00157	0.92301
nciabmt11_5_2_5_3	1.4	80	4636	3709	9338	65.72	1.0e-04	0.90533	0.00127	0.90787	hciabmt12_5_2_5_3	0.90772	0.00136	0.91044
nciabmt11_4_2_5_3	1.4	80	3709	2967	9387	82.59	1.0e-04	0.88537	0.00136	0.88808	hciabmt12_4_2_5_3	0.88792	0.00150	0.89092

Table 6.9.6-11. Results for HEU broken metal content in packaging calculation model

case name	np (in)	enr. (wt%)	U (g)	^{235}U (g)	H_2O (g)	h/x	moifr	k_{eff}	σ	$k_{eff}+2σ$	case name	k_{eff}	σ	$k_{eff}+2σ$
nciabmt11_11_2_4_3	1.4	70	10211	7148	9044	33.02	1.0e-04	0.93094	0.00141	0.93376	hciabmt12_11_2_4_3	0.93119	0.00138	0.93395
nciabmt11_10_2_4_3	1.4	70	9283	6498	9093	36.52	1.0e-04	0.92534	0.00139	0.92813	hciabmt12_10_2_4_3	0.92795	0.00129	0.93052
nciabmt11_9_2_4_3	1.4	70	8355	5848	9142	40.80	1.0e-04	0.91866	0.00122	0.92110	hciabmt12_9_2_4_3	0.92290	0.00125	0.92540
nciabmt11_8_2_4_3	1.4	70	7426	5198	9191	46.15	1.0e-04	0.91902	0.00137	0.92175	hciabmt12_8_2_4_3	0.91835	0.00126	0.92086
nciabmt11_7_2_4_3	1.4	70	6498	4549	9240	53.02	1.0e-04	0.90863	0.00152	0.91166	hciabmt12_7_2_4_3	0.91042	0.00137	0.91316
nciabmt11_15_2_3_3	1.4	60	14872	8923	8798	25.74	1.0e-04	0.93047	0.00133	0.93313	hciabmt12_15_2_3_3	0.93032	0.00114	0.93259
nciabmt11_14_2_3_3	1.4	60	13942	8365	8847	27.61	1.0e-04	0.92560	0.00138	0.92837	hciabmt12_14_2_3_3	0.92828	0.00143	0.93115
nciabmt11_13_2_3_3	1.4	60	12083	7250	8946	32.21	1.0e-04	0.91963	0.00126	0.92214	hciabmt12_13_2_3_3	0.92389	0.00124	0.92638
nciabmt11_12_2_3_3	1.4	60	11154	6692	8995	35.08	1.0e-04	0.91502	0.00155	0.91812	hciabmt12_12_2_3_3	0.91776	0.00138	0.92053
nciabmt11_11_2_3_3	1.4	60	10224	6135	9044	38.48	1.0e-04	0.90892	0.00140	0.91172	hciabmt12_11_2_3_3	0.91237	0.00133	0.91503
content in flooded containment vessel, array packaging model for CSI=0.4														
NCT											HAC			
no can spacers (np thickness = 0.0 in.)														
											hcf2bmt12_11_1_5_3	0.91900	0.00131	0.92163
											hcf2bmt12_10_1_5_3	0.91775	0.00161	0.92097
											hcf2bmt12_9_1_5_3	0.91229	0.00127	0.91483
ncf1bmt11_8_1_5_3	0.0	80	7417	5934	9804	43.13	1.0e-04	0.92824	0.00156	0.93135	hcf2bmt12_8_1_5_3	0.90367	0.00138	0.90643
ncf1bmt11_7_1_5_3	0.0	80	6490	5192	9854	49.54	1.0e-04	0.92088	0.00131	0.92349				
ncf1bmt11_6_1_5_3	0.0	80	5563	4450	9903	58.08	1.0e-04	0.91164	0.00153	0.91470				
ncf1bmt11_5_1_5_3	0.0	80	4636	3709	9952	70.04	1.0e-04	0.90130	0.00135	0.90400				
ncf1bmt11_4_1_5_3	0.0	80	3709	2967	10001	87.98	1.0e-04	0.88094	0.00128	0.88350				
											hcf2bmt12_15_1_4_3	0.91711	0.00152	0.92016
											hcf2bmt12_14_1_4_3	0.91432	0.00164	0.91760

Table 6.9.6-11. Results for HEU broken metal content in packaging calculation model

case name	np (in)	enr. (wt%)	U (g)	^{235}U (g)	H_2O (g)	h/x	moifr	k_{eff}	σ	$k_{eff}+2σ$	case name	k_{eff}	σ	$k_{eff}+2σ$
ncf1bmt11_13_1_4_3	0.0	70	12996	9097	9510	27.28	1.0e-04	0.93558	0.00138	0.93834	hcf2bmt12_13_1_4_3	0.91429	0.00141	0.91711
ncf1bmt11_12_1_4_3	0.0	70	11140	7798	9608	32.16	1.0e-04	0.92957	0.00130	0.93217	hcf2bmt12_12_1_4_3	0.90853	0.00161	0.91175
ncf1bmt11_11_1_4_3	0.0	70	10211	7148	9657	35.26	1.0e-04	0.92397	0.00139	0.92675				
ncf1bmt11_10_1_4_3	0.0	70	9283	6498	9706	38.99	1.0e-04	0.92240	0.00135	0.92510				
ncf1bmt11_9_1_4_3	0.0	70	8355	5848	9755	43.54	1.0e-04	0.91886	0.00139	0.92163				
											hcf2bmt12_21_1_3_3	0.91091	0.00139	0.91369
											hcf2bmt12_20_1_3_3	0.90915	0.00144	0.91203
ncf1bmt11_19_1_3_3	0.0	60	18589	11154	9216	21.57	1.0e-04	0.92771	0.00137	0.93044	hcf2bmt12_19_1_3_3	0.90638	0.00160	0.90958
ncf1bmt11_18_1_3_3	0.0	60	17660	10596	9265	22.82	1.0e-04	0.92867	0.00148	0.93164	hcf2bmt12_18_1_3_3	0.90466	0.00124	0.90715
ncf1bmt11_17_1_3_3	0.0	60	16731	10038	9314	24.22	1.0e-04	0.92948	0.00113	0.93173				
ncf1bmt11_16_1_3_3	0.0	60	15801	9481	9363	25.78	1.0e-04	0.92252	0.00158	0.92569				
ncf1bmt11_15_1_3_3	0.0	60	14872	8923	9412	27.53	1.0e-04	0.91999	0.00123	0.92246				
ncf1bmt11_14_1_3_3	0.0	60	13942	8365	9461	29.52	1.0e-04	0.91961	0.00144	0.92248				
with can spacers (np thickness = 1.4 in.)														
											hcf2bmt12_10_2_8_3	0.93154	0.00152	0.93458
ncf1bmt11_9_2_8_3	1.4	100	8323	8323	9142	28.67	1.0e-04	0.94429	0.00138	0.94704	hcf2bmt12_9_2_8_3	0.92329	0.00147	0.92622
ncf1bmt11_8_2_8_3	1.4	100	7398	7398	9191	32.43	1.0e-04	0.94337	0.00169	0.94674	hcf2bmt12_8_2_8_3	0.92153	0.00144	0.92442
ncf1bmt11_7_2_8_3	1.4	100	6473	6473	9240	37.26	1.0e-04	0.93117	0.00172	0.93460				
ncf1bmt11_6_2_8_3	1.4	100	5549	5549	9289	43.70	1.0e-04	0.92119	0.00147	0.92412				
											hcf2bmt12_13_2_7_3	0.93389	0.00167	0.93722
											hcf2bmt12_12_2_7_3	0.92649	0.00146	0.92941
ncf1bmt11_11_2_7_3	1.4	95	10179	9670	9044	24.41	1.0e-04	0.94326	0.00139	0.94604	hcf2bmt12_11_2_7_3	0.92061	0.00130	0.92320
ncf1bmt11_10_2_7_3	1.4	95	9254	8791	9093	27.00	1.0e-04	0.93829	0.00154	0.94138	hcf2bmt12_10_2_7_3	0.91423	0.00145	0.91712

Table 6.9.6-11. Results for HEU broken metal content in packaging calculation model

case name	np (in)	enr. (wt%)	U (g)	^{235}U (g)	H_2O (g)	h/x	moifr	k_{eff}	σ	k_{eff}+2σ	case name	k_{eff}	σ	k_{eff}+2σ
ncf1bmt11_9_2_7_3	1.4	95	8328	7912	9142	30.16	1.0e-04	0.93239	0.00181	0.93600	hcf2bmt12_9_2_7_3	0.90883	0.00137	0.91156
ncf1bmt11_8_2_7_3	1.4	95	7403	7033	9191	34.11	1.0e-04	0.92812	0.00144	0.93100				
ncf1bmt11_7_2_7_3	1.4	95	6478	6154	9240	39.19	1.0e-04	0.91938	0.00130	0.92199				
											hcf2bmt12_15_2_6_3	0.93106	0.00129	0.93364
											hcf2bmt12_14_2_6_3	0.92492	0.00129	0.92749
ncf1bmt11_13_2_6_3	1.4	90	12963	11667	8896	19.90	1.0e-04	0.94806	0.00123	0.95052	hcf2bmt12_13_2_6_3	0.92272	0.00138	0.92548
ncf1bmt11_12_2_6_3	1.4	90	11111	10000	8995	23.48	1.0e-04	0.93464	0.00123	0.93710	hcf2bmt12_12_2_6_3	0.91625	0.00149	0.91924
ncf1bmt11_11_2_6_3	1.4	90	10185	9167	9044	25.75	1.0e-04	0.93068	0.00148	0.93363	hcf2bmt12_11_2_6_3	0.91097	0.00136	0.91370
ncf1bmt11_10_2_6_3	1.4	90	9260	8334	9093	28.48	1.0e-04	0.92732	0.00150	0.93032				
ncf1bmt11_9_2_6_3	1.4	90	8334	7500	9142	31.81	1.0e-04	0.91744	0.00145	0.92034				
ncf1bmt11_8_2_6_3	1.4	90	7408	6667	9191	35.98	1.0e-04	0.91952	0.00133	0.92218				
ncf1bmt11_17_2_5_3	1.4	80	16688	13351	8700	17.01	1.0e-04	0.93531	0.00128	0.93787	hcf2bmt12_17_2_5_3	0.91255	0.00114	0.91482
ncf1bmt11_16_2_5_3	1.4	80	15761	12609	8749	18.11	1.0e-04	0.93511	0.00160	0.93832	hcf2bmt12_16_2_5_3	0.91363	0.00123	0.91608
ncf1bmt11_15_2_5_3	1.4	80	14834	11867	8798	19.35	1.0e-04	0.93431	0.00141	0.93713	hcf2bmt12_15_2_5_3	0.91038	0.00115	0.91268
ncf1bmt11_14_2_5_3	1.4	80	13907	11125	8847	20.76	1.0e-04	0.92939	0.00133	0.93205	hcf2bmt12_14_2_5_3	0.90762	0.00139	0.91041
ncf1bmt11_13_2_5_3	1.4	80	12980	10384	8896	22.36	1.0e-04	0.92453	0.00131	0.92715	hcf2bmt12_13_2_5_3	0.90539	0.00137	0.90812
ncf1bmt11_12_2_5_3	1.4	80	11125	8900	8995	26.38	1.0e-04	0.91584	0.00142	0.91868	hcf2bmt12_12_2_5_3	0.89295	0.00174	0.89642
ncf1bmt11_24_2_4_3	1.4	70	23207	16245	8357	13.43	1.0e-04	0.93515	0.00143	0.93801	hcf2bmt12_24_2_4_3	0.91356	0.00125	0.91606
ncf1bmt11_23_2_4_3	1.4	70	22279	15595	8406	14.07	1.0e-04	0.93264	0.00113	0.93490	hcf2bmt12_23_2_4_3	0.91116	0.00113	0.91342
ncf1bmt11_22_2_4_3	1.4	70	21351	14946	8455	14.77	1.0e-04	0.93058	0.00128	0.93314	hcf2bmt12_22_2_4_3	0.90737	0.00145	0.91027
ncf1bmt11_21_2_4_3	1.4	70	20422	14296	8504	15.53	1.0e-04	0.92635	0.00112	0.92859	hcf2bmt12_21_2_4_3	0.90516	0.00140	0.90796
ncf1bmt11_20_2_4_3	1.4	70	19494	13646	8553	16.36	1.0e-04	0.92535	0.00141	0.92818	hcf2bmt12_20_2_4_3	0.90283	0.00136	0.90555

Table 6.9.6-11. Results for HEU broken metal content in packaging calculation model

case name	np (in)	enr. (wt%)	U (g)	^{235}U (g)	H_2O (g)	h/x	moifr	k_{eff}	σ	k_{eff}+2σ	case name	k_{eff}	σ	k_{eff}+2σ
ncf1bmt11_19_2_4_3	1.4	70	18566	12996	8602	17.28	1.0e-04	0.92097	0.00177	0.92450	hcf2bmt12_19_2_4_3	0.89757	0.00144	0.90046
ncf1bmt11_18_2_4_3	1.4	70	17638	12346	8651	18.29	1.0e-04	0.91681	0.00140	0.91961	hcf2bmt12_18_2_4_3	0.89367	0.00144	0.89656
ncf1bmt11_36_2_3_3	1.4	60	35320	21192	7719	9.51	1.0e-04	0.93212	0.00121	0.93455	hcf2bmt12_36_2_3_3	0.90846	0.00137	0.91121
ncf1bmt11_35_2_3_3	1.4	60	34391	20634	7768	9.83	1.0e-04	0.93168	0.00129	0.93426	hcf2bmt12_35_2_3_3	0.90742	0.00118	0.90977
ncf1bmt11_34_2_3_3	1.4	60	33461	20077	7817	10.16	1.0e-04	0.93079	0.00145	0.93368	hcf2bmt12_34_2_3_3	0.90657	0.00134	0.90925
ncf1bmt11_33_2_3_3	1.4	60	32532	19519	7866	10.52	1.0e-04	0.92781	0.00131	0.93042	hcf2bmt12_33_2_3_3	0.90603	0.00117	0.90837
ncf1bmt11_32_2_3_3	1.4	60	31602	18961	7915	10.90	1.0e-04	0.92550	0.00131	0.92811	hcf2bmt12_32_2_3_3	0.90015	0.00127	0.90270
ncf1bmt11_31_2_3_3	1.4	60	30673	18404	7964	11.29	1.0e-04	0.92597	0.00128	0.92853	hcf2bmt12_31_2_3_3	0.90333	0.00122	0.90577
ncf1bmt11_30_2_3_3	1.4	60	29743	17846	8013	11.72	1.0e-04	0.92361	0.00120	0.92601	hcf2bmt12_30_2_3_3	0.89683	0.00144	0.89971
ncf1bmt11_29_2_3_3	1.4	60	28814	17288	8062	12.17	1.0e-04	0.92063	0.00143	0.92350				
content in flooded containment vessel, array packaging model for CSI=0.8														
NCT											HAC			
no can spacers (np thickness = 0.0 in.)														
ncf2bmt11_17_1_5_3	0.0	80	16688	13351	9314	18.21	1.0e-04	0.93655	0.00144	0.93942	hcf3bmt12_17_1_5_3	0.92003	0.00129	0.92262
ncf2bmt11_16_1_5_3	0.0	80	15761	12609	9363	19.38	1.0e-04	0.93242	0.00143	0.93529	hcf3bmt12_16_1_5_3	0.91399	0.00148	0.91694
ncf2bmt11_15_1_5_3	0.0	80	14834	11867	9412	20.70	1.0e-04	0.92982	0.00135	0.93251	hcf3bmt12_15_1_5_3	0.91169	0.00139	0.91448
ncf2bmt11_14_1_5_3	0.0	80	13907	11125	9461	22.20	1.0e-04	0.92699	0.00137	0.92972	hcf3bmt12_14_1_5_3	0.90943	0.00135	0.91213
ncf2bmt11_13_1_5_3	0.0	80	12980	10384	9510	23.90	1.0e-04	0.92634	0.00138	0.92909	hcf3bmt12_13_1_5_3	0.90348	0.00133	0.90615
ncf2bmt11_12_1_5_3	0.0	80	11125	8900	9608	28.18	1.0e-04	0.91826	0.00166	0.92158	hcf3bmt12_12_1_5_3	0.89805	0.00155	0.90115
ncf2bmt11_21_1_4_3	0.0	70	20422	14296	9117	16.65	1.0e-04	0.92723	0.00123	0.92968				
ncf2bmt11_20_1_4_3	0.0	70	19494	13646	9166	17.53	1.0e-04	0.92094	0.00124	0.92342	hcf3bmt12_20_1_4_3	0.90398	0.00124	0.90646
ncf2bmt11_19_1_4_3	0.0	70	18566	12996	9216	18.51	1.0e-04	0.92341	0.00144	0.92629	hcf3bmt12_19_1_4_3	0.90150	0.00151	0.90452
ncf2bmt11_18_1_4_3	0.0	70	17638	12346	9265	19.59	1.0e-04	0.91814	0.00135	0.92085	hcf3bmt12_18_1_4_3	0.89955	0.00134	0.90222

Table 6.9.6-11. Results for HEU broken metal content in packaging calculation model

case name	np (in)	enr. (wt%)	U (g)	^{235}U (g)	H_2O (g)	h/x	moifr	k_{eff}	σ	k_{eff}+2σ	case name	k_{eff}	σ	k_{eff}+2σ
ncf2bmt11_17_1_4_3	0.0	70	16709	11697	9314	20.78	1.0e-04	0.91793	0.00133	0.92058	hcf3bmt12_17_1_4_3	0.89730	0.00133	0.89996
ncf2bmt11_16_1_4_3	0.0	70	15781	11047	9363	22.12	1.0e-04	0.91629	0.00133	0.91895	hcf3bmt12_16_1_4_3	0.89458	0.00122	0.89702
ncf2bmt11_15_1_4_3	0.0	70	14853	10397	9412	23.63	1.0e-04	0.91068	0.00125	0.91317	hcf3bmt12_15_1_4_3	0.89088	0.00130	0.89347
ncf2bmt11_36_1_3_3	0.0	60	35320	21192	8332	10.26	1.0e-04	0.93348	0.00105	0.93558	hcf3bmt12_36_1_3_3	0.91223	0.00113	0.91450
ncf2bmt11_35_1_3_3	0.0	60	34391	20634	8381	10.60	1.0e-04	0.93036	0.00127	0.93290	hcf3bmt12_35_1_3_3	0.91033	0.00128	0.91288
ncf2bmt11_34_1_3_3	0.0	60	33461	20077	8430	10.96	1.0e-04	0.92584	0.00127	0.92837	hcf3bmt12_34_1_3_3	0.90950	0.00126	0.91202
ncf2bmt11_33_1_3_3	0.0	60	32532	19519	8479	11.34	1.0e-04	0.92680	0.00142	0.92965	hcf3bmt12_33_1_3_3	0.90720	0.00143	0.91007
ncf2bmt11_32_1_3_3	0.0	60	31602	18961	8529	11.74	1.0e-04	0.92588	0.00144	0.92877	hcf3bmt12_32_1_3_3	0.90425	0.00126	0.90678
ncf2bmt11_31_1_3_3	0.0	60	30673	18404	8578	12.17	1.0e-04	0.92420	0.00123	0.92665	hcf3bmt12_31_1_3_3	0.90271	0.00118	0.90506
ncf2bmt11_30_1_3_3	0.0	60	29743	17846	8627	12.62	1.0e-04	0.92236	0.00165	0.92566	hcf3bmt12_30_1_3_3	0.90323	0.00138	0.90599
ncf2bmt11_29_1_3_3	0.0	60	28814	17288	8676	13.10	1.0e-04	0.91822	0.00113	0.92047	hcf3bmt12_29_1_3_3	0.89982	0.00121	0.90224
with can spacers (np thickness = 1.4 in.)														
ncf2bmt11_12_2_8_3	1.4	100	11097	11097	8995	21.16	1.0e-04	0.93137	0.00124	0.93385	hcf3bmt12_12_2_8_3	0.91417	0.00139	0.91696
ncf2bmt11_11_2_8_3	1.4	100	10173	10173	9044	23.20	1.0e-04	0.92641	0.00144	0.92928	hcf3bmt12_11_2_8_3	0.91315	0.00164	0.91642
ncf2bmt11_10_2_8_3	1.4	100	9248	9248	9093	25.66	1.0e-04	0.92058	0.00138	0.92334	hcf3bmt12_10_2_8_3	0.90570	0.00166	0.90902
ncf2bmt11_9_2_8_3	1.4	100	8323	8323	9142	28.67	1.0e-04	0.91671	0.00138	0.91947	hcf3bmt12_9_2_8_3	0.89648	0.00131	0.89911
ncf2bmt11_8_2_8_3	1.4	100	7398	7398	9191	32.43	1.0e-04	0.91365	0.00171	0.91706	hcf3bmt12_8_2_8_3	0.89682	0.00139	0.89960
ncf2bmt11_7_2_8_3	1.4	100	6473	6473	9240	37.26	1.0e-04	0.90684	0.00166	0.91016	hcf3bmt12_7_2_8_3	0.88907	0.00143	0.89192
ncf2bmt11_6_2_8_3	1.4	100	5549	5549	9289	43.70	1.0e-04	0.89705	0.00145	0.89995	hcf3bmt12_6_2_8_3	0.87797	0.00166	0.88130
ncf2bmt11_14_2_7_3	1.4	95	13880	13186	8847	17.51	1.0e-04	0.93174	0.00131	0.93437	hcf3bmt12_14_2_7_3	0.91453	0.00162	0.91777
ncf2bmt11_13_2_7_3	1.4	95	12955	12307	8896	18.87	1.0e-04	0.92685	0.00140	0.92965	hcf3bmt12_13_2_7_3	0.91006	0.00135	0.91276
ncf2bmt11_12_2_7_3	1.4	95	11104	10549	8995	22.25	1.0e-04	0.91939	0.00136	0.92210	hcf3bmt12_12_2_7_3	0.89784	0.00132	0.90048
ncf2bmt11_11_2_7_3	1.4	95	10179	9670	9044	24.41	1.0e-04	0.91215	0.00134	0.91483	hcf3bmt12_11_2_7_3	0.89423	0.00146	0.89715

Table 6.9.6-11. Results for HEU broken metal content in packaging calculation model

case name	np (in)	enr. (wt%)	U (g)	^{235}U (g)	H_2O (g)	h/x	moifr	k_{eff}	σ	$k_{eff}+2σ$	case name	k_{eff}	σ	$k_{eff}+2σ$
ncf2bmt11_10_2_7_3	1.4	95	9254	8791	9093	27.00	1.0e-04	0.90898	0.00126	0.91151	hcf3bmt12_10_2_7_3	0.89121	0.00159	0.89438
ncf2bmt11_9_2_7_3	1.4	95	8328	7912	9142	30.16	1.0e-04	0.90123	0.00147	0.90416	hcf3bmt12_9_2_7_3	0.88311	0.00145	0.88602
ncf2bmt11_16_2_6_3	1.4	90	15741	14167	8749	16.12	1.0e-04	0.92855	0.00124	0.93103	hcf3bmt12_16_2_6_3	0.91007	0.00134	0.91276
ncf2bmt11_15_2_6_3	1.4	90	14815	13334	8798	17.22	1.0e-04	0.92599	0.00107	0.92813	hcf3bmt12_15_2_6_3	0.90421	0.00136	0.90693
ncf2bmt11_14_2_6_3	1.4	90	13889	12500	8847	18.47	1.0e-04	0.91938	0.00131	0.92200	hcf3bmt12_14_2_6_3	0.90163	0.00129	0.90422
ncf2bmt11_13_2_6_3	1.4	90	12963	11667	8896	19.90	1.0e-04	0.91387	0.00110	0.91607	hcf3bmt12_13_2_6_3	0.89824	0.00123	0.90069
ncf2bmt11_12_2_6_3	1.4	90	11111	10000	8995	23.48	1.0e-04	0.90989	0.00135	0.91258	hcf3bmt12_12_2_6_3	0.88832	0.00136	0.89105
ncf2bmt11_11_2_6_3	1.4	90	10185	9167	9044	25.75	1.0e-04	0.90334	0.00152	0.90637	hcf3bmt12_11_2_6_3	0.88574	0.00168	0.88911
ncf2bmt11_10_2_6_3	1.4	90	9260	8334	9093	28.48	1.0e-04	0.89868	0.00172	0.90212	hcf3bmt12_10_2_6_3	0.87986	0.00134	0.88254
ncf2bmt11_9_2_6_3	1.4	90	8334	7500	9142	31.81	1.0e-04	0.89190	0.00154	0.89499	hcf3bmt12_9_2_6_3	0.87453	0.00140	0.87733
											hcf3bmt12_24_2_5_3	0.90790	0.00134	0.91058
											hcf3bmt12_23_2_5_3	0.90282	0.00121	0.90523
ncf2bmt11_22_2_5_3	1.4	80	21324	17059	8455	12.94	1.0e-04	0.92358	0.00131	0.92619	hcf3bmt12_22_2_5_3	0.90006	0.00139	0.90284
ncf2bmt11_21_2_5_3	1.4	80	20397	16317	8504	13.60	1.0e-04	0.91640	0.00145	0.91930	hcf3bmt12_21_2_5_3	0.89948	0.00134	0.90216
ncf2bmt11_20_2_5_3	1.4	80	19470	15576	8553	14.33	1.0e-04	0.91428	0.00133	0.91694	hcf3bmt12_20_2_5_3	0.89698	0.00122	0.89941
ncf2bmt11_19_2_5_3	1.4	80	18542	14834	8602	15.14	1.0e-04	0.91020	0.00130	0.91281	hcf3bmt12_19_2_5_3	0.89282	0.00129	0.89541
ncf2bmt11_18_2_5_3	1.4	80	17615	14092	8651	16.02	1.0e-04	0.90784	0.00135	0.91054	hcf3bmt12_18_2_5_3	0.88897	0.00125	0.89148
ncf2bmt11_17_2_5_3	1.4	80	16688	13351	8700	17.01	1.0e-04	0.90364	0.00123	0.90610	hcf3bmt12_17_2_5_3	0.88452	0.00123	0.88697
ncf2bmt11_16_2_5_3	1.4	80	15761	12609	8749	18.11	1.0e-04	0.90402	0.00132	0.90666	hcf3bmt12_16_2_5_3	0.88688	0.00121	0.88929
ncf2bmt11_15_2_5_3	1.4	80	14834	11867	8798	19.35	1.0e-04	0.90496	0.00145	0.90786	hcf3bmt12_15_2_5_3	0.88496	0.00135	0.88765
ncf2bmt11_33_2_4_3	1.4	70	32490	22743	7866	9.03	1.0e-04	0.92631	0.00120	0.92871	hcf3bmt12_33_2_4_3	0.90516	0.00118	0.90752
ncf2bmt11_32_2_4_3	1.4	70	31562	22093	7915	9.35	1.0e-04	0.92304	0.00128	0.92560	hcf3bmt12_32_2_4_3	0.90236	0.00135	0.90507

Table 6.9.6-11. Results for HEU broken metal content in packaging calculation model

case name	np (in)	enr. (wt%)	U (g)	^{235}U (g)	H_2O (g)	h/x	moifr	k_{eff}	σ	k_{eff}+2σ	case name	k_{eff}	σ	k_{eff}+2σ
ncf2bmt11_31_2_4_3	1.4	70	30634	21444	7964	9.69	1.0e-04	0.92250	0.00132	0.92514	hcf3bmt12_31_2_4_3	0.90127	0.00111	0.90349
ncf2bmt11_30_2_4_3	1.4	70	29705	20794	8013	10.06	1.0e-04	0.92048	0.00138	0.92325	hcf3bmt12_30_2_4_3	0.89944	0.00124	0.90192
ncf2bmt11_29_2_4_3	1.4	70	28777	20144	8062	10.45	1.0e-04	0.91607	0.00135	0.91878	hcf3bmt12_29_2_4_3	0.89544	0.00139	0.89823
ncf2bmt11_28_2_4_3	1.4	70	27849	19494	8111	10.86	1.0e-04	0.91338	0.00129	0.91596	hcf3bmt12_28_2_4_3	0.89451	0.00127	0.89706
ncf2bmt11_27_2_4_3	1.4	70	26921	18844	8160	11.30	1.0e-04	0.91255	0.00127	0.91510	hcf3bmt12_27_2_4_3	0.88990	0.00135	0.89261
ncf2bmt11_36_2_3_3	1.4	60	35320	21192	7719	9.51	1.0e-04	0.90382	0.00130	0.90642	hcf3bmt12_36_2_3_3	0.88262	0.00120	0.88503
ncf2bmt11_35_2_3_3	1.4	60	34391	20634	7768	9.83	1.0e-04	0.90020	0.00136	0.90291	hcf3bmt12_35_2_3_3	0.87857	0.00132	0.88120
ncf2bmt11_34_2_3_3	1.4	60	33461	20077	7817	10.16	1.0e-04	0.89689	0.00121	0.89932	hcf3bmt12_34_2_3_3	0.87717	0.00111	0.87939
ncf2bmt11_33_2_3_3	1.4	60	32532	19519	7866	10.52	1.0e-04	0.89834	0.00117	0.90069	hcf3bmt12_33_2_3_3	0.87502	0.00127	0.87757
ncf2bmt11_32_2_3_3	1.4	60	31602	18961	7915	10.90	1.0e-04	0.89483	0.00136	0.89755	hcf3bmt12_32_2_3_3	0.87552	0.00129	0.87809
ncf2bmt11_31_2_3_3	1.4	60	30673	18404	7964	11.29	1.0e-04	0.89450	0.00137	0.89723	hcf3bmt12_31_2_3_3	0.87475	0.00139	0.87752
ncf2bmt11_30_2_3_3	1.4	60	29743	17846	8013	11.72	1.0e-04	0.89227	0.00133	0.89493	hcf3bmt12_30_2_3_3	0.87454	0.00121	0.87695
content in flooded containment vessel, array packaging model for CSI=2.0														
NCT											**HAC**			
no can spacers (np thickness = 0.0 in.)														
ncf3bmt11_24_1_5_3	0.0	80	23178	18542	8970	12.63	1.0e-04	0.92510	0.00131	0.92772	hcf4bmt12_24_1_5_3	0.88778	0.00138	0.89054
ncf3bmt11_23_1_5_3	0.0	80	22251	17801	9019	13.22	1.0e-04	0.92307	0.00144	0.92595	hcf4bmt12_23_1_5_3	0.88545	0.00131	0.88806
ncf3bmt11_22_1_5_3	0.0	80	21324	17059	9068	13.87	1.0e-04	0.91977	0.00125	0.92228	hcf4bmt12_22_1_5_3	0.88238	0.00140	0.88519
ncf3bmt11_21_1_5_3	0.0	80	20397	16317	9117	14.58	1.0e-04	0.91607	0.00134	0.91876	hcf4bmt12_21_1_5_3	0.87917	0.00128	0.88173
ncf3bmt11_20_1_5_3	0.0	80	19470	15576	9166	15.36	1.0e-04	0.91812	0.00123	0.92059	hcf4bmt12_20_1_5_3	0.87731	0.00132	0.87995
ncf3bmt11_36_1_4_3	0.0	70	35275	24693	8332	8.81	1.0e-04	0.93179	0.00144	0.93467	hcf4bmt12_36_1_4_3	0.89390	0.00117	0.89625
ncf3bmt11_35_1_4_3	0.0	70	34347	24043	8381	9.10	1.0e-04	0.92998	0.00125	0.93248	hcf4bmt12_35_1_4_3	0.89164	0.00140	0.89444
ncf3bmt11_34_1_4_3	0.0	70	33419	23393	8430	9.41	1.0e-04	0.92792	0.00128	0.93049	hcf4bmt12_34_1_4_3	0.88829	0.00123	0.89075

Table 6.9.6-11. Results for HEU broken metal content in packaging calculation model

case name	np (in)	enr. (wt%)	U (g)	^{235}U (g)	H_2O (g)	h/x	moifr	k_{eff}	σ	k_{eff}+2σ	case name	k_{eff}	σ	k_{eff}+2σ
ncf3bmt11_33_1_4_3	0.0	70	32490	22743	8479	9.73	1.0e-04	0.92421	0.00134	0.92690	hcf4bmt12_33_1_4_3	0.88600	0.00117	0.88834
ncf3bmt11_32_1_4_3	0.0	70	31562	22093	8529	10.08	1.0e-04	0.92329	0.00131	0.92591	hcf4bmt12_32_1_4_3	0.88581	0.00140	0.88861
ncf3bmt11_31_1_4_3	0.0	70	30634	21444	8578	10.44	1.0e-04	0.91896	0.00132	0.92160	hcf4bmt12_31_1_4_3	0.88314	0.00132	0.88577
ncf3bmt11_36_1_3_3	0.0	60	35320	21192	8332	10.26	1.0e-04	0.90201	0.00123	0.90447	hcf4bmt12_36_1_3_3	0.86792	0.00130	0.87053
ncf3bmt11_35_1_3_3	0.0	60	34391	20634	8381	10.60	1.0e-04	0.90103	0.00130	0.90363	hcf4bmt12_35_1_3_3	0.86477	0.00150	0.86777
ncf3bmt11_34_1_3_3	0.0	60	33461	20077	8430	10.96	1.0e-04	0.89984	0.00147	0.90278	hcf4bmt12_34_1_3_3	0.86396	0.00137	0.86670
ncf3bmt11_33_1_3_3	0.0	60	32532	19519	8479	11.34	1.0e-04	0.89745	0.00130	0.90004	hcf4bmt12_33_1_3_3	0.86136	0.00134	0.86404
ncf3bmt11_32_1_3_3	0.0	60	31602	18961	8529	11.74	1.0e-04	0.89310	0.00137	0.89585	hcf4bmt12_32_1_3_3	0.86115	0.00124	0.86362
ncf3bmt11_31_1_3_3	0.0	60	30673	18404	8578	12.17	1.0e-04	0.89440	0.00135	0.89711	hcf4bmt12_31_1_3_3	0.85909	0.00151	0.86212
with can spacers (np thickness = 1.4 in.)														
ncf3bmt11_19_2_8_3	1.4	100	18496	18496	8602	12.14	1.0e-04	0.93577	0.00135	0.93847	hcf4bmt12_19_2_8_3	0.89811	0.00149	0.90110
ncf3bmt11_18_2_8_3	1.4	100	17571	17571	8651	12.85	1.0e-04	0.93186	0.00154	0.93494	hcf4bmt12_18_2_8_3	0.89794	0.00151	0.90096
ncf3bmt11_17_2_8_3	1.4	100	16646	16646	8700	13.64	1.0e-04	0.92731	0.00135	0.93002	hcf4bmt12_17_2_8_3	0.89377	0.00134	0.89644
ncf3bmt11_16_2_8_3	1.4	100	15721	15721	8749	14.53	1.0e-04	0.92992	0.00126	0.93244	hcf4bmt12_16_2_8_3	0.89138	0.00121	0.89379
ncf3bmt11_15_2_8_3	1.4	100	14796	14796	8798	15.52	1.0e-04	0.92597	0.00134	0.92865	hcf4bmt12_15_2_8_3	0.89085	0.00130	0.89345
ncf3bmt11_14_2_8_3	1.4	100	13872	13872	8847	16.65	1.0e-04	0.91788	0.00124	0.92037	hcf4bmt12_14_2_8_3	0.88486	0.00143	0.88772
ncf3bmt11_13_2_8_3	1.4	100	12947	12947	8896	17.94	1.0e-04	0.91410	0.00116	0.91642	hcf4bmt12_13_2_8_3	0.88161	0.00147	0.88454
ncf3bmt11_12_2_8_3	1.4	100	11097	11097	8995	21.16	1.0e-04	0.90586	0.00164	0.90915	hcf4bmt12_12_2_8_3	0.87451	0.00129	0.87708
ncf3bmt11_11_2_8_3	1.4	100	10173	10173	9044	23.20	1.0e-04	0.90034	0.00144	0.90322	hcf4bmt12_11_2_8_3	0.86789	0.00129	0.87047
ncf3bmt11_24_2_7_3	1.4	95	23134	21977	8357	9.92	1.0e-04	0.93439	0.00143	0.93724	hcf4bmt12_24_2_7_3	0.89896	0.00122	0.90141
ncf3bmt11_23_2_7_3	1.4	95	22209	21098	8406	10.40	1.0e-04	0.93453	0.00131	0.93716	hcf4bmt12_23_2_7_3	0.89761	0.00131	0.90024
ncf3bmt11_22_2_7_3	1.4	95	21283	20219	8455	10.91	1.0e-04	0.92992	0.00130	0.93252	hcf4bmt12_22_2_7_3	0.89290	0.00142	0.89574
ncf3bmt11_21_2_7_3	1.4	95	20358	19340	8504	11.48	1.0e-04	0.92588	0.00136	0.92860	hcf4bmt12_21_2_7_3	0.89171	0.00135	0.89441